Reply to the reviewers

We thank the reviewers and editor for their time evaluating our manuscript. Here we reply to their helpful suggestions, pointing out changes made to the revised manuscript. First, the main issues:

The major criticism of reviewers 1 and 3 was the length or organization. We responded by reducing the length of the main body of the manuscript by about half. Our other large change is to the introduction, which reviewer 2 expressed a need for more general background. So, we broke the original Introduction into Introduction and Background, adding general information in Background. Except for Appendix A, which is needed for the test of facet spreading, all theory sections are moved to a separate manuscript. The remaining parts have been significantly reorganized, and much rewritten, to make reading easier. All detailed discussion of the secondary habits was moved to the appendix, and some figures have been revised to help clarify the content. Finally, the title has changed to better reflect the content.

Shown below are the complete reviewer comments, separated by our replies with a red dashed line and made distinct with larger font. Also, in yellow highlighting are changes in the revised manuscript.

Anonymous Referee #1 Received and published: 26 April 2019

The authors studied the formation mechanisms of air pockets and other secondary habits in snow crystals. The topics coincide with the scope of Atmos. Chem. Phys. Discuss., and the secondary habits of snow crystals are interesting from the fundamental viewpoint. However, first of all, this manuscript is too lengthy (26 figures are shown in the manuscript of 51 pages in total), and too many subjects are included in a mixedup way. Therefore, I need to say the presentation quality is poor. Second, the authors insist that the formation of corner air pockets (the main subject in this manuscript) cannot be explained by the traditional growth mechanisms based on lateral step motion, and by the morphological instability based on the inhomogeneous distribution of vapor density. Then the authors conclude that the lateral-type (protruding) growth, which is the key mechanism in this study, is a novel concept. However, I cannot agree with such authors' claims (for details, see the comment 2). Hence, I believe that the scientific significance of the present manuscript is also poor. Since the amount of revisions is significantly large and the conceptual revisions are necessary, I do not recommend the publication of this manuscript.

Our reply:

Thank you for your comments. We address these issues below. In brief, the manuscript is reorganized, with a main body half as long. The issue with comment 2) seems to be based on a misreading as explained below.

Following 1-3 are major comments.

1. Too lengthy: one paper should have one main claim. Then, I believe that the following topics should be presented in separated papers: # the formation mechanism of the corner air pockets, # quantitative discussion about the kinetics of the lateral-type (protruding) growth, and # secondary habits other than the corner air pockets (these topics can be also moved into supplementary information)

Our reply:

We followed your suggestions in part by moving most theory subsections to a separate manuscript. The secondary habits discussion is a crucial part of our main claim and remain in this paper, but due to their length we moved them to the appendices and simply summarize the findings in the main body. They remain in the paper because they give further support for the importance of lateral growth and provide numerous tests of the phenomenon, but do not interrupt the flow. More importantly for us, they may satisfy readers curiousity about how some very unobvious crystal forms can arise.

Our main claim is that lateral growth should be included in any complete model of ice growth. We stated this in the introduction and in the conclusions, but neglected to explicitely state it in the abstract. This omission has been corrected. Appearing at the end of the abstract:

Although these suggested mechanisms may presently lack quantitative detail, the overall body of evidence here demonstrates that any complete model of ice growth from the vapor should include lateral-type growth processes.

The title was also changed to better reflect the content.

---

2. The formation mechanism of the corner air pockets: the authors mentioned that the normal growth via step motion and the standard hollowing theory based on the morphological instability caused by the inhomogeneous vapor density cannot explain the formation of the corner air pockets. Then, I shall explain the formation of the corner air pockets by the traditional concepts. The key is the morphology of a snow crystal at the beginning of the growth. 1) When a starting crystal is fully faceted, the local vapor density becomes maximum at the corner of the crystal, providing a hollow not at the corner but at the center of the crystal face, as the authors explained. 2) In contrast, when a starting crystal is partly rounded, the layer-by-layer growth of the faceted face (located at the center of the crystal) proceeds. Then a spreading edge appears as shown in Fig. 1b (marked by e) and Fig. 8c. Since the spreading edge shows an angular shape and the corner of the crystal is still rounded, the local vapor density at the tip of the spreading edge becomes higher than that at the rounded corner, providing the overhang as shown in Fig. 1d and Fig. 8d. After once the overhang was produced, the overhang is developed spontaneously (the authors call this process the protruding growth), and the corner air pocket is formed. These processes never violate the traditional concepts of the layer-by-layer growth and the morphological instability.

Our reply:

Thank you for the suggested mechanism. We agree that the vapor-density gradients should promote protruding growth and that "traditional concepts" are involved. In the first paragraph of §3.6 (which the comment addresses), we are referring to hollows forming on a fully facetted face as being incompatible with the observed corner pockets. To reduce chances of the same misunderstanding, we changed the wording (now section 4.1.2):

Existing views on normal growth via step motion cannot readily explain corner pockets on fully facetted crystals. With normal growth, each pocket must have at one time been a hollow (lacuna or concave feature) before closing-off to enclose the air. And standard hollowing theory (e.g., Kuroda et al., 1977; Frank, 1982; Nelson and Baker, 1996) predicts that hollows form around a local vapor-density minimum, not at a corner where the driving force for normal growth is instead a local maximum. Moreover, the standard theory relies upon step clumping on a facetted surface.

We agree with the reviewer's ideas about protrusion initiation. But they were already in the manuscript—in the 2nd paragraph of §3.22. This section is now moved to section 5.1. The passage, from line 20

A possible answer to (1) is a large vapor-density gradient. Consider again the sketch in Fig. 2b. If the vapor-density contours closely parallel the surface, but "skim over" the inside corner **c**, then the vapor density would sharply decrease from **e** to **c** provided that this distance exceeded the vapor mean-free path. In such a case, the AST flux may build up nearer to **e** and not reach **c**, initiating the protrusion.

Thus, the reviewer simply misread what we had written. Hopefully, it is now clear. Finally, whether or not one refers to lateral-type growth as a "traditional concept" is immaterial (we never say it is not); the fact we emphasize is that it has not been considered in ice-crystal growth models, which is our main point.

In addition, the authors emphasize the importance of the diffusion of admolecules on the crystal surface (the surface diffusion of admolecules). Then the authors named this process “adjoining surface transport (AST)”. I fully agree with the importance of the surface diffusion for the formation of the overhang and the subsequent protruding growth. However, the concept of the surface diffusion of admolecules is very traditional (firstly proposed by Frank and coworkers in the 1960s, and then experimentally proved by the growth of various crystals). Therefore, the authors should clearly show what is the authors’ novel concept and what is not.

Our reply:

One paragraph in the original introduction was devoted to prior work on surface transport over crystal edges (page 8, paragraph starting on line 12). There are 8

references to prior work on the topic. So, we made no new additions to this discussion, as we feel the 8 citations are sufficient. Moreover, the overhanging aspect of protruding growth appears in none of these previous papers. The reviewer appears to be confusing surface diffusion with surface transport over the edge to the lateral-growth front. These are distinct processes that we have tried to further clarify in the new Background section.

Concerning the point that we should clarify what is new and what is not: We have followed the long-standing scientific practice of giving references to all relevant prior work except when long-established (e.g., kinetic theory of gases), with all else being presumably new. If we were to start saying "this is novel" every time we express a new result or idea, the reader would soon tire of the repetition and deem us arrogant. Even though some authors break with this practice and announce their result as "novel", most do not, and for good reason—that is the job of others to declare. Relevant changes to the manuscript are in our next reply.

---

3. Throughout the manuscript, the authors should clearly explain what is the authors' new finding and what is not, with respect to phenomena and formulas as well. Followings are minor comments.

Our reply:

Whatever does not have a citation is thought to be new, as per standard scientific writing practices. However, several additions help clarify our contributions: In the introduction to the role of AST on secondary habits (Appendix B)

Most of these features and habits appear inexplicable with normal-type growth processes only, and only a few of them have even seen attempts at explanation.

And in the introduction to the main results (§4)

The following subsections survey, and partly explain, observations made in CC2, including previously unreported "corner pockets", "planar pockets", and "elongated edge pockets".

---

4. The term "droxtal": since many readers (including me) are not familiar with this term, the authors need to explain it properly at the beginning.

Our reply:

In the revised manuscript, we define the term in the new background section, page 3 as

Atmospheric ice crystals generally begin with the simplest of shapes, a solid ice sphere, also called a droxtal.

The term is no longer used in the abstract, as we now refer to the droxtal center as

small circular centers in dendrites

The term is also defined in the figure with droxtal images. Before, this was Fig. 2, now it is Fig. 1:

Figure 1: Crystals at different stages between large droxtals (just-frozen droplets) and prisms

---

5. The section 1.2 gives the impression that the authors do not fully understand the fundamental growth mechanism of crystal growth. The concept of the surface diffusion of admolecules (AST) is widely accepted in the crystal growth of wide variety of materials: not only for the metal whiskers, but also for semiconductor crystals, molecular crystals and ice crystals as well (as studied by Hallett, Mason et al, Kobayashi, and Asakawa et al.) Hence, for me, the application of the surface diffusion to the lateral and protruding growth by Yamashita (2015) does not look a significant revision, since the lateral and protruding growth can be explained easily, as shown in my above-mentioned comment 2.

Our reply:

We do not see the relation here between the first sentence and the rest of the paragraph. We agree that surface diffusion is widely accepted, and cite these and other authors for work on AST in the Background section. But surface diffusion is not AST: AST is defined as adjoining surface transport to the lateral "growth front" as stated on lines 11-14 of the abstract. AST was defined elsewhere as well. To help reduce this confusion, we briefly list the relevant definitions now at the end of the background section. The previous section 1.2 has been expanded to the new Background section, so this "impression" should no longer be present.

Concerning comment 2, we address that confusion above. However, whether or not the reviewer considers lateral and protruding growth a "significant revision", the fact remains that it had not been considered as an important aspect of ice growth from the vapor. Lateral-type growth does not appear in the ice-growth literature, and AST is generally ignored. For example, at the end of the new section 5.2.1, after briefly summarizing how AST-driven lateral growth can explain seven secondary habits and features, we add

A recent review of ice growth from the vapor suggested that AST may be unnecessary for understanding ice growth forms (Libbrecht, 2005). The above examples suggest otherwise, instead arguing that many oft-observed secondary features may be inexplicable without the AST mechanism.

Getting back to the reviewer's first sentence, do we "fully understand the fundamental growth mechanism of crystal growth"? Does anyone?

By the way, it is impossible to obtain the reference Yamashita 2015. The page numbers of the references Yamashita 2013 and 2016 should be 165-176 and 393-400, respectively: the page numbers of 23-33 and 15-22 are those in the issues 60 (3) and 63 (5).

Our reply:

Yamashita 2015 is a conference proceeding paper. Indeed, such papers are often hard to obtain, but not impossible (we found it). The reference serves the purpose of giving credit to the originator of the idea. Given that this is a common practice in scientific papers, we keep the reference. We have a few other cases like this, but the vast majority of our references are easy to access.

Thank you for the corrected page numbers for Yamashita 2013, 2016. The Tenki journal has two page numbering systems on each page, and, being unfamiliar with this journal's system, it seems we picked the wrong one. This has been corrected.

---

6. The authors should show the schematic illustration of the new crystal-growth apparatus (CC2) in this study, since the reference Swanson and Nelson 2019 is still in preparation.

Our reply:

The manuscript is under review and available for viewing, so we did not include a drawing here. We updated the reference so readers can view the apparatus. Please see the link in the new references:

Swanson, B., and Nelson, J.: Low-Temperature Triple-Capillary Cryostat for Ice Crystal Growth Studies. Atmos. Measurement Techniques, https://doi.org/10.5194/amt-2019-137, 2019.

---

7. In the section 3.4, from Fig. 4, I cannot understand the difference between the expanding boundary of the basal face and growing macro-steps. The authors also should clearly explain the kinetic models I, II and III in the main

text (of a separated paper), since the quantitative discussion has no meaning without obtaining the complete understanding of the models.

Our reply:

A macrostep exists as a large step within a facet and it arises from the clustering of smaller steps. Neither apply here. The case here, as we try to clarify in the main text and the appendix, is a facet expanding over a rough, round surface. The rough, round surface is not yet a facet, and thus our case is not a macrostep; moreover, the facet edge did not arise from step clustering. To help clarify, we added the following text where we discuss the plot:

…, but it is a reasonable fit to the initial cross-section profile. This profile is that of a flat facet out to a radius $r < a$, and a curved profile between r and a where the crystal had rounded during sublimation. (Refer to Fig. A1 for further details.)

We now discuss macrosteps in a few places in the new Background section, clarifying their difference with a spreading facet.

Finally, we keep the appendix here to explain the calculations for the plot, but as suggested will have further details of the model in a separate paper.

By changing the value of h/xs arbitrarily, one can easily fit the experimental data. Hence, here the authors need to explain the causes of the change in the value of h/xs (I believe that the cause of the change is the evolution of macro-steps) and also whether the change is appropriate or not. The authors also need to discuss the values of h and xs.

Our reply:

Yes, changing h/xs allows us to fit the data. We made no claim to the contrary and write that accurate measurements with a different apparatus are needed. Nevertheless, the qualitative trend in the fitted curve is consistent with the cross-sectional profile of the crystal when the facet began expanding. It has nothing to do with macrosteps because the expanding facet is not a macrostep. The cause of the change in h is shown in Fig. A1, and explained in the caption:

At a later time t', the value of h is larger (light shading) due to the advancement to $r(t')$, making a larger distance between the rough surface and basal surface at c.

Of course, it is likely that some normal growth on the basal facet occurred that contributed to h, but this rate of growth in this case is negligible compared to the

rate of lateral growth, also making the contribution to *h* negligible. (Other cases may differ, so we do not claim this contribution can always be ignored.)

Without an accurate measure of the crystal profile and an established value for *x*s, providing separate numbers for *h* and *xs* here is largely pointless; the trend is clearly consistent with the profile, but accurate measurements are needed. The whole point of the comparison is to show that the AST is the only process capable of explaining the data. Nevertheless, we added the following discussion of *h* and x_s:

A reasonable estimate of height *h* upon reaching the edge is 1–5 μm. With this range, the fit in Fig. 6 (inset) predicts $h/x_s = 0.3$, giving x_s = 3–17 μm at this temperature, which is comparable to the value of about 2 μm found by Mason et al. (1963).

But to emphasize the main point here, the last paragraph was modified slightly as

Nevertheless, the observed behavior clearly shows that mechanisms I and III cannot explain the observed lateral growth. Only growth driven by a flux of surface mobile molecules, the AST mechanism, from the facet to the lateral-growth front is capable of fitting the observations.

Also, to help reduce confusion on this issue, we removed the two intermediate curves with high supersaturations from the plot. Now there are just three curves for the three models, all at the same supersaturation.

---

8. In the section 3.9, the authors should explain the impossibility and instability much more in detail.

Our reply:

Detailed examination of impossibility and instability theories are covered well in the literature (though the term 'impossibility' is not used elsewhere). However, we agree that a little more explanation and rewording will help. In this section, after the 2nd sentence, we have the following rewrite that expresses the key differences between these two types of behavior:

In the standard treatment, however, the hollow occurs when the gradient in supersaturation needed for uniform growth can no longer be compensated for by the step density (e.g., Kuroda et al., 1977; Frank, 1982). In other words, normal growth of the entire facet becomes impossible, which is different from being unstable. In this "impossibility" case, one expects the hollow initiation and shape to be nearly identical on identical faces in a nearly uniform environment as well as being highly reproducible when other crystals grow under the same conditions. If merely an unstable phenomenon, then a sufficiently uniform, constant condition may be expected to circumvent the hollowing. Conversely, if hollows do form, then their initiation and shape should differ between identical faces due to minute differences in

conditions. We suggest here that inclusion of lateral-type growth processes predicts qualities of unstable growth at low supersaturations, leading to hollow close-off and terracing features.

---

9. The sections 3.10-3.22: If these sections have scientific significance, the authors should explain them in separated papers. If their scientific significance is not so large, the authors should move them into the supporting information.

Our reply:

These sections provide explanations for commonly observed ice-crystal forms and secondary features, making them significant to anyone interested in the causes of crystal shapes. Please compare to any paper (*of thousands*) that have been written about dendrite branching or some of the cited ones dealing with trigonal growth.

As these crystal forms and features had not been satisfactorily explained by other mechanisms, the explanations here involving lateral-type growth provide support for the importance of lateral-type growth, the main point of our paper.

We understand that the volume of information makes reading in one push difficult, so we moved these subsections to the appendix, instead summarizing them in the new subsection 5.2.1. We also added text and two figures showing images of two such crystal forms to more clearly motivate the need for explanation.

Perhaps what we failed to express here is that the extreme complexity of ice-crystal growth in air warrants a variety of approaches. At this stage, we need to at least know which processes to include in a crystal growth model. No model has yet included lateral-type growth. By including evidence that such a growth process can explain numerous micron-scale features in vapor grown ice (the secondary features), this paper shows just how prevalent the lateral-type growth is.

If getting the relevant growth processes right is not significant, then we do not know what is.

Anonymous Referee #2 Received and published: 30 April 2019

The paper “Air pockets and secondary habits in ice from lateral-type growth” presents extensive collection of micrographs of growing ice. I am very pleased by its esthetical beauty. I think it should be published for its experimental value, regardless the theoretical explanations. The explanation of air pockets formation is elegant. I cannot judge on its correctness. Nevertheless, I have some suggestions stemming mostly from the fact that I am not an expert in the field of ice grow from the vapor phase and thus I would welcome some introduction and generalizations. That may be a case for most of the readers, though. I suggest the paper be published after considerations the comments.

Our reply:

Thank you very much for recognizing the extent and significance of the work in this paper and making these suggestions. We have added some more general background in the beginning, breaking the introduction into a shorter introduction section that gives our motivation, similar to before, and a new background section that covers the more general topic (or "generalizations").

I would think that such extensive work deserves broader introductions and connections to what “general ice knowledge” may cover. I started form Hobbs: Physics of ice Ch. 8: I found the description of the growth in the direction of c and a-axis easier to understand then to consider the basal face and prismatic face in presented manuscript. Can both description be shown in the pictures?

Our reply:

Yes. We revised the sketches in Fig. 1 (now Fig. 2) to include different views and the principle axes as expressed in Hobbs. As mentioned above, we have broadened the introductory section, adding a section 3 "Background". This section explains the normal growth directions.

In Hobbs (ch. 8.3) the linear growth (here named normal) is defined as normal to crystallographic face. Is the here discussed lateral growth perpendicular to both c-axis and a-axis? Would not that be more exact definition than that given on the line 5 of page 2?

Our reply:

Lateral growth of a basal face is growth perpendicular to the c-axis, but the same cannot be said for the prism face. However, the maximum dimensions normal to the c-axis tends to be in the a-axes directions as shown in the revised Fig. 1, now Fig. 2.

We also improved the sketches in this new Fig. 2 to help explain what we mean by lateral growth. Also, in the Introduction, we help to clarify lateral growth:

The rate is often called the linear growth rate (e.g., Lamb and Scott, 1972), but to help distinguish this face-normal growth from face-lateral (or areal) growth, we refer to it as the normal growth rate.

Also, we try to clarify the types of lateral growth with a bulleted list of definitions at the end of the new Background section.

I think, that schema in Figure 1a suggests that the droxtal has 8 prismatic phases –should not there be only 6 of them?

Our reply:

There are just two prism faces in back. The figure has been revised to help address your previous concern, and now makes the six prisms clear by showing the top view at right in the new Fig. 2.

I had some previous knowledge of "snow morphology diagram", where temperature and humidity is decisive for the shape of snowflakes. Thus I was surprised that the current paper does not describe the humidity in details or does not attempt systematic study of the influence of temperature and humidity. Is reasonable to suppose the dependence? Is AST necessarily needed for the observations or would the vapor deposition normal to a-axis be sufficient?

Our reply:

Lateral-type growth should depend on temperature and humidity. We plan to investigate this experimentally, and also hope that this paper spurs others to investigate as well. We now mention some expected dependences. For example, in the Background section, pg. 3, lines 3-5, we mention the temperature dependence of x_s:

Experiments reported in the 1960s indicated that x_s on the basal face varied dramatically with temperature, changing by a factor of 5–7 between about −7 and −12 °C (Mason et al., 1963; Kobayashi, 1967). Although the exact values of x_s may be disputed, both studies independently found the values to be largest in the tabular regime, smallest in the columnar.

In other parts of the manuscript, we refer to this temperature dependence for the basal as being potentially important for various features, such as the two-level structure of planar crystals, capped columns, and trigonals. But the values for the basal have not been verified by other experiments and we do not have measurements for the prism. For protruding growth, another length scale may be important as well, the migration distance on rough faces, which may depend on temperature and supersaturation, but we have no theory or experiments to guide us. We mention this in the new Background section. Thus, we do not attempt anything like the snow crystal habit diagram for lateral-type growth features. However, we now mention the snow-crystal habit diagram in the introduction:

The primary and secondary habits depend on temperature and humidity as often portrayed on the habit diagram. This diagram has generally remained the same since Ukichiro Nakaya first proposed it (Nakaya, 1954), though some extensions and modifications have come from subsequent studies (e.g., Hallett and Mason, 1958; Takahashi et al., 1991; Bailey and Hallett, 2004; Takahashi, 2014).

It would be nice to shortly connect current observations to those of “classical” snowflakes formations. Is there AST mechanism needed there? I would appreciate if some discussed term are more explained and/or shown in the pictures (droxtal, adjoining facets, basal and prismatic facets in Figure 2).

Our reply:

We make several connections to the classical stellar crystal, but do not suggest that the main features such as the branches and sidebranches are due to lateral growth. In the main body, we make the connection to corner pockets in classical snow crystals in Fig. 8 and section 4.5, as well as discussing the two-level structure in section 5.2. Several other aspects of the classic snow crystal are addressed in Appendix B. We now list the common lateral-growth terms at the end of the Background section.

I think the abstract should be modified according the final content. Currently, I find some disagreement between it and the content of the manuscript. Also the name of prof. Yamashita in the abstract does not seem appropriate to me.

Our reply:

We are not sure what "some disagreement" refers to here, but we have assumed the reviewer means that some findings are not explicitly mentioned in the abstract. In response, we added our model fit to the abstract and mention other results from the experiments:

Further experiments revealed other types of pockets that are difficult to explain without invoking AST and protruding growth. We develop a simple model for lateral growth on a tabular crystal in air, finding that AST is also required to explain observations of facet spreading.

and added some words to help clarify our applications to observed secondary features:

Applying the AST concept to observed ice and snow crystals, we argue that AST promotes facet spreading, causes protruding growth, and increases layer nucleation rates. In particular, depending on the crystal shape and conditions, combinations of these lateral-type processes with normal growth can help explain presently inexplicable features and secondary habits such as air pockets, small circular centers in dendrites, hollow terracing and banding, multiple-capped columns, scrolls, trigonals, and sheath clusters. For dendrites and sheaths, AST may increase their maximum dimensions and round their tips. Although these applications presently lack quantitative detail, the overall body of evidence here demonstrates that any complete model of ice growth from the vapor must include these lateral-type growth processes.

About mentioning Prof. Yamashita in the abstract, we realize that the practice is not common. But it is done (see e.g., some abstracts from the physicist J. A. Wheeler, and the one by Frenkel that we cite), and in this case we prefer to have his name. He has promoted the idea of AST and protruding growth for years, often communicating with one of us, but has had difficulty writing his results up for an English journal. We reference all of his relevant work in the main text, but some readers only read the abstract and we feel that he deserves recognition for the concepts on the front page lest readers mistakenly think we originated the concepts of AST and protruding growth. But to help address your concern, we shortened the mention of his name in the abstract.

Anonymous Referee #3 Received and published: 7 May 2019

This paper reports an experimental study of ice growth from vapor in air, with a focus on the formation of air pockets and secondary habits. It ultimately looks to explain a wide variety of experimental observations on lateral-type growth and looks to relate the observed behaviour to a surface flux of water molecules, which the authors call "adjoining surface transport" (AST). As a non-expert this specific field (experimental studies of ice growth from vapor), I found this paper rather difficult to read, and I felt I learned very little in reading it. I found it to be not well written, and a bit of a jumble of data and ideas with no clear narrative. Hence, I think it could be considerably improved by shortening (i.e. less would be more here) and organizing the material better.

Our reply:

We are sorry to read that you learned very little from it. We agree that the original was hard to read completely through due to the length of the main body. To improve the narrative, we have reduced by half the main body, largely reorganized the paper, rewriting many parts, adding more motivation for the work, removed most theory sections, and added to the introduction a background section to put the work in context of standard crystal growth theory.

Applications to secondary features, which occupied much of the main body of the original, no longer appear before the summary, instead appearing in Appendix B, beginning with a list of the content. The main point is now emphasized more, which should also improve the narrative.

Also, the paper often seems to read more like a review, where it was often unclear where the authors' work started and ended. Perhaps after considerable revision with work might be appropriate for publication.

Our reply:

We understand how one might read the paper in this way because we have examined many observed crystal types. And in a sense, it is a review of our own work going back six years. But whether one considers it a review or not, it is all tied together by the clear evidence that lateral-type growth is needed to understand many ice-crystal forms. That this point should be emphasized is given by the fact

that a previously published review considered it unnecessary to include AST in growth models. We now explicitely state this at the end of section 5.2.1:

A recent review of ice growth from the vapor suggested that AST may be unnecessary for understanding ice growth forms (Libbrecht, 2005). The above examples suggest otherwise, instead arguing that many oft-observed secondary features may be inexplicable without the AST mechanism. Additional cases, including aspects of primary habit, are briefly examined in the appendix as well. The arguments are mostly qualitative; nevertheless, they may help stimulate new measurements of x_s, further observations, and more detailed modeling of these interesting crystal forms.

However that review examines cases of normal growth for the primary habit and "morphological instability", but does not consider some of the secondary features like we do.

Concerning where our work started and others' ended, we reply to this point in a previous reply: we have followed standard procedure and given references for any work or results that are not ours.

Finally, we have made considerable revisions, as suggested.

I was also unable to make sense of their physical model.

Our reply:

For the examination of facet spreading in Fig. 5 (now Fig. 6), the model we used is the BCF model as justified in the Background section. Starting in the first paragraph:

The most widely used model for the growth of crystal faces from the vapor is the BCF model (Burton et al., 1951; Woodruff, 2015). This model supposes that a given molecule in the vapor above a faceted surface strikes the crystal surface and become temporarily trapped in a mobile state until either desorbing back to the vapor or migrating along the surface and reaching a more strongly bound state at a step edge….

Then at the end of the third paragraph

…Hence, at least as a first approximation, it is still useful to compare observed behavior of ice to the BCF model and make use of measured x_s values.

The basic physical model involves AST, which is not new. From the old Introduction, now near the end of the new Background:

The types of lateral growth here are driven by AST. Evidence for AST on ice is indirect, partly coming from early studies of spreading ice layers on covellite (Hallett, 1961; Mason et al., 1963, Kobayashi, 1967). In these studies, the rates of approaching micron-scale layers, also known as macrosteps (arising from clustering of smaller steps or contact between crystals of differing height) changed in a way consistent with a flux of molecules over the top edge of the layer. The concept has long been applied to the growth rates of metal whiskers (e.g., Sears, 1955; Avramov, 2007), but rarely applied to ice.

Most theory sub-sections have been removed (put in a separate manuscript). The details of the model calculation for Fig. 6 are in the first appendix. In the rest of the manuscript, we are only arguing qualitatively for AST effects. The reason is two-fold: 1) calculations of an AST for most secondary features would require much more space in a separate paper (e.g., for the needle crystals) and 2) the key parameter x_s is poorly constrained, particularly for the prism face. Our hope is that this study stimulates work on the topic, allowing such quantitative treatment in the future.

It has now be very well established that the surface of ice features a layer water molecules that exhibit mobility (this is sometimes referred to as the quasi-liquid-layer – QLL; see Rosenberg, Phys. Today 2005, 58, 50; Li and Somorjai, J. Phys. Chem. C 2007, 111, 9631; Björneholm et al., Chem. Rev. 2016, 116, 7698). While different experiments report different thickness for the QLL, they generally agree on its presence, and that its thickness (and other properties) are strongly temperature dependent. One would expect any surface flux to then depend on the thickness of the QLL and the mobility within the layer (which will also be strongly temperature dependent). Thus, AST should exhibit strong temperature dependence, and one would expect to observed "protruding growth" only when the effect of AST is large compared with the rate of vapor deposition (which will depend on the level of supersaturation).

Our reply:

Thank you for pointing this out. We agree that the surface of ice has significant mobility and that many researchers have found evidence for a QLL. In the background section, we now briefly discuss the apparently disordered nature of the ice surface, its role in growth, and our reasoning for using BCF with the parameter x_s:

The BCF model of surface diffusion assumes that the mobile surface molecules are sparse and non-interacting. For ice, this assumption is widely believed to be violated over much of the atmospheric temperature range where the surface is thought to contain significant disorder (e.g., Rosenberg, 2005). Yet the BCF model is nevertheless often used to interpret experimental results (e.g., Sei and Gonda, 1989; Asakawa et al., 2014). A key parameter in the model is the mean migration distance x_s of a mobile molecule on the surface before desorbing, a distance that should differ between the basal (***b***) and prism

(***p***) faces as well as depend on temperature. With interactions between these surface-mobile molecules (e.g., Myers-Beaghton and Vvedensky, 1990), x_s may also depend on supersaturation. In addition, the migration of surface vacancies may also affect x_s (Frank, 1993). Experiments reported in the 1960s indicated that x_s on the basal face varied dramatically with temperature, changing by a factor of 5–7 between about −7 and −12 °C (Mason et al., 1963; Kobayashi, 1967). Although the exact values of x_s may be disputed, both studies independently showed that the values are largest in the tabular regime, smallest in the columnar. Corresponding values for the prism have not been determined. Later, Nelson and Knight (1998) found a similarly sharp behavior in basal-face critical supersaturation between these temperatures. A possible link between these two parameters is clustering of the mobile species responsible for growth: when the temperature is such that clustering is strong, the critical supersaturation is low and surface-mobile molecules would become temporarily trapped in sub-critical nuclei, giving them very low mobility. Thus, the critical supersaturation would be low when x_s is low and vice-versa as found by experiments. The values of the measured critical supersaturations led Nelson and Knight to conclude that the surface was indeed disordered but " ...the [common] view of the ice surface as a liquid layer is not a useful idealization for crystal growth processes." Hence, at least as a first approximation, it is still useful to compare observed behavior of ice to the BCF model and make use of measured x_s values.

That passage also includes the review article by Rosenberg that you cited. Also, in the discussion of hollows and center-pocket formation, we mention a newer study of step dynamics in a disordered region (now in Appendix B.1):

(Neshyba et al. (2016) proposed a more detailed model of step dynamics for ice with a thick surface-disordered region, but it is not yet clear how a hollow would develop in that model.)

Finally, we consider that with or without a thick disordered layer, the AST process may continue. Even as isolated mobile molecules, the simple calculation using BCF gives a significant contribution to growth, the amount depending on the ratio of the surface-migration distance x_s to the edge thickness t. In the new section 5.1, at the start, we added

The microscale mechanism of facet spreading involves AST, which is the migration of molecules, first over the edge of the facet, and second with their finding a high-density of growth sites on the other side. The first may occur via isolated molecules or as a more cooperative phenomena in a thicker disordered region, but either case may be consistent with the observations here.

Concerning the temperature dependence of AST, this will largely depend on x_s, which is presently poorly constrained, and the thickness of the lateral-edge front. Other factors will be addressed in a follow-up paper.

In the section on the two-level formation on droxtals, now appendix B.3, we describe the temperatures that these are found and make the connection to the high x_s values measured by Mason et al. (1963) at these temperatures. In this

section and elsewhere, we refer to their finding a temperature-dependence of x_s on the basal face.

Yet, the authors do a rather poor job of characterizing the conditions, temperatures and supersaturations, in the reported experiments. Moreover, in a carefully designed set of experiments (when one varies one of these, for example), it should be possible to see the effect become manifest. I would find such a set of data much more convincing. As a minimum, the authors should do a much better job of describing the conditions for each experiment, and then comparing and contrast the behaviour on the basis of these conditions.

Our reply:

We have included the conditions whenever possible. When they are only partly known, the examples are nevertheless useful to help support the roles of lateral-type growth. For example, in Fig. 1 (old Fig. 2), the main points of showing them are the spreading facets and the pockets. In this case, we give references to other cases with more precisely known conditions. For the case in Fig. 3, we give the temperature, supersaturations, and crystal sizes. For the case in the old Fig. 4 (now Fig. 5), we had the conditions in Appendix A, but now added them in the main text. Conditions were given for the crystal in Fig. 6 (now Fig. 7). We added the conditions in the caption of Fig. 12, but we empasize at the beginning that the behavior being reported occur over a wide range of conditions. This range will be explored quantitatively in a future study. In general, the effects of AST described here will be larger when the mean migration distance is larger than the edge-front or protrusion thickness. These quantities are not known very well, so testing the predictions will require their measurements. Our task here has been to establish that AST occurs and is worthy of further study.

~~Air pockets and secondary habits in ice from l~~Lateral-type growth of ice facets I: observations and applications to secondary habits of snow crystals

Jon Nelson[1], Brian Swanson[2,3]

[1]Redmond Physical Sciences, Redmond, 98052, USA
[2]Earth and Space Sciences, University of Washington, Seattle, 98195, USA
[3]Laucks Foundation Research, Salt Spring Island BC, V8K2E5, Canada

Correspondence to: Jon Nelson (jontne@gmail.com)

Abstract. Often overlooked in studies of ice growth is how the crystal faces grow laterally. This paper reports on observations and applications of such lateral-type growth for vapor-grown ice in air. Using a new crystal-growth chamber, we observed air pockets forming at crystal corners when a sublimated crystal is regrown. This observation indicates that the lateral spreading of a face can, under some conditions, extend as a thin overhang over the adjoining region. We argue that this extension is driven by a flux of surface-mobile molecules across the face to the lateral-growth front. Following the pioneering work on this topic by A. Yamashita, we call this flux "adjoining surface transport" (AST) and the extension overgrowth "protruding growth". Further experiments revealed other types of pockets that are difficult to explain without invoking AST and protruding growth. We develop a simple model for lateral growth on a tabular crystal in air, finding that AST is required to explain observations of facet spreading. Applying the AST concept to observed ice and snow crystals, we argue that AST promotes facet spreading, causes protruding growth, and alters layer nucleation rates. In particular, depending on the conditions, combinations of lateral-type processes with normal growth can help explain presently inexplicable secondary features and habits such as air pockets, small circular centers in dendrites, hollow structure, multiple-capped columns, scrolls, sheath clusters, and trigonals. For dendrites and sheaths, AST may increase their maximum dimensions and round their tips. Although these applications presently lack quantitative detail, the overall body of evidence here demonstrates that any complete model of ice growth from the vapor should include lateral-type growth processes~~Often overlooked in studies of ice growth is how the crystal faces grow laterally. This paper explores the implications of such lateral-type growth and how it may explain air pockets and other secondary features of vapor-grown ice in air. For example, using a new crystal-growth chamber, we observed air pockets forming at crystal corners when a sublimated crystal is regrown. This and other observations support the idea that the lateral spreading of a face, and its (in some cases) extension as a thin overhang over the adjoining region, is driven by a flux of surface-mobile admolecules across the face to the lateral-growth front. Inspired by recent work on this topic by Prof. A. Yamashita of Osaka Kyoiku University, we call this flux "adjoining surface transport" (AST) and the extension overgrowth "protruding growth", then apply the concepts to observed ice and snow crystals, including some from a cloud chamber and others from our experiments. We also suggest that such lateral-type growth may explain other air pockets, droxtal centers in dendrites, hollow terracing and banding, multiple-capped columns, scrolls, trigonals, and sheath clusters. For dendrites and sheaths, AST may increase their maximum dimensions and round their tips. .

1 Introduction

~~### 1.1 Normal growth, primary vs secondary habits, and interior features~~

Both primary and secondary habit depend on temperature and humidity as often portrayed on the Nakaya habit diagram. This diagram has generally remained the same since Ukichiro Nakaya first proposed it (Nakaya, 1954), though some extensions and modifications have come from subsequent studies (e.g., Hallett and Mason, 1958; Takahashi et al., 1991; Bailey and Hallett, 2004; Takahashi, 2014). Concerning the mechanism for these habits, at liquid-water saturation the primary habit likely arises from the temperature dependence of the layer-nucleation rates (Nelson and Knight, 1998), but at the lower supersaturations, defects likely control the primary habit (e.g., Bacon et al., 2003; Harrington et al., 2019).

Secondary features have been observed for a long time, but have seen relatively little study. Wilson Bentley, known for his extensive photo-micrography work, paid much attention to the crystals' interior markings including various air enclosures (Bentley, 1901, 1924). For example, in his 1901 paper, he suggested that these markings and air pockets (enclosures) give clues about the crystal's trajectory, an idea no doubt true, yet both unexploited and unexplained. Later, Maeno and Kuroiwa (1966) examined the patterns of apparent air enclosures in snow crystals, verifying through sublimation and melting that they were indeed enclosed pockets of air and not surface features. More recently, Yamashita categorized 16 types of pockets in tabular crystals (2016, 2019). Several examples of air enclosures in small prisms can be seen in Fig. 1d–f. Studies of other interior markings include those of hollows (Mason et al., 1963) and of ridges and ribs on branch backsides (Nelson, 2005; Yamashita, 2013; Shimada and Ohtake, 2016, 2018). Such features have recently attracted attention because the crystal "complexity" also affects radiative scattering of ice-containing clouds (e.g., Smith et al., 2015; Järvinen et al., 2018).

Although the normal-growth mechanisms, including layer nucleation and defect-driven steps, provide a solid framework for understanding the primary habit and other crystal features, many secondary habits remain inexplicable. In addition to the air pockets, these other habits include i) the small spherical form at the center in many dendritic snow crystals, ii) the thin basal planes in capped and multiple-capped columns, iii) the abrupt bending of thin prism planes in scroll crystals, iv) the structure of sheath clusters, and v) trigonal crystals. Can lateral-type growth processes help explain these forms? We argue here that they can, and thus should be included in any complete ice-growth model.~~Research on ice-crystal growth from the vapor usually focuses on the rates and mechanism of growth normal to the basal and prism faces (e.g., Takahashi et al. 1991). The rates are sometimes called the linear growth rates, but to help distinguish normal from lateral growth, we use the other common term, the normal growth rates. These rates determine the crystal's maximum dimensions and aspect ratio, thus defining the primary habit. But ice and snow crystals usually have more complex shape features, such as hollows and branches, known as the secondary habit (e.g., Kikuchi et al., 2013). These features have recently attracted attention because the crystal "complexity" affects radiative scattering of ice-containing clouds (e.g., Smith et al., 2015; Järvinen et al., 2018).~~

~~Although normal-growth processes, including the various growth mechanisms, provide a solid framework for understanding the primary habit and some other crystal features, several common secondary habits remain inexplicable. These puzzling habits~~

The most widely used model for the growth of crystal faces from the vapor is the BCF model (Burton et al., 1951; Woodruff, 2015). This model supposes that a given molecule in the vapor above a faceted surface strikes the crystal surface and becomes temporarily trapped in a mobile state until either desorbing back to the vapor or migrating along the surface and reaching a more strongly bound state at a step edge. Individual steps are abrupt changes in surface height, generally just one or two crystal layers, a height much less than their separation and thus the face appears flat.

As a source of step edges, BCF and later studies considered layer nucleation and defect-generated steps, most commonly spiral-step sources. The former has been argued to be the main source for ice-crystal growth from the vapor under most atmospheric conditions (e.g., Knight, 1972; Nelson and Knight, 1998), but not for many other crystals (Frank, 1982). Under relatively low supersaturations, defect-generated step sources usually dominate. Once a step is generated, the flow of molecules to the step edge causes it to sweep across the macroscopically flat facet (or face, the terms used interchangeably here). When one step sweeps past a given position, that point on the face has advanced normally by the step height, and thus the frequency of the sweeping steps gives the normal growth rate. Normal growth rates are thus proportional to the step-generation rate. In contrast, non-flat surface regions are said to be "rough" and grow at the maximum rate allowed by the rate of impingement of vapor molecules. Such growth is called continuous growth, with individual steps close together compared to their height. In ice growth from the melt, continuous growth dominates for non-basal orientations, but for vapor growth, all thick surface regions leading growth are usually facetted. Individual steps, and steps clumped into macrosteps, instead tend to have a rough edge.

The BCF model of surface diffusion assumes that the mobile surface molecules are sparse and non-interacting. For ice, this assumption is widely believed to be violated over much of the atmospheric temperature range where the surface is thought to contain significant disorder (e.g., Rosenberg, 2005). Yet the BCF model is nevertheless often used to interpret experimental results (e.g., Sei and Gonda, 1989; Asakawa et al., 2014). A key parameter in the model is the mean migration distance x_s of a mobile molecule on the surface before desorbing, a distance that should differ between the basal (***b***) and prism (***p***) faces as well as depend on temperature. With interactions between these surface-mobile molecules (e.g., Myers-Beaghton and Vvedensky, 1990), x_s may also depend on supersaturation. In addition, the migration of surface vacancies may also affect x_s (Frank, 1993). Experiments reported in the 1960s indicated that x_s on the basal face varied dramatically with temperature, changing by a factor of 5–7 between about −7 and −12 °C (Mason et al., 1963; Kobayashi, 1967). Although the exact values of x_s may be disputed, both studies independently found the values to be largest in the tabular regime, smallest in the columnar. Corresponding values for the prism have not been determined. Later, Nelson and Knight (1998) found a similarly sharp behavior in basal-face critical supersaturation between these temperatures. A possible link between these two parameters is clustering of the mobile species responsible for growth: when the temperature is such that clustering is strong, the critical supersaturation is low and surface-mobile molecules would become temporarily trapped in sub-critical nuclei, giving them very low mobility. Thus, the critical supersaturation would be low when x_s is low and vice-versa as found by experiments. The values of the measured critical supersaturations led Nelson and Knight to conclude that the surface was indeed disordered but " ...the view of the ice surface as a liquid layer is not a useful idealization for crystal growth processes." Hence, at least as a first approximation, it is still useful to compare observed behavior of ice to the BCF model and make use of measured x_s values.

A second simplification of BCF is the assumption of a uniform vapor density. This condition should hold in a pure vapor, but not for ice growth from the vapor in an atmosphere of air. Gilmer et al. (1971) showed that an exact treatment predicts vapor-depleted air immediately adjacent to a step edge, slowing the crystal growth rate over that of BCF, but the exact calculation is difficult for a 3-D polyhedral crystal such as that for ice (Nelson, 1994). Instead, atmospheric ice models usually assume a locally uniform vapor near the step source. As the crystal shape presents a greater modeling challenge, recent work has focused less on the exact surface model than on the modeling of more realistic crystal shapes (e.g., Wood et al., 2001).

Atmospheric ice crystals generally begin with the simplest of shapes—a solid ice sphere, also called a droxtal. The droxtal forms when a droplet freezes. That freezing is a crucial first step for atmospheric ice was greatly supported by the extensive cloud studies of Hobbs and Rangno (e.g., Hobbs and Rangno, 1985). This two-step process of vapor-to-droplet then droplet-to-ice, instead of direct vapor nucleation to ice, is thought to prevail because the nucleation rate is exceedingly sensitive to the

interfacial surface energy, with the surface energy for the liquid–vapor case being lower than that for the ice–vapor case (e.g., ten Wolde and Frenkel, 1999).

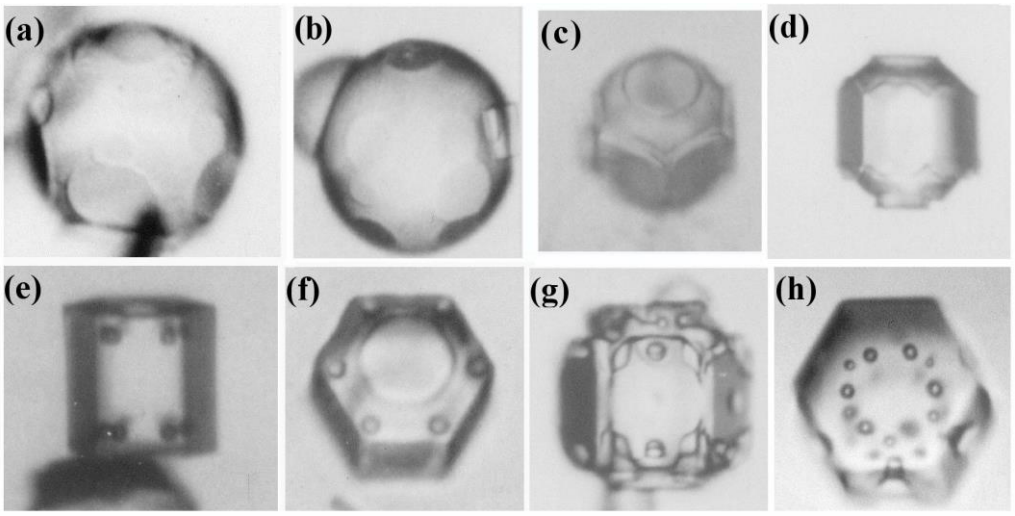

Figure 1: Crystals at different stages between large droxtals (just-frozen droplets) and prisms at temperatures between −6 and −12 °C. Top row shows initial development of basal and prism faces, with some pyramidal faces in (a) and (b). Bottom row shows filled-out faces with corner pockets in (e) and (f). In (g) and (h), pockets appear where pyramidal faces may have hollowed before being overtaken by basal and prism faces. Sizes are within 45–90 µm. (From a cloud chamber, courtesy of A. Yamashita.)

After the ***b*** and ***p*** faces fill out, the crystal is more easily described by its normal growth rates N_B and N_P, though the faces are also growing in area. This type of lateral growth is a standard aspect of polyhedral growth, so we refer to it as "S-type", but we focus on the F- and P-types (described next). During the facet-spreading phase (b), normal growth may also be occurring, but surface-mobile molecules on the relatively small facet are already close to the molecular sink at the lateral-growth front e–c. Thus, nucleation of new growth layers will be greatly impeded until the facet radius m–e exceeds the surface migration distance x_s. Also, if x_s and radius m–e both exceed the thickness e–c, then this AST flux may lead to a lateral growth rate F that is much greater than the normal rates N due to the relatively large molecular collection region on the facet.

Under some conditions, the facet spreading may produce an overhanging planar extension. Following Yamashita (2014), we call the growth of this planar overhang "protruding growth" or "P-type", marking it "P" in Fig. 2b'. Here, the lateral-edge front e–i extends over the inside corner c, becoming narrower than the case in Fig. 2b. The thickness of this edge-front should depend on how far surface-mobile molecules can migrate on the rough edge. If this length-scale is l_r, then the edge thickness should be of order l_r and less than x_s for P-growth. This length-scale has not been studied, so we will not analyze it further except to note that the high-density of growth sites on a rough edge compared to that on a facet would suggest that $l_r << x_s$. Such P-growth from two intersecting faces, such as ***b*** and ***p*** in Fig. 2c', produces a pocket. The examples in Fig. 1e,f show pockets in the corners, which likely formed from the intersection of three protruding faces. The pockets in Fig. 1g are less clear, but the pocket may be due to

Formatted: Normal

protruding growth from opposing directions on the pyramidal face. This image also seems to show thickened protrusions at the four corners of the front prism face. The case in Fig. 1h seems to show both sets of pockets (i.e., both cases f and g).

~~normally, such as through direct vapor deposition. But lateral growth can also occur when there is no adjoining facet. We focus here on this latter, more interesting, case. Specifically, we assume the growth front for this lateral growth is a relatively small adjoining area at the face perimeter.~~

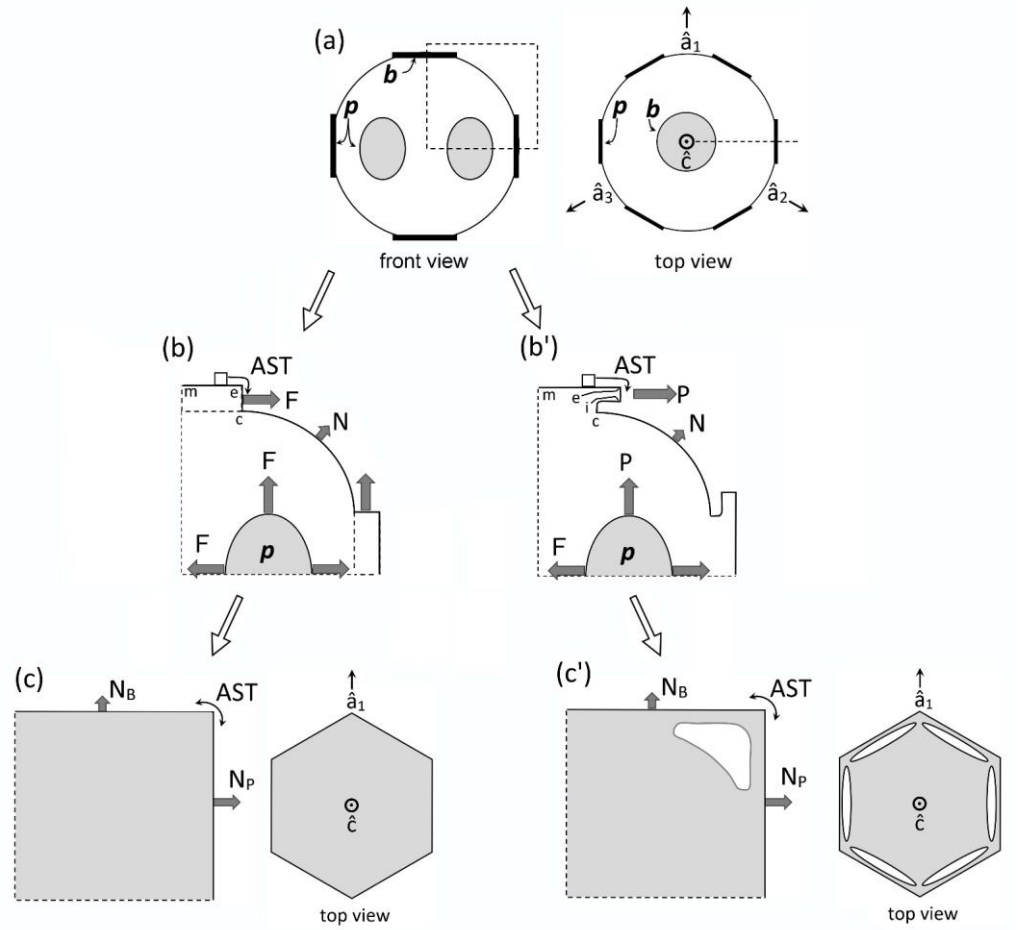

Figure ~~1~~2: Concepts of lateral-type growth **(F, P, S)** for the~~,~~ droxtal-to-prism transition, driven by AST. (a) Droxtal ~~front view showing~~with small ~~small~~ basal ***b*** and prism ***p*** faces. Front view at left shows four prism and both basal faces. The top view at right shows all six prisms and the crystallographic directions of the c-axis ĉ and the a-axes â. (b) Upper-right quadrant of (a) in dashed box, front view. ~~Lateral growth~~ Facet spreading ~~L~~**F** on top basal and ~~right side~~two prism faces largely driven by adjoining surface transport AST. Normal growth **N** occurs on rough regions between faces (continuous growth). m is the middle of the facet. (c) Filled-out basal and prism faces. AST continues, likely with net amount to faster-growing face. Top view shows crystallographic directions. (~~d~~b') ~~Different case following~~Like (~~a~~b), ~~instead~~ except having protruding growth **P** between basal

and prism faces. e–i is the new lateral-growth front. (c') Like (c), except with air enclosure. After (c) and (c'), standard lateral growth (**S**-type) occurs due to normal growth of adjoining faces on a fully facetted crystal.

Concerning the conditions needed for such droxtal pockets, the size of the droxtals may be important. In the cases shown here, the radii are all above 22 μm. In the figures of Gonda and Yamazaki (1978, 1984), the droxtals have radii of about 10 and 15 μm, yet do not reveal any pockets upon filling out. Their study examined droxtals at −7 and −15 °C with air present and supersaturations from 1–2% (1984 study) to water saturation (1978 study). Thus, the overhanging aspect of P-growth may require a larger-area rounded region as occurs on a larger droxtal. If x_s depends on temperature as experiments suggest (Mason et al., 1963) or if l_s depends on temperature, then droxtal pockets should also depend on temperature. Both quantities may also decrease with increasing supersaturation.

The F- and P- types of lateral growth here are driven by AST. Evidence for AST on ice is indirect, partly coming from early studies of spreading ice layers on covellite (Hallett, 1961; Mason et al., 1963, Kobayashi, 1967). In these studies, the rates of approaching micron-scale layers, also known as macrosteps (arising from clustering of smaller steps or contact between crystals of differing height) changed in a way consistent with a flux of molecules over the top edge of the layer. The AST concept has long been applied to the growth rates of metal whiskers (e.g., Sears, 1955; Avramov, 2007), but rarely applied to ice. More recent experiments on ice find evidence for the flux over the tops of much thinner layers (Asakawa et al. 2014). In both the macrostep cases (Kobayashi, 1967) and in many other observations of thinner layers (e.g., Gonda et al., 1990; 1994), the step-front is rough, or rounded. The cause of this rounding may be the thermal roughening proposed by Frenkel (1945) and BCF (1951), but may also involve other processes and apply to the growth-front of F- and P-growth.

For applications, earlier studies applied the concept of AST to the primary-habit change. Mason et al. (1963) considered it the main factor driving primary habit, but the specific mechanism has been criticized because it does not consider the role of critical supersaturation on the nucleation of new layers. Frank (1982) argued instead that AST should make the change of primary-habit with temperature more abrupt due to layer nucleation on one face hindering nucleation on the adjoining face. Yamashita (2015, 2016, 2019) has revived the general concept, expanding its applications to secondary features via lateral and protruding growth.

Finally, to help clarify subsequent discussion, we use the following definitions:

- **Lateral-type growth** = areal growth on fully facetted faces, includes S-, F-, and P-types.
- **Standard lateral growth (S-type)** = areal growth of a facet bound by other facets, determined by their normal growth.
- **Facet spreading (F-type)** = areal increase of a facet on a rounded surface, driven mainly by AST.
- **Protruding growth (P-type)** = extending growth of thin, usually planar, face region that extends over adjoining regions, driven mainly by AST.
- **Adjoining surface transport (AST)** = surface transport of mobile molecules from a face, over the edge of the face, to the adjoining region where the growth occurs.

~~But in some cases, the AST flux plus the direct vapor flux does not completely fill out region **e**–**c**, and so the face extends as a thin planar overhang as shown in (d). Following Yamashita (2014), we call the growth of this planar overhang "protruding growth". With protruding growth **P**, the prism may incompletely fill out following the sequence (a), (d)–(f). The result of this protruding growth is an air inclusion, or pocket. The AST likely continues after the facets fill out, with the net flux possibly going in either direction as sketched in (c).~~

For this work, we used a new crystal-growth apparatus, hereafter CC2, that improves upon the capillary method in Nelson and Knight (1996). Like that apparatus, the observed crystal hangs pendant on an ultra-thin glass capillary within an isothermal,

Formatted: Bullets, Space After: 0 pt, No bullets or numbering

stagnant atmosphere. But in CC2, the ambient supersaturation around the crystal is controlled by the surface temperature of one of two vapor-sources in its own adjoining chamber, the connection of which is controlled by a translatable valve stopper. With this system, we can grow and then sublimate a given crystal without changing the temperature surrounding the crystal. The temperatures of the vapor-source surfaces are controlled by a thermoelectric element below each vapor-source container. The block encasing all three chambers is made of gold-plated, high-conductivity Te-Cu of dimensions 3" x 5" x 7" and submerged in optically clear cooling fluid pumped with a Neslab ULT-80 circulating cooler. To start an experiment, we insert HPLC water into the vapor-source containers and the capillary. The source water and capillary are cooled to the desired temperature and frozen. We then monitor the crystal at the capillary tip using back illumination and a full-frame DLSR 24-megapixel tele-microscope-camera system in the front. For more details of this apparatus and method, see Swanson and Nelson (2019).

We report here images collected from CC2 during their growth as well as images of crystals grown by AY in a cloud chamber~~collected post-growth in sub-zero silicone oil by AY~~. The latter crystals were nucleated at the top of a tall (15-m) cloud chamber (Yamashita, 1971), ~~and~~ fell while growing for about 3–4 minutes under relatively uniform conditions, and then collected post-growth in sub-zero silicone oil. Although they provide only a snapshot of a crystal's growth, the high-magnification imaging provides greater detail of the early growth stages as well as growth at higher supersaturations, thus complementing our CC2 results. Other crystal images were provided by Mark Cassino, ~~and~~ Martin Schnaiter, and Art Rangno.

The following subsections ~~is more a~~ survey ~~of topics than detailed analyses of a given crystal feature~~observations made in CC2, including previously unreported "corner pockets", "planar pockets", and "elongated edge pockets". ~~As such, most subsections largely stand-alone with few references to others. Observations of lateral growth and various air pockets comprise most of the first 10 subsections. Specific habits are examined in §3.12, 3.14, 3.16–3.19, and 3.21. Lateral-growth theory is in §3.15 and the appendices.~~

~~**3.1 Lateral growth and corner pockets in droxtals**~~

4.1.1 Observations

Formatted: Heading 3

In our CC2 experiments, we observed the appearance of 12 small pockets, one in each corner, after a thick prism crystal resumed growth after a period of sublimation. The crystal, shown in Fig. 3, remained at −29 °C with a supersaturation that began at about 0.5%, then spent less than an hour at a small negative value, then went back to about 0.5%.

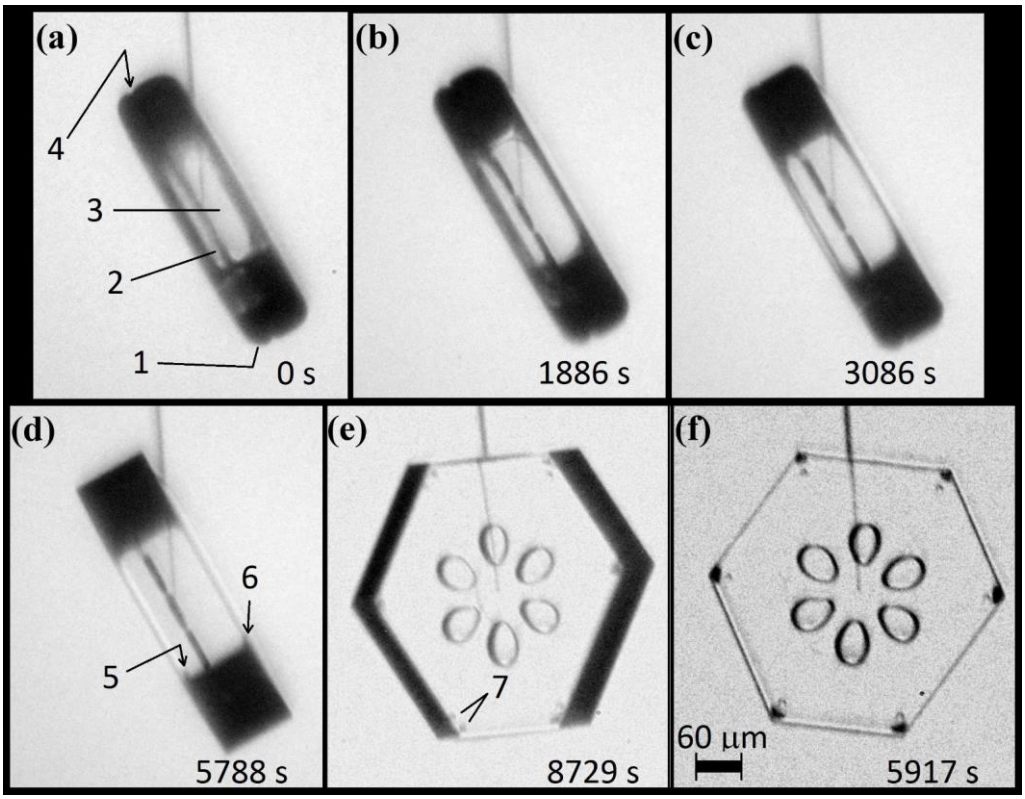

Figure 3: Corner-pocket formation at −29 °C after sublimation rounding. (a) Side-view of crystal at end of sublimation run. Marked point 1 shows a rounded basal-prism corner; 2, side view of interior planar air pockets; 3, view through two prism faces showing curved bounding edges (evidence from lack of sharpness); and 4, a perimeter groove bounding the same interior basal plane as the interior air pockets. (b)—(e) Subsequent sharpening of the basal-prism corner under growth conditions. Marked points 5 and 6 appear to show side views of the corner pockets. (e) The basal face partly turned into view, showing a corner-pocket pair near each prism–prism edge at 7. (f) Front view showing the 12 corner pockets (two pockets per prism-prism edge, each pocket near opposing basal faces). Line coming down from the top is the capillary, terminating in the crystal at the nucleation point.

Consider the sequence in more detail. Figure 3a begins after the sublimation, just as the growth condition has returned. The lack of sharpness viewed through opposite prism faces ~~in (a)~~ shows that the faces retain some curvature. At the edge, the rounding appears to have a radius of about 30 µm. As time elapses in (b)–(d), the boundaries sharpen, becoming fully facetted in (e) and showing six pairs of pockets near the corners in (f). The slightly rotated view in (e) shows that each pair consists of one pocket near each basal face (top and bottom), and these pockets may be barely discerned even in (d) at "5" and "6". This particular cycle is the second one we imposed on this crystal, but it shows the corner pockets more clearly than the first growth-sublimation sequence on the same crystal.

The corner pockets in this case occurred on a tabular crystal, but the tabular shape is not crucial to the pocket formation. In ~~another~~ a case we consider later for a different phenomenon, we had 10 crystals of various aspect ratios, including a long column, ~~on three capillaries~~ all undergo a growth–sublimation–growth cycle, and all exhibited the corner pockets~~.~~ (e.g., on the

nearly isometric crystals of Fig. 12b,d). All of the cases though have been on large crystals (~200–400 μm) at a temperature near −29 °C. In previous experiments (Nelson and Knight, 1998), we grew, sublimated, then grew crystals that were about 10x smaller (~15–40 μm) and at temperatures above −15 °C, yet never observed corner pockets. The literature shows cases that were not recognized as corner pockets. For example, similar corner pockets appear on a ~100 μm crystal studied by Kobayashi and Ohtake (1974) above −20 °C after a sublimation cycle. In that case, the radius of curvature at the corner was about 20 μm, but they show another case without corner pockets in which the corner radius was only about 10 μm. Also, Magono and Lee (1966) show a solid, thick plate (photo #30) with corner pockets. In this case, the crystal was about 150 μm across with a curvature at the corner near 20 μm adjacent to the upper basal. Near the lower basal, the curvature appeared a little smaller and the corner pockets were smaller. Thus, although the phenomenon can appear on a range of crystal shapes, it may require that the corner radius exceed a certain value. At about one atmosphere pressure and temperatures near −20 and −30 °C, this critical radius may be between 10 and 20 μm, but the value may depend on temperature and pressure.

4.1.2 Basic mechanism

Existing views on normal growth via step motion cannot readily explain corner pockets on fully facetted crystals. With normal growth, each pocket must have at one time been a hollow (lacuna or concave feature) before closing-off to enclose the air. And standard hollowing theory (e.g., Kuroda et al., 1977; Frank, 1982; Nelson and Baker, 1996) predicts that hollows form around a local vapor-density minimum, not at a corner where the driving force for normal growth is instead a local maximum. Moreover, the standard theory relies upon step clumping on a facetted surface. We argue here that the pockets instead form via protruding growth adjacent to a rounded corner, similar to that in Fig. 2b',c'. But unlike the droxtal case, the rounding here came from sublimation.

Consider the stages in Fig. 4, with an oblique view at left and a cross-section through a corner at right. In (a), the crystal is a thick prism and fully facetted, representing a growth condition. In (b), the crystal has transitioned to a sublimation condition, thus rounding its corners and edges. Then, in (c), a growth condition resumes, causing the basal and prism facets to grow laterally, primarily via AST over the spreading edge-front where they bond. As the spreading edge becomes thicker (viewed in cross-section), this rate will slow because the same number of molecules must spread over a wider front region. This growing front becomes too wide in (d), and the AST flux of molecules builds up an overhang on the spreading facet edge, initiating protruding growth. Where the protrusions from two faces intercept, they merge, halting further protrusion there. This merging occurs first further back along the edge from the corner, but progresses to the corner at (e), sealing-off the corner pocket. Later, sublimation and deposition within the sealed-up pocket will round out its interior, making the pocket more spherical. This mechanism does not include normal growth because normal growth in the experiment was extremely low.

The case in Fig. 3 shows six dark corner pockets on one basal, six lighter pockets slightly further inside (radially) on the other basal. This difference may have arisen from having different degrees of initial rounding, or by one basal face having more basal-normal growth than the other. The side views show how the planar pockets are closer to the left basal face, indicating both that the left-side rounding may have a smaller radius and also that the right basal face has a greater normal growth rate. Further considerations of how normal growth may affect pocket formation is in §4.6.2.

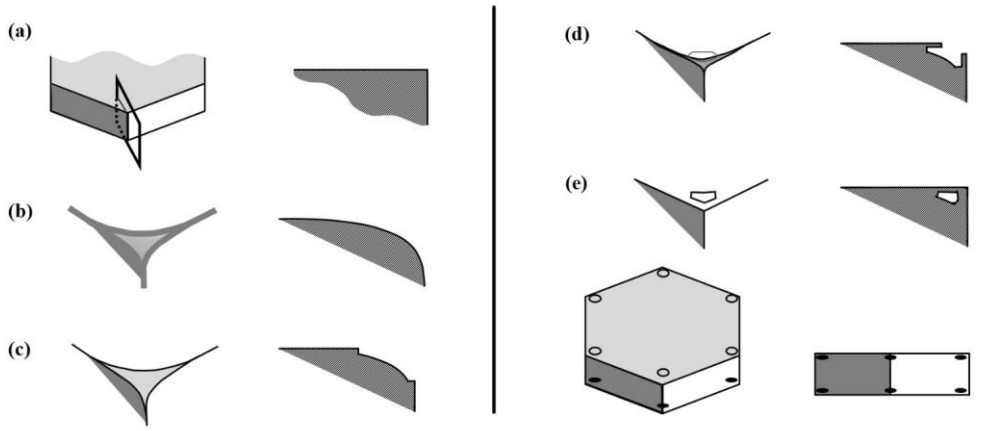

Figure 4: Corner-pocket formation after sublimation rounding. (a) Oblique (left) and cross-section (right) view of edge of a tabular crystal during growth. The top face is basal, the sides are prism. (b) Same views after net sublimation rounded the edge. (c) After growth conditions resume. Basal and prism have facet-edge fronts (same as Fig. 2b). (d) Protruding growth begins. (e) Corner pocket forms. Overall oblique and front view at bottom.

~~3~~4.~~3~~ 2 Planar pockets formed under constant conditions

The crystal in Fig. 3 exhibits another notable feature—its six thin, petal-shaped pockets. These "planar pockets" appeared well before the formation of the corner pockets, and did not require a sublimation event before formation. From the front (f), they appear typical of common center hollows (i.e., formed in face centers) that later closed up, but the side view (d) shows them to be unusually thin, or planar. In (a), the planar pockets appear to be in the same plane as the small notch marked "4". The notching suggests a disordered region, like the eroded region at the grain boundary near the center of bullet rosettes. However, the prism planes align on both sides of the notch, showing both sides have the same crystal orientation. Thus, the notch and plane must have a stacking fault, not a grain boundary, with the depth of the pockets suggesting that a region of faults may be present. Itoo (1953) called such crystals "twin prisms", and found them to be very common in a light precipitation at −30 °C. Kobayashi and Ohtake (1974) made a similar observation to that here, suggesting a specific type of stacking fault. A more recent study found that extended regions of stacking disorder are common when small water droplets freeze near −40 °C (Malkin et al., 2012), but are unlikely to form during vapor growth (Hudait and Molinero, 2016). The crystal of Fig. 3 began with a freezing event at the tip of the capillary, where the apparent stacking-disorder region intercepts, and then grew from the vapor. Thus, the argument for the source of the notch and planar pockets is consistent with these recent studies.

Another distinctive feature of these pockets is their near-perfect six-fold symmetry. Such symmetry of both the pockets and the crystal is unusual for a crystal grown at such low supersaturation. ~~A r~~Reasons for their symmetry and their closing-off ~~is~~ are given in ~~§3.11~~Appendix B.2.

4.3 Facet spreading on the basal face

4.3.1 Observations

Formatted: Heading 3

In some crystals, we can observe the spreading of the basal facet when the partly sublimated crystal begins to grow. For example, the sequence in ~~Fig. 4~~Fig. 5a–e shows an expanding ring on the basal face. The temperature was about −30 °C and from (b) to (f), about 1% supersaturation. When this ring reaches the perimeter, the crystal appears fully facetted and the corner pockets appear (arrows in (e)). Thus, the rings mark the expanding boundary of the basal face (as opposed to a macro-step on a growing face). The positions of these rings are marked in (f), with the time interval (units of 5 min) between marked positions in the upper right. The markings show a significant slowdown as the facet perimeter approaches the crystal perimeter, and in this process, the facet perimeter becomes more distinct. The latter observation is consistent with a thicker height difference *h* between the rounded surface and the facet upon reaching the perimeter, consistent with having a rounded edge, and lateral growth driven by AST. Also, one can see that the prism–prism edges appear to sharpen by (d), before the basal face fully spreads out. We ~~can see~~saw similar behavior in ~~our next case~~other cases.

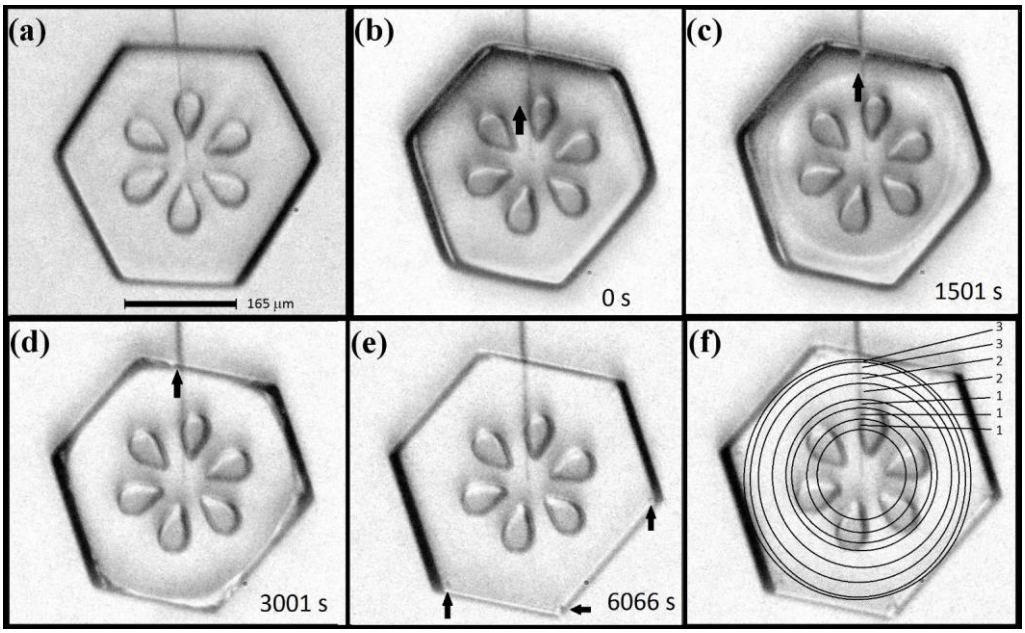

Figure 45: Expanding basal facet with corner pocket formation. (a) Crystal just before sublimation. (b)—(e) Same crystal, during a second growth period, just after the sublimation period. The thick arrow marks a barely visible boundary of the basal facet, roughly forming a circle. In (c), two such circles can be seen, representing the boundaries on both basal facets. The times of the images are in their bottom right corner. In (e), the arrows mark the corner pockets. (f) Same image as (e), but with the estimated basal perimeters sketched with circles. Numbers at right are the times between the perimeter sketches in units of 5 minutes. Data is plotted in ~~Fig. 5~~Fig. 6.

4.3.2 Test of AST-driven facet spreading

Formatted: Heading 3

To test the AST-driven ~~lateral growth explanation~~facet-spreading mechanism, we ran ~~several~~ calculations ~~involving~~ for three ~~models for the~~possible mechanisms of lateral growth. Results are in Fig. 6. The first model, marked ~~(~~I~~)~~, is normal growth of the

lateral-growth front (i.e., **e–c** in Fig. 1b) driven by direct vapor flux. This case shows a resulting advance about two-orders of magnitude too slow. Also, the trend, which can only be seen with a much higher supersaturation (not shown), does not capture the slowdown that begins within about 1000 s of the start. Model II is the AST-driven case, and this fits the data well provided that the calculation uses the inset trend of h/x_s (normalized height of lateral-growth front). This profile of the growth-front height h is difficult to compare to the crystal, as it requires frequent side views of the crystal that we did not obtain, but it is a reasonable fit to the initial cross-section profile. This profile is that of a flat facet out to a radius $r < a$, and a curved profile between r and a where the crystal had rounded during sublimation. (Refer to Fig. A1 for further details.) A reasonable estimate of height h upon reaching the edge is 1–5 μm. With this range, the fit in Fig. 6 (inset) predicts $h/x_s = 0.3$, giving $x_s = 3$–17 μm at this temperature, which is comparable to the value of about 2 μm found by Mason et al. (1963). Model III is an approximate rate based on normal growth of the rough region beyond the lateral-growth front. It does not fit the data well, but is better than case I. Also, case III is sensitive to the profile of the rough region. Thus, the failure to fit the curve may be partly due to profile inaccuracy. Appendix A has details of all three model calculations. A better test of the lateral-growth mechanism requires better data, such as interferometry data (e.g., Shimada and Ohtake, 2016) and possibly a model that includes processes in both mechanisms II and III.

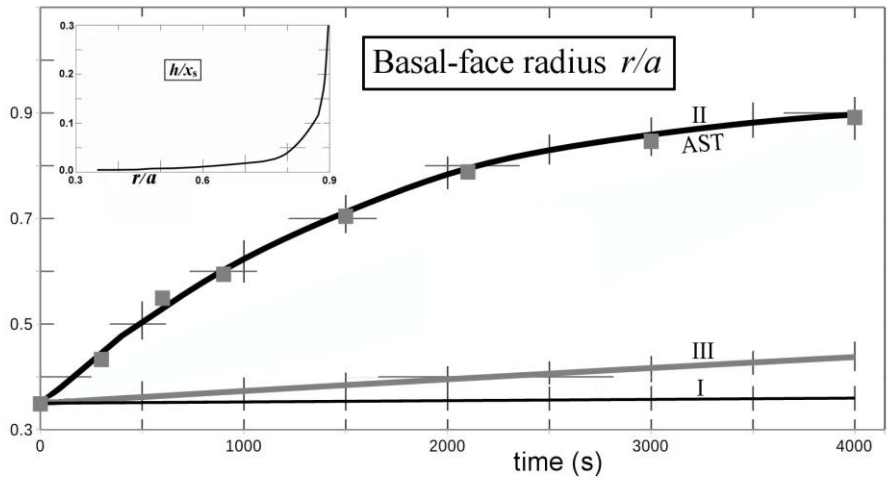

Figure 6: Facet spreading of basal from Fig. 5 (solid squares) with model fits I–III from Appendix A (curves). (I): Normal growth of the facet edge. (II): Facet spreading from AST. (III): Normal growth of the rough, rounded region. Assumed supersaturation of 1% and temperature of −30 °C. Calculation details are in Appendix A. The radius a is the mean value out to the prism–prism edge. Hatch marks are truncated gridlines. Inset plot shows values of facet-edge height h used in the fit for case II, x_s is the surface migration distance.

Nevertheless, the observed behavior ~~is consistent with~~clearly shows that mechanisms I and III cannot explain the observed facet spreading. Only growth ~~being~~ driven by a flux of surface mobile molecules, the AST mechanism, from the facet to the lateral-growth front is capable of fitting the observations.~~. Also, one can see that the prism–prism edges appear to sharpen by (d), before the basal face fully spreads out. We can see similar behavior in our next case.~~

~~3~~4.5~~.~~4 Corner pockets on a non-symmetric thick plate ~~and on naturally formed crystals~~

In another case, we ran a growth–sublimation–growth cycle on a tabular prism at −30 °C with unequal prism faces. In this case, shown in ~~Fig. 6~~Fig. 7, the initial crystal in (b) is more rounded than that in the previous case, with a radius of ~30–40 μm. After regrowth (supersaturation below 1%), the facetted crystal emerged with larger corner pockets that are elongated along the edges (e). And, as with the previous case, the spreading of the basal facet slows down upon nearing the edge in (b) to (d). Later in the growth, in (e), a large basal hollow appears. But the larger size of the corner pockets in this case compared to those in the cases in Figs. 3 and 4 is consistent with the pocket size being larger for cases with larger initial corner radii.

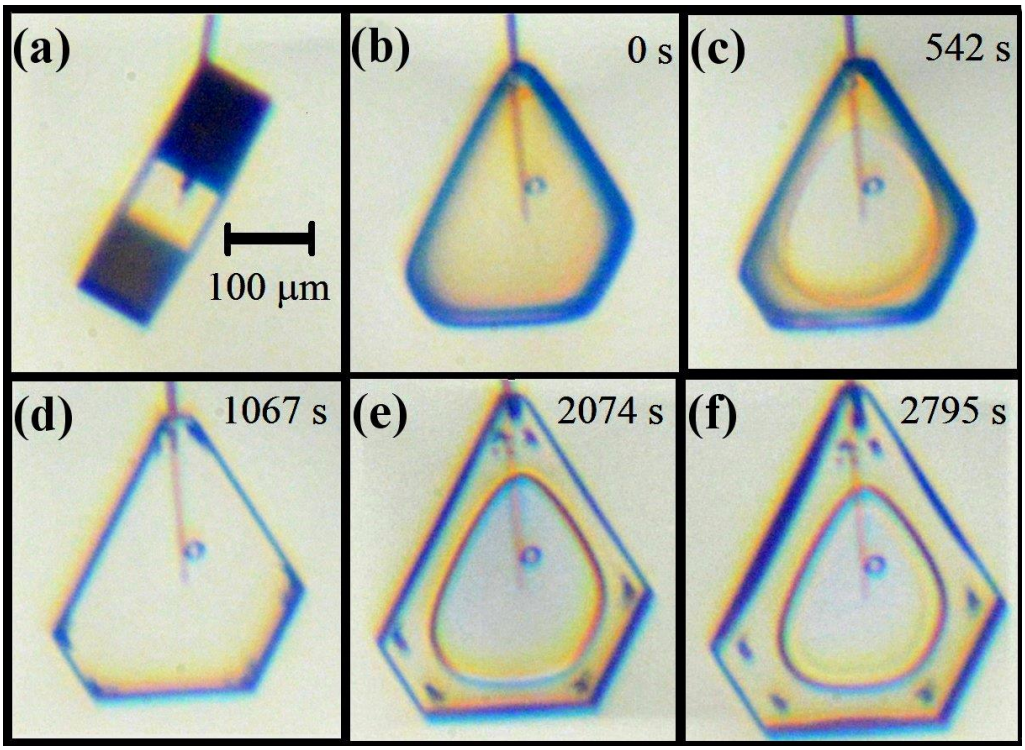

Figure 7: Corner-pocket and center hollow formation and changes on a non-symmetric crystal. (a) About 2 h before sublimation. (b) Immediately after sublimation, growth period starting. (c) Basal facet spreading. (d) Clear corner pockets formed. (e) After normal growth, a center hollow on one basal and on top prism. (f) Further growth, some hollowing starting on wider prism faces.

4.5 Corner pockets on naturally formed crystals

Formatted: Heading 2

Corner pockets such as those described here also appear on natural snow and ice crystals. The center of the snow crystal in ~~Fig. 7~~Fig. 8a, collected and photographed at the ground, shows pockets "CP" in the corners of the central plate. Case (b) shows apparent corner pockets in a thin, solid tabular prism collected in-cloud. In (c), we see six pocket pairs near the center of another collected snow crystal. ~~This case is not as clear as~~The mechanism in this case may differ from that in (a) because they appear on a two-level crystal. We also show other pockets further up a main ridge in the smaller inset at bottom. Thus, these do not appear to be the same corner pockets that we have discussed above. This type is discussed later, in ~~§3.13~~Appendix B.4. For the cases in (a) and (b), we conclude that the crystals ~~may have~~likely underwent~~gone~~ a sublimation period to produce the corner pockets.

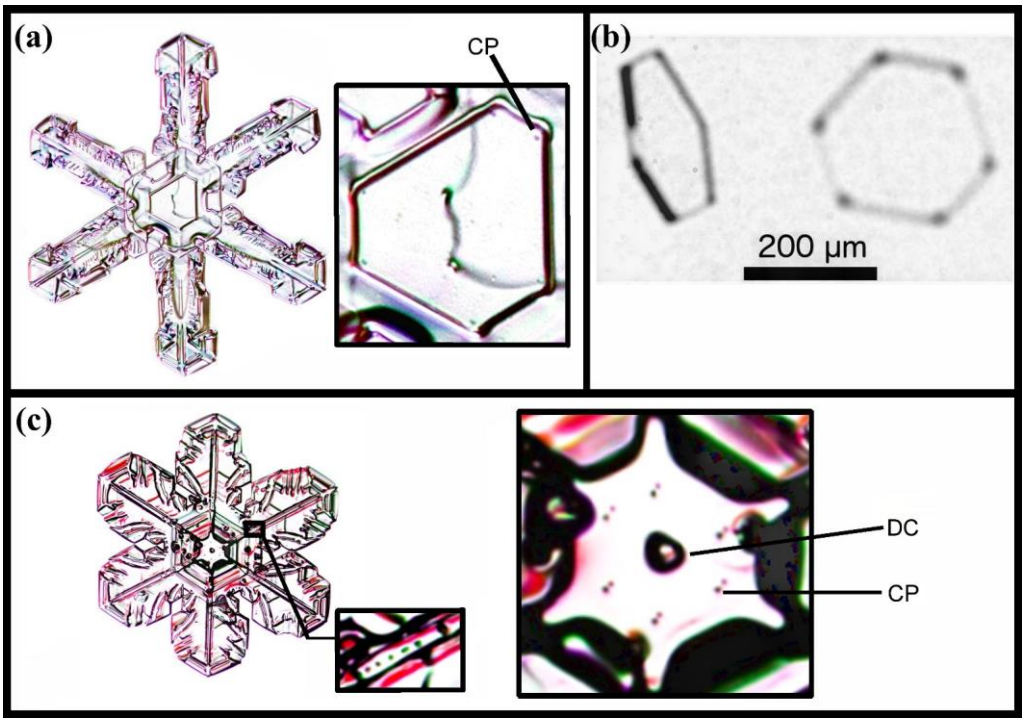

Figure ~~7~~8: Corner pockets (CP) and droxtal centers (DC) on natural snow and ice crystals. (a) A narrow broad-branch crystal. (Curved line through crystal center is an imperfection on the glass slide.) (b) Crystal collected on the SOCRATES mission at -24.9 °C, viewed at two angles. Image courtesy of Martin Schnaiter. (c) Case of a wide broad-branch, large inset at right showing a close-up of center, small inset shows pockets along one ridge (nearly identical to pockets along the other five main ridges). Snow crystal images in (a), (c) courtesy of Mark Cassino.

~~**3.6 A basic mechanism of corner-pocket formation**~~

4.6.1 Observations

Formatted: Heading 3

The corner pockets can vary in size and shape, with those in ~~Fig. 6~~Fig. 7 being larger and longer along the edge than those in Figs. 3 and ~~4~~5. This elongation can extend along the edge, traversing nearly the entire edge. The example in Fig. 9 ~~also~~ involves a more complex crystal than the previous ones~~, with interior edges~~. It begins from a sublimated, rounded form at 0 s. After 180 s, small prism facets started to appear (not shown). These facets grow both normally and laterally as the other facets become defined. At 541 s, the edge at 'A', as well as the edges of face 1, extend slightly above the plane of the adjacent faces. By 1083 s, some normal growth can be discerned. From 1444 s, the two opposing edges of faces 2 and 3 become clear, and these edges approach each other at 'C' (2138 s)~~at later times~~, appearing to be facets. These two facets completely merge~~ing~~ before 8448 s. Later, the final front and side view shows that this edge region has a long pocket along this prism–prism edge marked 'E'. Thus, the merging of two lateral-growth regions created an elongated edge pocket between prism faces. As this is the only case we observed, we do not know if the complex nature of the crystal was essential or the greater amount of normal growth than those in the previous cases. Below, we suggest a mechanism involving S-type and P-type lateral growth.

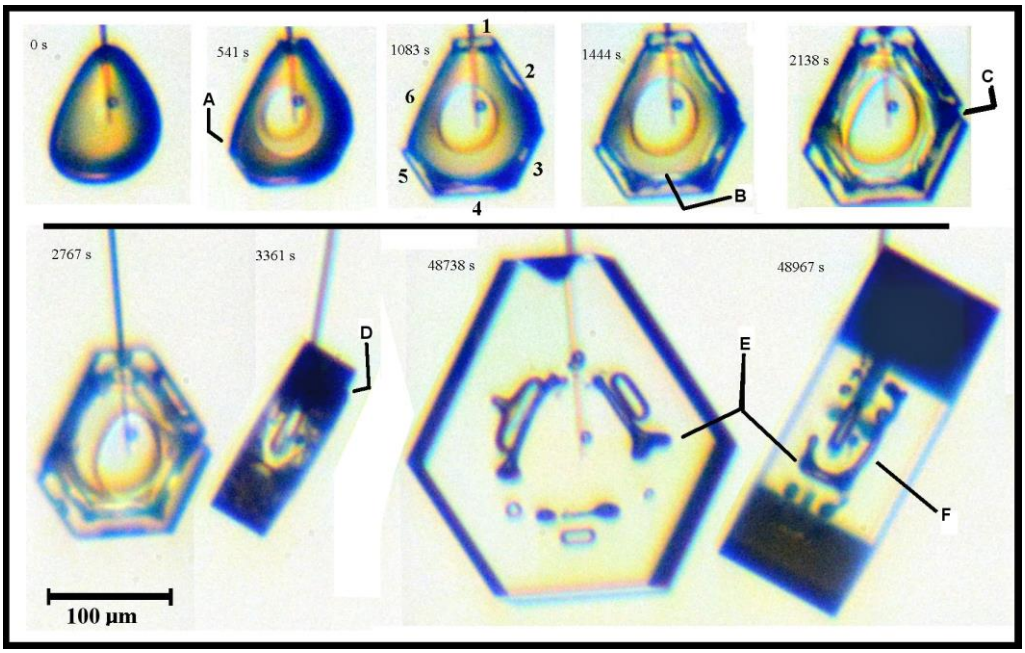

Figure 9: Elongated edge pockets and lateral face growth on a complex crystal growing under constant conditions. Time 0 s is just after sublimation, the crystal just starting to grow. At 541 s, **A** marks the edge of prism face 5, growing laterally over face 6. The prism faces are filled out by 1083 s and numbered clockwise from top. Face 5 growing laterally over face 6. The **B** at 1444 s shows a boundary with straight edge. **C** at 2138 s shows two adjacent prism faces closing up via lateral growth (completed before 8448 s, leaving an elongated edge pocket). At 3361 s, **D** marks an interior edge of a thick layer on the bottom basal face. **E** marks two views of an edge pocket between prism faces (same as that tracked by **C**). **F** is an elongated edge pocket between the bottom basal face and prism face 2.

Such merging of straight-edged sections may be occurring on the basal face as well. By 1444 s, dark regions appear along basal-prism edges, suggesting that the corners are connected by long pockets. Such an edge pocket is confirmed and marked 'F' in the final side view. However, unlike the prism–prism-edge case, the lateral growth involved in this feature's formation is unclear. Standard S-type ~~The~~ lateral spreading of a thick layer on the old basal face, with edge boundaries parallel to the basal ~~–~~ prism edge, may explain this edge pocket. Two indications that such a thick layer may have spread as such are marked as 'B' and 'D'.

The dendrite in ~~Fig. 23~~Fig. B13c shows similar edge pockets at sidebranch "D", but the formation conditions are likely different. The formation of elongated edge pockets in both cases likely require protruding growth even if the details of the mechanism differ.

~~3~~4.~~8~~ 6.2 Mechanism of edge, elongated-edge, and edge-pair pockets

Formatted: Heading 3

The formation of edge and elongated-edge pockets should be similar to that of the corner pockets. For the elongated-edge pockets in Fig. 9, one difference from the corner pocket case is that the advancing front of the laterally growing facet is straight and parallel to the crystal edge. In the view marked 'C' in Fig. 9, these fronts appear to be prism facets indicating S-type lateral growth. Another difference may be the higher normal-growth rate (though still quite low). These differences suggest the mechanisms in Fig. 10.

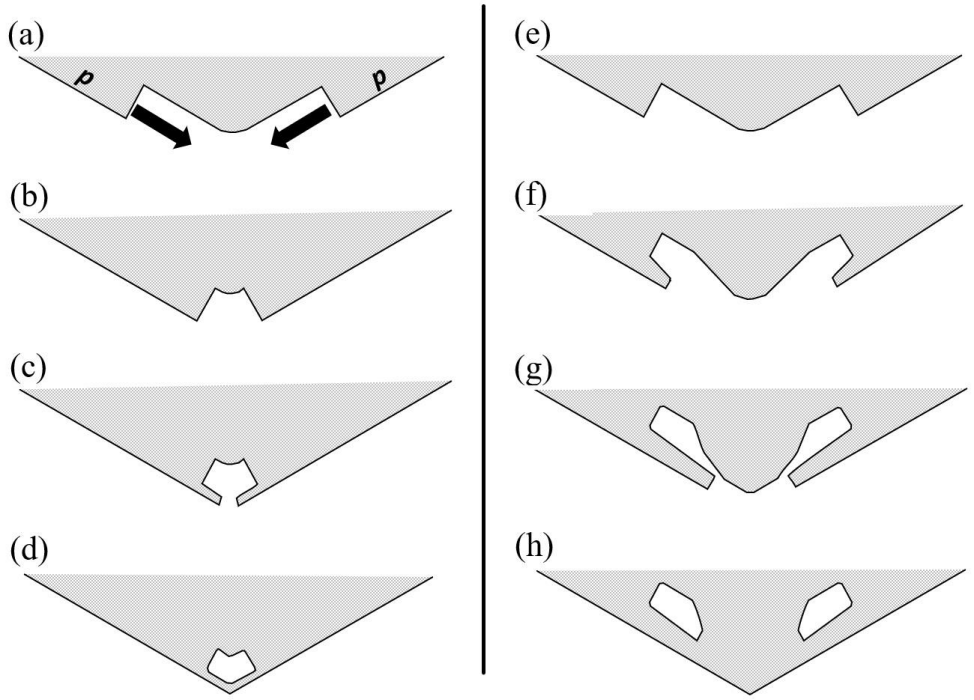

Figure 10: Edge-type pocket formation between prism faces. (a) Each prism face has a large advancing front or side-face growing laterally towards the edge. This lateral growth is marked by the solid arrows and is driven by both direct vapor flux and the AST flux. (b) The two large fronts are close enough to effectively 'shadow' the inside edge from the vapor flux. (c) Vapor gradients along front leads to protruding growth, driven by AST. (d) Protrusions merge, making an elongated edge pocket. Case (e)–(h) is similar except with greater normal growth. The two side fronts may also be non-crystallographic as in scallop-type rounded growth.

In Fig. 10~~(~~a~~)~~, the two new prism facets converge on an existing prism–prism edge. Their advancing fronts may be prism faces (as in Fig. 9) or non-crystallographic. ~~If the front is thin, then protrusive growth may occur only near the corner where the rounding is greater. So, we consider thicker fronts in this mechanism. T~~For a thicker, facetted front, the two fronts are cases of S-type lateral growth that intersect, with their motion ~~is~~ initially driven ~~largely~~ by both AST and ~~, but some~~ direct vapor deposition to the front ~~will contribute~~. But when the two fronts converge, the interior region would get increasingly shielded and shut ~~–~~out from vapor (b) at the same time that the front height ~~starts to~~ increases (the rounded edge means the base of the front recedes, increasing the front height) ~~due to the rounding~~. Thus, the AST should eventually dominate, producing two~~es~~ protrusions (c). Upon merging, they leave a pocket parallel to the edge (d). This pocket may be nearly equidimensional for ~~the~~ an edge pocket on a thin tabular crystal, and elongated if the prism–prism edge is long. This enclosure would then be completely sealed up by lateral-type ~~and protruding~~ growth on the basal faces (not shown).

A pair of pockets may form near an edge or corner instead of one. Although all stages in this process have not been observed, Libbrecht (2003) shows a double-edge case in a thin plate grown at −15 °C, and Knight (2012, Fig. 3c) appears to show some

that are more widely spaced at −5 °C. Bentley (1924) shows several cases (e.g., his figures 6, 32). Such cases may arise when even greater normal growth occurs with the protruding growth as sketched in Fig. 10e–h. Although the normal vapor flux may compete with the AST flux, it may also create vapor-density gradients that can favor protrusion formation on one face versus another. For example, if the case in (e)–(h) represents a thin plate, the vapor-density gradients (discussed in Appendix B.1) would favor initiation of protrusions on the prism faces as shown, but not necessarily from the AST flux from the basal. However, as argued in Appendix B.7, the AST flux from the basal should be larger for points nearly $\sim x_s$ back from the tip. Thus, the AST flux from the basal could produce protrusive growth away from the corner, but not at the exact corner. Thus, the corner can fill-out as shown due to both normal flux and AST flux from the basal. The result is a pair of pockets as shown in (h). This process requires that the initial stage (e) have a rounded prism–prism edge. Knight (2012) observed that the thin plates often began rounded, and scallopped, lacking any prims faces, and later became fully facetted plates (see Appendix B.7 for similar cases). Thus, this mechanism does not require a period of sublimation rounding.

~~3~~4.~~9~~ 7 Hollow close-off to center pockets and terracing

Under a wide range of growth conditions, a small ~~center~~ hollow may form in the center of~~n~~ one or more crystal faces. Once such a "center hollow" begins, it can enlarge (in width) as it grows, eventually overtaking most of the face, or it can vary in width, perhaps even closing-off. In the case that the width enlarges, the hollow deepens and develops structure. Figure 11 has a crystal showing some hollows that oscillate in width and some hollows that close-off.~~Libbrecht (2005) and other authors (e.g., Gonda and Gomi, 1985) have referred to the process as an instability. In the standard treatment, however, the hollow occurs when normal growth of the entire facet becomes impossible (e.g., Kuroda et al., 1977; Frank, 1982). Impossibility or instability, which is it? The standard "impossibility" treatment seems qualitatively successful in some cases of middling supersaturation (e.g., Nelson and Baker, 1996) and at relatively high supersaturation where the hollow tends to keep enlarging in width (e.g., hollow columns) or advance into branches (e.g., dendrites) in a generally consistent, repeatable fashion. But at low supersaturations, the hollow often varies in width, getting wider, then getting narrower, and finally closing-off into a center pocket. Oscillations also occur at middling-to-high supersaturations (e.g., Smith et al., 2015), but are much more pronounced at the low supersaturations in our experiments here. Gonda and Koike (1983) also observed the closing-off of hollows during growth at one atmosphere and supersaturations up to 33% at −30 °C. At low supersaturations, otherwise identical faces can have different patterns of hollows and pockets. Thus, at least at low supersaturations, the hollow phenomenon does seem to have some qualities of an instability. We provide supporting evidence here, and suggest a basic instability for low growth rates in §3.10.~~

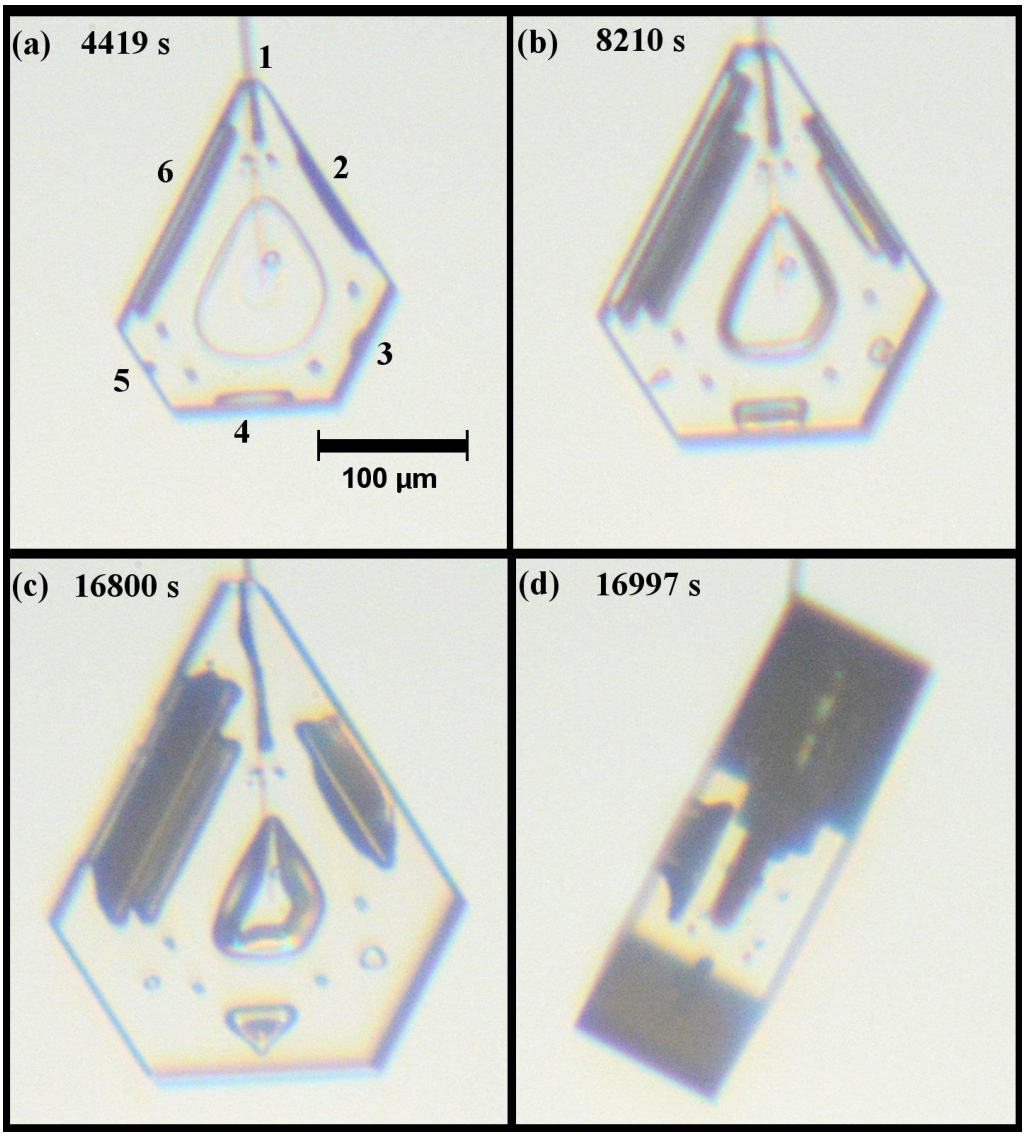

Figure 11: Center hollow development and center pocket formation. The crystal is the same as that in ~~Fig. 6~~Fig. 7, but at later times. The scale in (a) applies to all images. Numbers in (a) label the six prism faces. Image (d) is a side view.

This oscillating-width nature of some of the prism hollows also occurs with basal hollows. In Fig. 12, we show two cases. In the top row, initially, in (a), the basal faces have hollows that 'fan open' at their start, that is, have an increasing width during growth, but then have nearly straight sides, indicating a constant rim diameter of the hollows. Soon thereafter, the hollow rim suddenly widens, forming a terrace feature in (b). A similar progression occurs in the crystal in the bottom row, with two such

terraces forming on the face on the right in (d). Except for a brief sublimation period (note the corner pockets), the growth conditions remained constant throughout the 47 hours of growth. Factors influencing the pockets and terraces in Figs. 11, 12 are likely complex, but in Appendix B.1 we suggest a simple model involving F- and P-growth to help explain them.

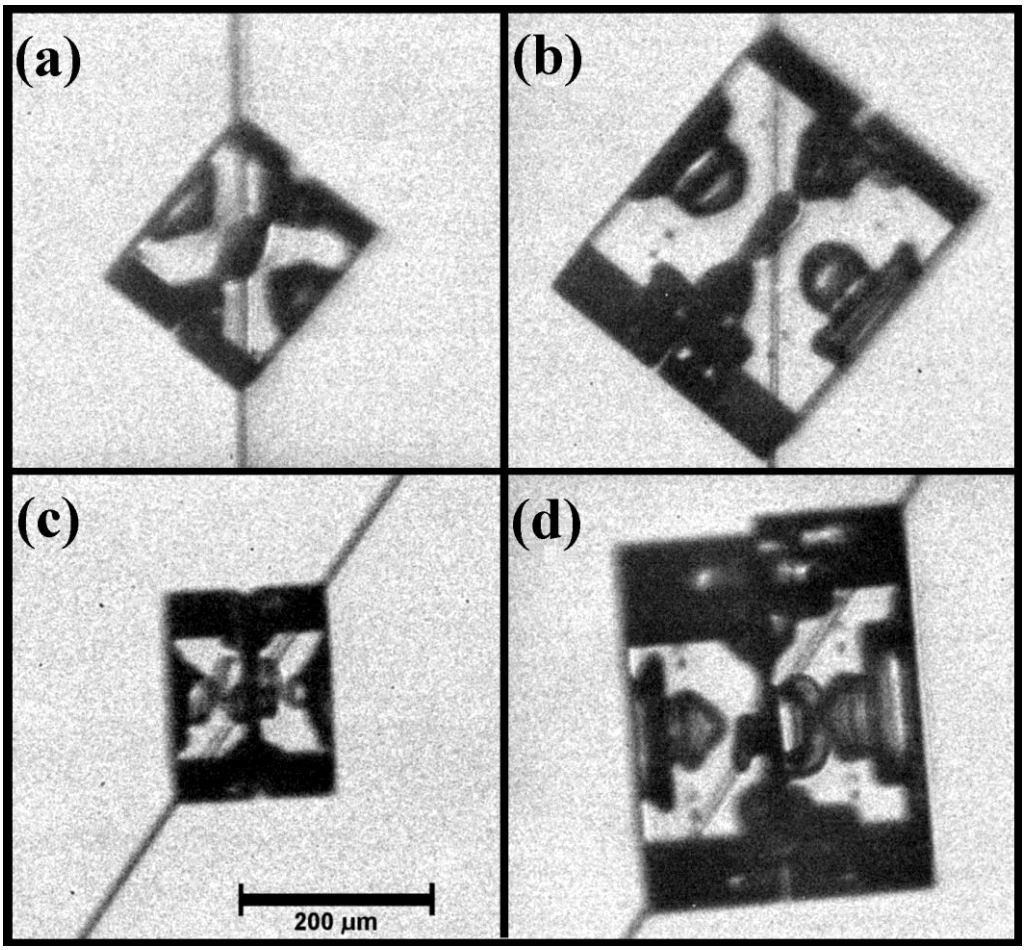

Figure 12: Center hollow terracing on twinned crystals grown under constant conditions of about −30 °C and 0.5% supersaturation. (a) Side view of crystal in middle of one capillary, basal faces pointing NW and SE. (b) Crystal in (a), but 46 hours later. (c) Different crystal under the same conditions, but on a different capillary. (d) Crystal in (c), but 47 hours later. Small corner pockets also appear in (b) and (d) due to a brief sublimation period after images in (a) and (c). Scale in (c) applies to all images.

~~3.2~~25.1 Microscale mechanisms of facet spreading and protruding growth

The microscale mechanism of facet spreading involves AST, which is the migration of molecules, first over the edge of the facet, and second with their finding a high-density of growth sites on the other side. The first may occur via isolated molecules or as a

more cooperative phenomena in a thicker disordered region, but either case may be consistent with the observations here. The second argues that the direction of this AST flux will largely be towards the side with the greater density of growth sites. The observations in Figs. 1, 5 show this lateral-growth front to be rough, thus indicating that the flux should be to this front. The reason for the roughness is not clear, but may be partly a result of the thermal roughening analyzed in BCF (1951). BCF argued that single steps should be rough, but surfaces should be flat except at or above their roughening temperature. Observations of steps on ice show them to be rough, even when collected into macrosteps (e.g. Kobayashi, 1967). The lateral-growth fronts may be rough for a similar reason even though they advance on a rough surface, not a facet, and may be thicker. That they may be significantly thicker than single steps might be connected to thermal roughening of facets. There have been reports of a roughening temperature near −2 °C (e.g., Elbaum, 1991), and thus ice facets at even lower temperatures may be close enough to roughening that macrosteps and other thin crystal regions such as the lateral-growth front can be rough even though larger faces remain facetted. Other causes of roughening are discussed below and in Appendix B.7.

For the microscale mechanism of protruding growth, two obvious questions arise: (1) How does a thin protrusion start? That is, instead of the AST molecules spreading out on the adjoining surface region to build-up a thick facet, why is the flux concentrated to a thin region? (2) As with F-growth, why would the thin front of the protrusion have a higher density of growth sites than the analogous facet to efficiently collect all the AST flux and continue protruding?

A possible answer to (1) is a large vapor-density gradient. Consider again the sketch in Fig. 2b. If the vapor-density contours closely parallel the surface, but "skim over" the inside corner **c**, then the vapor density would sharply decrease from **e** to **c** provided that this distance exceeded the vapor mean-free path. In such a case, the AST flux may build up nearer to **e** and not reach **c**, initiating the protrusion. Consistent with this argument is the observation that no cases of the corner pockets have been reported for small crystals and on crystals grown and sublimated in a pure vapor. Regardless, if one instead argues more generally that if we have a mechanism that answers (2), forming a high-density of growth sites in a thin region just over the edge of a facet, then a net flow of mobile surface molecules would not migrate any further than this thin region. If this migration on the rough surface has length scale l_t, then a region of thickness $t \sim l_t$ would start protruding. Thus, it becomes even more important to find a possible mechanism that answers (2); that is, why the edge is rough. Rough edges on thin-face regions have been observed in numerous cases as discussed in Appendix B.7. Thus, rough, thin protrusions may form and produce fast growth rates. However, it is not clear why only thin, and not also thick, protrusions would be rough.

A possible answer was proposed by Libbrecht (2003), who argued that thin plates must have a different structure at their leading fronts that leads to a high deposition coefficient (i.e., a high density of growth sites such as a rough edge), and then suggested a type of nanoscale surface-melting effect. However, at nanometer sizes, the small radius of curvature may also increase the rate of sublimation, causing a compensating decrease in lateral growth rate. And though such a mechanism may help explain the fast-growing serrated dendrites at −2.0 °C and thin discs at slightly lower temperatures, it would be less likely at the much lower-temperature protruding-growth effects found here near −30.0 °C. Another possible answer is that the edge region consists of rough, high-index planes that essentially vanish on larger surfaces due to their rapid growth but cannot vanish on a thin protrusion due to a curvature effect. Other possible factors are considered in Appendix B.7, but clearly more experiments are needed to understand the mechanism of protruding growth as well as relations between thickness, roughness, and temperature.

~~That is, instead of the AST molecules spreading out on the adjoining surface region to build-up a thick facet, why is the flux concentrated to a thin region? (2) Why would the thin front of the protrusion have a higher density of growth sites than the analogous facet to efficiently collect all the AST flux and continue protruding?~~

5.2 General implications

5.2.1 How AST may help explain secondary features and habits

Ice growth in the atmosphere is affected by many processes. A first step towards an understanding is to identify which processes may play the dominant role in a given situation. We found above that AST appears crucial to understanding the observed facet spreading as well as the formation of corner and edge pockets. Although these exact situations may rarely occur in the atmosphere, AST itself cannot be "turned off", and thus AST-driven phenomena may have a key role in other situations as well. And as it turns out, there are numerous features on atmospheric ice crystals that are routinely observed yet have no clear explanation. Here we consider some of these features, proposing explanations that include F- and P-growth driven by AST. Detailed discussion and diagrams are in Appendix B.

Center pockets A center pocket is a center hollow that has closed-up. The closing-up involves growth lateral to the face in which the hollow sits, similar to that modeled in Fig. 6. As we found, the rate of the lateral-type growth via AST in that case was much faster than normal growth, making the closing up of hollows into center pockets a likely consequence of AST. Such pockets are more common at lower normal growth rates, a situation that can allow such protruding growth to occur from opposite directions of a given facet. The normal-growth process, in contrast, does not explain the closing-up because the vapor impingement would be increasingly impeded in the narrow crevice region that closes up.

Terracing and banding in hollows Even when the hollow cannot close-up, facet spreading can occur on the inside surface of the hollows. When such spreading starts in a given region, adjoining regions sharpen. The vapor-density gradients near the sharpened region can then influence the facet spreading such as to amplify the effect. This may be the cause of the wide terraces in hopper crystals and the "band-like" lines in narrow hollow columns.

Two-level planes with center droxtals The center circle in some branched, tabular snow crystals around −15 °C have long been identified with the crystal's original droxtal, but it has never been clear how the circular form could remain as the droxtal grew outward via normal growth. Protruding growth from both basal planes has been observed in larger droxtals and likely also occurs in smaller droxtals such as those that are more common seeds of snow crystals. With AST-driven protruding growth of the basal faces, the basal planes can extend over the middle of the droxtal, leaving it behind in a vapor-shielded, still circular, region that hardly grows. This process likely explains the observed center droxtals.

Capped and multiple-capped columns When a columnar crystal moves into a temperature at which tabular crystals form, thin tabular extensions develop at the ends. These ends appear to start very thin, a situation in which AST should significantly contribute to their growth. Another driving process is likely the large supersaturation gradients near the tip, which may help to initiate the thin plates at the ends. But initiation of interior plates in the multiple-capped columns are much harder to explain without AST. Here, the appearance of a small basal face is all that is needed for a large plate to develop. Such a basal face may even arise from the side of a rime droxtal.

Scrolls The scroll form involves prism faces that bend inward, extending in the directions of the a-axes and c-axis. If this was due to normal growth, then why would a face bend? Instead, their appearance suggests lateral-type growth in a prism plane, driven by AST. Once the thin plane thickens such as to be no longer primarily driven by AST, a new prism plane forms. Once a new prism plane forms, the extending growth changes direction such as to extend the new prism plane inward. In this way, the prism face bends inward, resembling a scroll. Nakaya et al. (1958) shows the form appearing around −9 °C, at relatively high supersaturation, consistent with that reported by Magono and Lee (1966). This temperature is close to that at which they reported the columnar habit changing to tabular.

Bundles of sheaths and needles Needle crystals grow around −5 °C, even at sub-liquid saturation (e.g., Knight, 2012). In the atmosphere they often appear not as a simple needle shape, but instead in a bundled form. The sheath bundle is sometimes

distinguished from the needle bundle, though they may be slight variations on the same form. Takahashi et al. (1991) reports sheath needles forming at −4.4 to −6.4 °C and liquid water saturation, with columns forming at immediately lower and higher temperatures. No other crystal form appeared in the columnar regime reported to lie between −4.0 and −8.1 °C. The non-bundled needle crystals observed by Knight (2012) had almost no normal growth of the prism faces, and thus it is hard to see how normal growth can explain the relatively wide diameters, and abrupt changes in diameter, of the bundled crystals. However, AST-driven lateral growth of prism faces could lead to extensions in a-axis directions, abruptly increasing the diameter and sprouting a new needle or sheath in the bundle. In this way, they are similar to the scroll forms.

Trigonal crystals These crystals have just three clearly distinguished prism faces, the other three being much smaller or indiscernible. A few possible explanations have been proposed for trigonal ice crystals, but they are either inconsistent with the observations of Yamashita (1973) or lack a specific growth mechanism. Yamashita (1973) argued that the trigonal forms grew from sub-micron droxtals, and more recently argued that AST-driven growth on an initial sub-micron prism face (more generally, of order x_s or less) would dominate the droxtal, overgrowing the two immediately neighboring prism faces (Yamashita, 2014). The process may also promote the formation of next-neighboring prism faces, but even if the remaining three prism faces have equal chance of developing next, the sequence of events would lead to trigonal crystals in most such cases. These small crystals might not remain trigonal during growth, however, unless a mechanism exists that can maintain a stable trigonal structure. We suggest that the larger crystal with a small prism between two large prism faces would have vapor-density contours that allow slightly faster rates of layer nucleation on the small prism face. A small difference in layer nucleation rates would be amplified to a larger difference due to net AST from the large to the small prism, possibly stabilizing the trigonal form.

A recent review of ice growth from the vapor suggested that AST may be unnecessary for understanding ice growth forms (Libbrecht, 2005). The above examples suggest otherwise, instead arguing that many oft-observed secondary features may be inexplicable without the AST mechanism. Additional cases, including aspects of primary habit and rounding, are briefly examined in the appendix as well. The arguments are mostly qualitative; nevertheless, they serve to put very different growth forms into a common framework. They may also help stimulate new measurements of x_s, further observations, and more detailed modeling of these interesting crystal forms.

5.2.2 Implications for modeling and light scattering

Formatted: Heading 3

To test the general magnitude of the AST role in ice growth, lateral-growth measurements are needed with greater precision than those given here. An interferometry study may provide sufficient precision of the lateral-front height and contour of the perimeter. For deducing the resulting x_s values, the model introduced in Appendix A may be used. To test specific habit mechanisms proposed here, we need better modeling—including vapor diffusion to realistic crystal shapes and relevant surface processes.

Presently, the most realistic crystal-growth model is that of Wood et al. (2001), but it is limited to hexagonal prisms. Some modeling approaches, such as cellular automata (Kelly and Boyer, 2014) and phase-field (Demange et al., 2017) ~~model~~ simulate much more complex shapes, but they unfortunately do not appear to include any of the relevant surface microscale processes directly. The list of relevant surface processes includes layer nucleation, defect-step sources, step clumping, and non-crystallographic regions (Nelson, 2005). To this list, we must now add that lateral-type growth processes with AST must be included.

Concerning light scattering from atmospheric ice, some studies have suggested that the outermost ice-crystal faces can introduce "roughness" that affects the visible-light scattering (e.g., Voigtländer et al., 2018). But in the crystal-growth field, going back many decades (e.g., Frenkel, 1945; BCF, 1951; Woodruff, 2015), crystal faces are known to grow as atomically flat

surfaces with nanoscale steps at low supersaturations, as occur in the atmosphere, except where hollows or branches sprout. Our experiments and observations are consistent with this well-established view of growth. However, the interior regions such as backsides, hollows, and pockets can show bumpier structures, and these interior regions are the more likely source of the "roughness" implied by the scattering results. The pockets, however, cannot be detected using the oft-used method (e.g., in Smith et al., 2015) of examining ice-crystal replicas. In addition, for sublimation, our experiments showed no indication of rough features on the outermost surfaces (except the nanoscale roughness of a smoothly curved edge), such as those found in recent SEM studies (e.g., Magee et al., 2014; Pfalzgraff et al., 2010). In those experiments, little air was present, thus differing from atmospheric ice crystals. The presence of air had been argued previously to be important for the observed smoothly rounded shapes of sublimating ice (Nelson, 1998).

~~5~~ 6 Summary

We have described here some previously unreported features on vapor-grown ice, including corner pockets, planar pockets, and elongated edge pockets, ~~and planar pockets,~~ as well as provided more detailed observations of hollow terracing and hollow close-off. We argued that such features arose partly from ~~lateral~~ facet spreading ~~or~~and protruding growth, both phenomena driven largely by surface transport across the boundary of a face to the advancing edge, a process we termed adjoining surface transport or AST. Several quantitative models have been introduced that apply to lateral growth, including a model for center-pocket formation, and several qualitative models have been presented linking lateral-type growth to known secondary habits of snow crystals.

Our central point is that such lateral-type ~~and protruding~~ growth, long neglected in ice and snow research, may help explain a wide range of complex features and phenomena related to ice- and snow-crystal growth in the atmosphere, particularly when combined with normal growth. Protruding growth itself likely produces the two-level structure on many stellar snow crystals and also helps to explain capped columns, multiple-capped columns, florid crystals, sheath growth, scrolls, sheath clusters, as well as various branch pockets and planar extensions. ~~As argued here, l~~Lateral-type ~~and protruding~~ growth ~~are~~ is also a likely factor~~s~~ in hollow terracing, banding, and close-off to make center pockets. Finally, the AST process itself likely contributes to the growth rates of sheath and dendritic crystals where it may substantially increase the growth rates and round-out the shape of the leading tip or corners. Finally, AST may also affect layer nucleation rates and explain trigonal forms.

As for immediate practical applications, we may infer the occurrence of an undersaturated cloud region via the observation of 12 corner pockets in a collected crystal, with the positions of the pockets providing the crystal size and aspect ratio at the time immediately after sublimation. ~~However, such an interpretation requires care because c~~Corner pockets may also form whenever a change in growth conditions leads to a transition between rounded and facetted growth, such as on branch backsides. Similar inferences of crystal conditions based on other crystal features will likely be revealed in subsequent experiments. Thus, gaining a greater understanding of the formation of hollows, pockets, and various thin protrusions may lead to a more detailed knowledge of cloud conditions, and conversely, lead to better predictions of their occurrence in models. In turn, the improved predictions may improve the modeling of radiative transfer through ice-containing clouds. With such widespread potential applications, the phenomenon of AST-driven lateral and protruding growth deserves greater study.

Appendix A: Modeling lateral and protruding growth

We introduce the three mechanisms for the lateral growth of a face for the fits in ~~Fig. 5~~Fig. 6. Referring now to Fig. A1, assume *r* marks the radial edge-front of the face with height *h*. The rate *dr/dt* is affected by I) direct vapor deposition to the edge-front, II)

AST flux from the top basal face, from within x_s of r, and III) normal growth of the rough region laying between radial position r and the radius a of the crystal. Cases I and II involve a face edge-front of height h, whereas h is assumed zero for III. In case III, the position r is the intersection of the curved face and the basal-face position $z = c$, marked with a dot in the sketch.

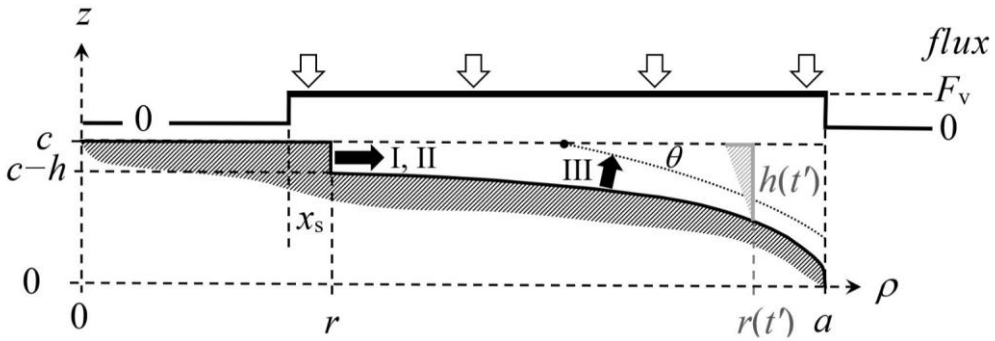

Figure A1: ~~Lateral growth~~Facet spreading models. Dark shading shows the surface region of one quadrant of the crystal cross-section at a given time t. The flux calculation treats the crystal as a thin disc of radius a with flux F_v uniform between $r–x_s$ and a, zero elsewhere (upper plot). The face edge-front at radial position r has height h for mechanisms I and II. At a later time t', the value of h is larger (light shading) due to the advancement to $r(t')$, making a larger distance between the rough surface and basal surface at c. For III, the edge-front is instead assumed to lie at the intersection of the laterally growing face at c (dashed line) and the dotted curve, intersecting with angle θ.

Formatted: Font: Symbol

All three mechanisms for dr/dt depend on the vapor flux to the face, so we first estimate this flux. Assuming zero normal growth of the face (the basal face in this case), the flux normal to the face must be zero out to within x_s of the face-edge at r. Beyond this point we assume a uniform flux F_v (#/m^{2}s) in the z direction out to the edge of the crystal and then zero beyond. For the flux calculation, the crystal is assumed to be an infinitesimally thin disc of radius a. As done for other uniform-flux calculations (e.g., Nelson and Baker, 1996), the value of F_v is determined self-consistently through an assumed surface response (deposition-coefficient function) to the vapor density at the surface, with the vapor density depending on F_v. The rates for I–III, top-to-bottom are

$$\frac{dr}{dt} = \begin{matrix} \Omega F_v \\ \Omega F_v \frac{x_s}{h}\left(1 - \frac{x_s}{2r}\right) \\ \Omega F_v \frac{1}{\sin(\theta)} \end{matrix} , \qquad (A1)$$

where Ω is the volume occupied by a water molecule in ice (mass of molecule/mass-density), and θ is the angle between the rough surface beyond r and the basal face (see Fig. A1). To calculate this angle for case III, we assume ~~that this~~the rough surface ~~is~~ to be the perimeter of an expanding ellipsoid of the same, fixed aspect ratio of the crystal. Such an assumption is unlikely to be accurate in detail, but nevertheless ~~includes the influence of an increasing~~predicts angle θ to increase ~~as the face grows laterally~~with r as we expect. For the calculations, we ~~followed~~ use the treatment of the ellipsoidal coordinate system in Moon and Spencer (1961), and do not give the details here. For cases I and III, the flux is assumed to be in the normal direction ~~to~~ right at the surfaces (edge h and rough region, respectively) in Eqs. A1, even though the flux is assumed as along the z-axis for the

calculation of F_v. For case II, the prefactor comes from Eqs. B4 and B5, with the second factor in parenthesis arising from the curvature of the disc. The value of h is not known from the measurements, and thus is treated as a fitting parameter here and then compared with the initial crystal profile. It only remains to determine F_v.

In a stagnant atmosphere of air, the vapor density N surrounding a thin disc of radius a has flux $D\partial N/\partial z$ at the surface. For the first step of the calculation, we assume this flux is uniform over the entire top surface (i.e., $0 \le \rho \le a$). Shifting and normalizing as

$$\begin{aligned} \Delta N' &\equiv \frac{N(\rho',z')-N_\infty}{N_\infty} \\ F_v' &\equiv \frac{\partial \Delta N'}{\partial z'} \\ \rho' &\equiv \frac{\rho}{a} \\ z' &\equiv \frac{z}{a} \end{aligned} \quad , \qquad (A2)$$

with N_∞ the far-field vapor density, the solution for uniform F_v' can be shown to equal

$$\Delta N'(\rho',z') = -F_v' \cdot h_{td}(\rho',z') \ , \qquad (A3)$$

where the thin-disc basis function h_{td} is an integral of Bessel functions (Nelson, 1994). (This function is defined the same in A3 as are the analogous basis functions h for the cylinder (Nelson and Baker, 1996; Nelson, 2001) and Q for the hexagonal prism (Wood et al., 2001).) At the surface ($z' = 0$), this function simplifies to

$$h_{td}(\rho',0) \equiv \begin{cases} {}_2F_1\left(\frac{1}{2},-\frac{1}{2},1,\rho'^2\right) & \rho' \le 1 \\ \frac{2}{\pi}E\left(\rho'^2\right) & \rho' > 1 \end{cases} \ , \qquad (A4)$$

where ${}_2F_1$ is the hypergeometric function and E the elliptic integral. The curve is roughly bell-shaped about the origin, where it equals one, then nearly equaling $1/2\rho'$ for $\rho' > 1.5$. Consider now the "thin-ring" basis function h_{tr} defined as

$$h_{tr}(\rho',z',r',x_s') \equiv h_{td}(\rho',z') - \frac{1}{\gamma}h_{td}(\rho'\gamma,z'\gamma) \ , \qquad (A5)$$

where

$$\gamma \equiv \frac{a}{r-x_s} \equiv \frac{1}{r'-x_s'} \ , \qquad (A6)$$

always exceeds one. Eq. A6 defines r' and x_s'. You can readily show that the derivative of this function normal to the surface ($\partial/\partial z'$) gives a non-zero value at the surface only in the ring $r-x_s \le \rho \le a$ (or $1/\gamma \le \rho' \le 1$), where the value equals −1. For the edge-front, the relevant part of the function lies at $\rho = r$. We plot h_{tr} at this position in Fig. A2.

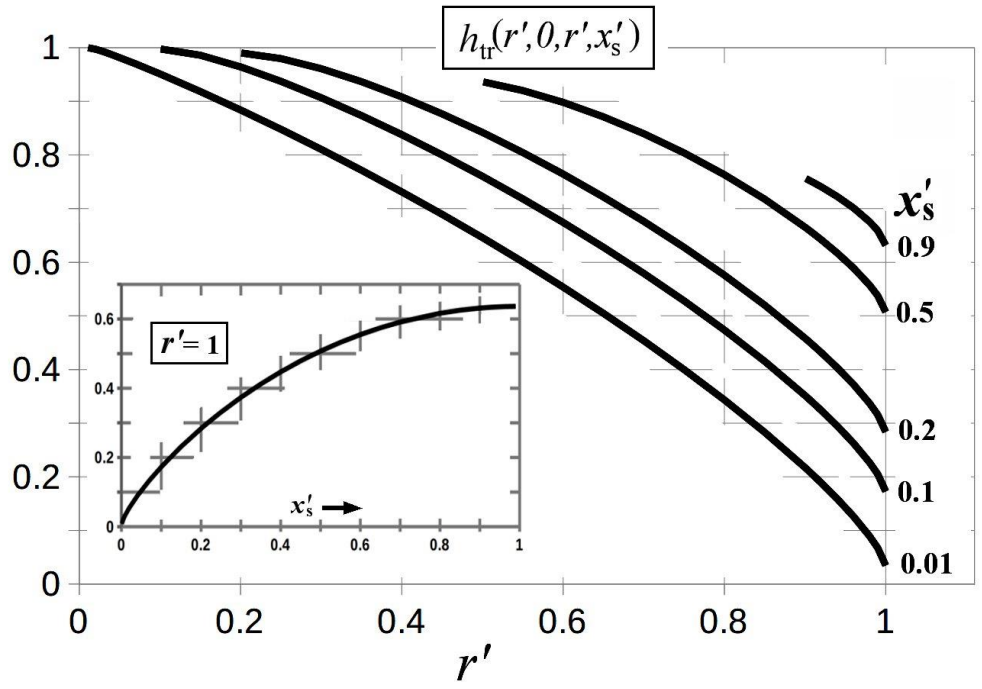

Figure A2: Basis function h_{tr} for the thin ring. The function is evaluated at $z' = 0$ (i.e., the surface) and ρ' at the position of the growing face edge-front (r'). The five curves are for the x'_s values given at right. Inset plot shows the dependence on x'_s when the edge-front reaches the crystal perimeter at a (i.e., $r' = 1$). Hatches show the grid.

As the face edge-front r' moves towards the crystal perimeter, the area that collects vapor decreases. This behavior is reflected in the decrease in h_{tr} as $r' \rightarrow 1$ for all values of x_s. Each curve for a given x'_s value begins at $r' = x'_s$ because the vapor-collection region starts at $r' - x'_s$, which cannot be negative. And when this starting point at x'_s increases, the function decreases because h_{td} decreases away from the origin. Exactly at the rim, where $r' = 1$, the only region of vapor collection is the ring of width x'_s (Fig. A1). Thus, in this case, h_{tr} approaches zero as $x'_s \rightarrow 0$, as shown in the inset plot; that is, a thin ring of growth hardly depletes the surrounding vapor.

Calculating the flux requires the surface-kinetic expression for the flux. Assuming a rough surface, the flux at the edge-front is one-fourth the vapor mean speed v times $N(r',0) - N_{eq}$ (see, e.g., Nelson and Baker, 1996), which can be rewritten as

$$F'_v = a'(\Delta N'(r',0) - \frac{N_{eq}}{N_\infty}\sigma_\infty) \quad , \qquad \text{(A7)}$$

where $a' \equiv va/4D$ is approximately the crystal radius divided by the vapor mean-free-path. From Eqs. A3 and A7, one can eliminate $\Delta N'$ to derive

$$F_v = \frac{\frac{v}{4}N_{eq}\sigma_\infty}{1+a'h_{tr}(r')} \quad , \qquad \text{(A8)}$$

where $h_{tr}(r')$ is shorthand for the full expression plotted in Fig. A2. This expression is used with Eqs. A1 to plot the curves in Fig. 6.

The method of linear superposition of basis functions, as shown in Eq. A5, can be extended by adding more terms to properly treat the case of rough growth in the region $r-x_s \le \rho \le a$. That is, instead of a single ring of uniform flux with deposition coefficient unity, one can break the ring into many smaller rings, and then sum the terms. Nevertheless, the treatment here should capture the essential features of the diffusion field $\Delta N'$.

For protruding growth, the behavior of h_{tr} for $r' = 1$ (inset, Fig. A2) is relevant. For example, having $x_s = 5$ μm with a face radius $a = 100$ μm gives h_{tr} of only ~ 0.08. Moreover, this value will decrease further as the protrusion grows due to a increasing at fixed x_s. Having such low vapor depletion will not only speed up the lateral growth, but may also allow the protrusion to nucleate layers more closely, possibly aiding a roughening transition ~~as discussed in Appendix B~~. Of course, this treatment assumes no normal growth of the face and no direct vapor flux to the edge in the radial direction. Such modifications can be added. The resulting expression will be similar in form to Eq. A8, but with added terms in the denominator that reduce the flux.

Appendix B: ~~Nucleation on a thin edge face~~Secondary features and habits

Further evidence that lateral-type growth is a common factor in ice growth comes from examination of various secondary features and secondary habits. We examine here several cases, but as ice-growth from the vapor in air is often complex, having several competing processes on complex shapes, each case requires a different approach and presently can only be treated in a qualitative fashion. Most of these features and habits appear inexplicable with normal-type growth processes only, and only a few of them have even seen attempts at explanation. Addressed here are ~~As argued by Frank (1982), nucleation of layers on snow crystals differs from the classical multinucleation treatment (e.g., Arima and Irisawa, 1990) due to the lateral supersaturation gradients on a face. Specifically, the new layers will repeatedly nucleate at the spot of highest supersaturation. In addition, the nucleation of a layer can locally reduce the surface ad-molecule supersaturation, meaning that a new layer will not nucleate until the step-edge of the previously nucleated layer moves a certain distance *l*. This *l* will be approximately the distance from the step-edge, where the surface supersaturation is relatively low, to the point where the surface supersaturation reaches the critical value σ_{cr} to nucleate the next layer. This process is described in Nelson (2001, Appendix A) for the case of nucleation on a wide terrace (step-free facet region). The purpose here is to examine how this process may differ on a thin-edge face, particularly in regards to reduced step-spacings and effectively rough growth.~~

- Center pockets, terracing, and banding from hollows (B.1)
- Center pocket variability (B.2)
- Two-level formation and center droxtals on planar forms (B.3)
- Corner pockets on rounded tabular backsides (B.4)
- Capped columns, multiple-capped columns, and florid crystals (B.5)
- Rounding of plates and tips of fast-growth forms (B.6)
- Tip shapes of sheath and sharp needles (B.7)
- Scroll crystal features (B.8)
- Bundles of sheaths and needles (B.9)
- Protruding growth on branch backsides and ridge pockets (B.10)
- AST contributions to trigonal formation and primary habits (B.11)

Formatted: Bullets

B.1 Hollow close-off to center pockets, hollow terracing and banding: mechanisms

Center hollows show variable behavior. Concerning their formation, Libbrecht (2005) and other authors (e.g., Gonda and Gomi, 1985) have referred to the process as an instability. In the standard treatment, however, the hollow occurs when the gradient in supersaturation needed for uniform growth can no longer be compensated for by the step density (e.g., Kuroda et al., 1977; Frank, 1982). In other words, normal growth of the entire facet becomes impossible, which is different from being unstable. In this "impossibility" case, one expects the hollow initiation and shape to be nearly identical on identical faces in a nearly uniform environment as well as being highly reproducible when other crystals grow under the same conditions. If merely an unstable phenomenon, then a sufficiently uniform, constant condition may be expected to circumvent the hollowing. Conversely, if hollows do form, then their initiation and shape should differ between identical faces due to minute differences in conditions. We suggest here that inclusion of lateral-type growth processes predicts qualities of unstable growth at low supersaturations, leading to hollow close-off and terracing features.

The standard facet-impossibility approach seems qualitatively successful in some cases of middling supersaturation (e.g., Nelson and Baker, 1996) and at relatively high supersaturation where the hollow tends to keep enlarging in width (e.g., hollow columns) or advance into branches (e.g., dendrites) in a generally consistent, repeatable fashion on all identical face types. But at low supersaturations, the hollow often varies in width, getting wider, then getting narrower, and may even close-off into a center pocket. Large changes in width also occur at middling-to-high supersaturations (e.g., Smith et al., 2015), but are much more pronounced at the low supersaturations here. Gonda and Koike (1983) also observed the closing-off of hollows during growth at one atmosphere and supersaturations up to 33% at −30 °C. At low supersaturations, otherwise identical faces can have different patterns of hollows and pockets. Thus, at least at low supersaturations, the hollow phenomenon does seem to have some qualities of an instability. We provide supporting evidence here, and suggest a basic model of instability at low growth rates.

In the cases shown here, Tthe center hollows ~~shown here exhibit variable behavior at low supersaturations~~vary considerably, even ~~under~~though the conditions are nearly ~~-~~constant ~~conditions~~. For example, the hollow's size and shape can vary considerably between different faces of the same crystal in Figs. 11 and 12. Also, a given hollow's width can change suddenly, often showing periodic terrace-like features, and sometimes closing-off completely, leaving a center pocket. Such behavior suggests a complex process involving competing influences and a possible instability. Here we describe a simplified mechanism for such an instability between normal and protruding growth, and argue that the growth behavior of adjacent faces may influence hollows, particularly at low supersaturations, possibly leading to the above-mentioned observations.

First, consider the initial hollowing. The overall driver of hollowing of a surface is lateral supersaturation (σ) gradients across the surface. These gradients are influenced by growth on the crystal faces such that, for example, normal growth on the basal face produces a decrease in surface supersaturation, starting from a high value in the middle of the prisms ***p***, as sketched in Fig. B1a, to the ***p***–***b*** edge, to the smallest value in the center of the basal. Normal growth only on an adjacent prism faces produces the opposite gradient on the basal (dotted lines). In general, normal growth occurs on all faces, and thus the contributions from both sets of contours in (a) are superimposed with a weight in proportion to the normal growth rates (Nelson and Baker, 1996). The normal growth rate of a given face is proportional to the areal flux F_v to the surface, which is mainly the vapor-diffusion flux

$$F_v = DN_{eq}\nabla\sigma \cdot \hat{n}\,, \quad \text{(B1)}$$

where D is the vapor diffusion constant, $\hat{n}$ is the surface normal, and N_{eq} is the equilibrium vapor density at the local surface temperature. This means that a larger growth rate of a face implies a larger normal gradient, which should positively correlate to a larger lateral surface gradient. Hence, taken together, the surface gradient in supersaturation that leads to hollowing, say on the

basal face, will be weaker at low normal growth rates of the basal and also weaker at high normal growth rates of the adjacent prism faces. That is, the growth on one face influences the lateral gradients on the other faces.

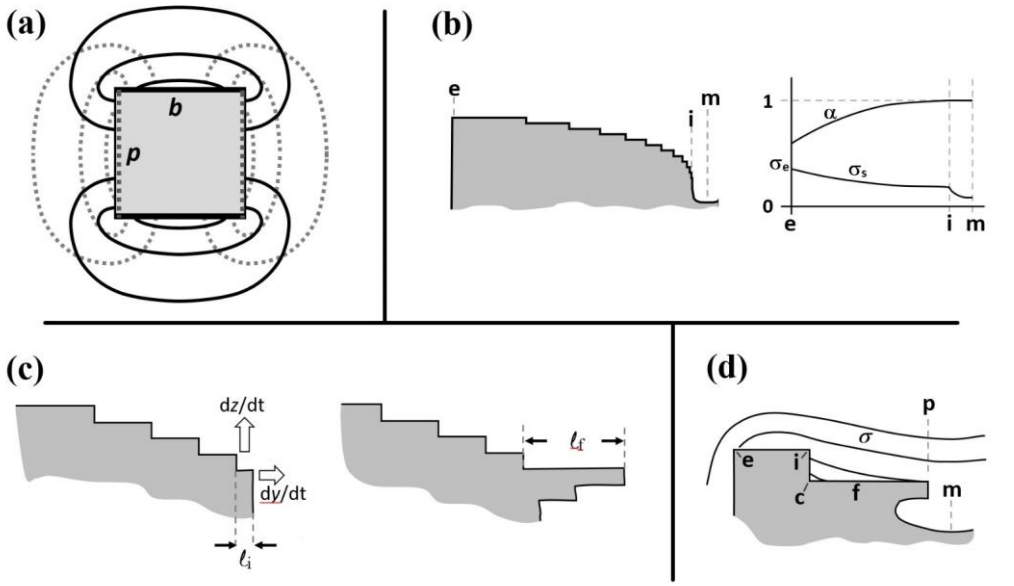

Figure 13B1: Processes involved in hollow close-off and terrace formation. (a) Basic patterns of vapor-density contours on a solid prism for growth only on the basal faces ***b*** in solid, dark curves, and for growth only on the prism ***p*** in dotted grey curves. The general case has a linear superposition. (b) Standard picture of hollow formation. Steps coming from edge at **e** become closer towards the inside edge **i** at right. Face middle is **m**. **(**Other half of face, as well as steps on side face, are not shown.) The plot on the right side shows the deposition-coefficient function α at top, with the trend in surface-supersaturation σ_s sketched below. (c) Close up of step-clumping region near inside edge **i** where the steps are separated by $l = l_i$. Protruding growth can occur towards the right (dy/dt), normal growth upward (dz/dt). Protrusion shown at right, last step length now $l = l_t$. (d) Supersaturation contours when a terrace **f** forms via lateral growth. Here, **c** is the inside corner, **p** is the protrusion.

The lateral surface gradient in supersaturation leads to hollowing via its effect on the surface steps (e.g., Frank, 1982; Nelson and Baker, 1996; Wood et al., 2001). Briefly, as sketched in Fig. B1b, steps originate from the crystal edge **e** and flow towards the face center **m** on the right. The sketch on the right shows the trends of vapor supersaturation along the surface and deposition coefficient function α. Near the edge, the vapor supersaturation σ_e is relatively high and the steps are relatively far apart, but there is a relatively high fraction that desorb, which is described by its low deposition coefficient α_e. As the steps move toward **m**, they slow down and become more densely packed, thus increasing the local deposition coefficient. At the edge **i** of the hollow, essentially all the incident molecules reach a step and the steps are clustered together to the point that they hardly move. A wall of steps builds up here, at the step-clumping region (SCR), forming the edge of the hollow. (Neshyba et al. (2016) proposed a more detailed model of step dynamics for ice with a thick surface-disordered region, but it is not yet clear how a hollow would develop in that model.)

However, after the hollow forms, the local supersaturations may change. This change could be due to either a change in external conditions (e.g., temperature or supersaturation), a change in growth rate of a face due to a changing activity of the step source, or simply the increasing size of the crystal. For example, an increase in crystal size will generally decrease σ_s. Regardless of the cause, consider now the sketch in Fig. B1c in which a slight change in local conditions near the hollow edge **i** has occurred, causing a slight increase in the local step separation l. The normal growth rate dz/dt at **i** is the step height h divided by the step-passage time τ (time between successive passings of a step at **i**). The latter time is the step separation divided by the step speed v_s. However, for a protrusion of thickness nh ($n \geq 1$) that starts into the hollow, the protruding growth rate $dy/dt = v_s/2n$, with the factor ½ due to the AST flux coming only from the top side. Comparing the two rates,

$$\frac{dy}{dt} = \frac{l}{2nh} \cdot \frac{dz}{dt}, \quad \text{(B2)}$$

When the hollow first forms, l may be of order h. But ~~with the~~an increase in l, causes~~as sketched in (c), then~~ dy/dt to increase~~s~~, further increasing l and thus further increasing dy/dt. Eventually dy/dt may greatly exceed dz/dt. Hence, in this very basic description, some change in step spacing near the hollow may become unstable, leading to a protrusion that can continue to grow, eventually sealing-off the hollow into a center pocket. Initially, there will also be some direct vapor-flux to the side of the hollow at the lip, but this contribution to ~~lateral~~protruding growth would vanish due to shielding from the opposite side as the pocket closes off.

This basic treatment neglects lateral supersaturation gradients and advancement of the crystal face. Briefly, these factors make sealing-off of a hollow less likely at higher growth rates because the initial protrusion will become left behind in a lower supersaturation region as the rim grow higher. As the supersaturation drops, the protrusion grows slower, amplifying the effect. Also, as the protrusion grows inward, the supersaturation should decrease (except in the case mentioned next), thus hindering or possibly preventing the instability. Thus, the above suggests a hollow instability at low growth rates, but not at high rates.

Concerning terracing, if the SCR develops nearer the rim and becomes elevated as in Fig. B1~~(d)~~, the interior region **f** may flatten. This flattening would be aided by a reversed surface supersaturation gradient; that is, if the inside corner **c** ~~in (d)~~ becomes isolated in an effective vapor shadow (height **i**–**c** exceeding the vapor mean-free path), then the steps in region **f** will speed up as they go towards the higher supersaturations near the center. This would produce an interior face that ~~grows~~spreads laterally, flattening region **f** into terrace features such as those in Figs. 11,12. ~~(It may also drive protruding growth to make a center pocket as also shown in (d).)~~

The growth of crystals with many terraces has been called skeletal or hopper growth, but the structure differs between that in relatively squat hollows and that in narrow columns. Referring to ~~Fig. 14~~Fig. B2, we call the former as terraced (a) and the latter as banded (b). A sequence showing banding during growth at atmospheric pressure, −30 °C, and 8.8% supersaturation is in Gonda et al. (1985). Schnaiter et al. (2018) shows the banding in hollow bullet rosettes from clouds and Nakaya et al. (1958) shows numerous cases on hollow columns and sector-like forms. The bands are much denser in the latter forms. Indeed, terracing and banding are very common in natural snow and hoarfrost.

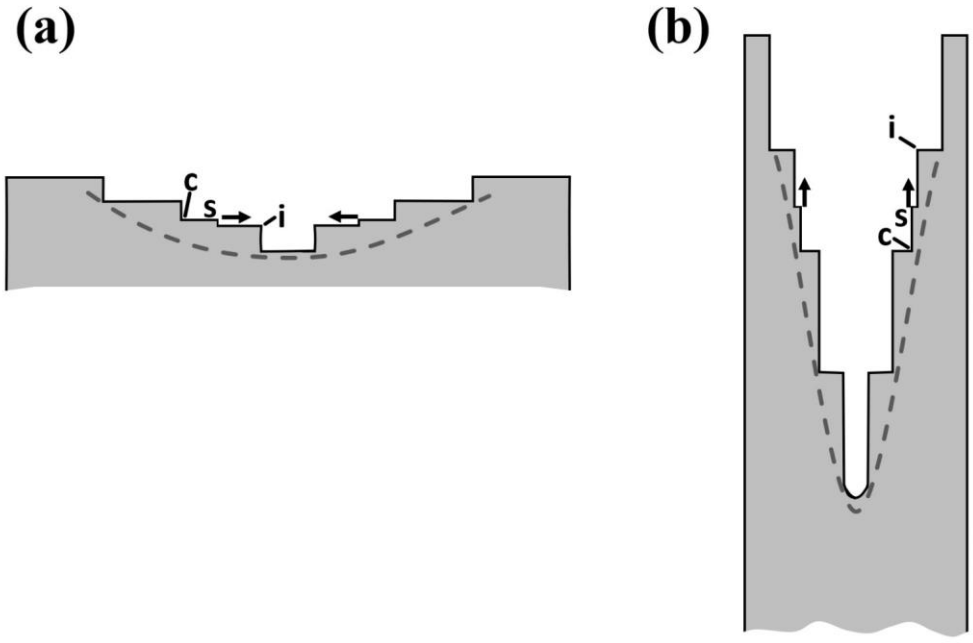

Figure ~~14~~B2: Terracing and banding in hollows. Sketches are cross-sections of top half of crystal, the dashed lines representing previous, smooth profiles. (a) A hollow on a squat crystal with terraces. On a sufficiently recessed terrace, the surface supersaturation increases towards the center from **c** to **i**, and thus single step **s** speeds up as it traverses the face, flattening the terrace. (b) A hollow on a long column or sheath with bands. The large macrosteps with inside corner such as **c** may produce the observed banding. A single step **s** starting between **c** and edge **i** would speed up upon approaching **i**, flattening the band region.

Concerning the formation of a terraced hollow, initially, the inner surface may be smoothly curved, as shown in the dashed line in Fig. B2a~~(a)~~. Starting from such a smoothly curved surface, the closely spaced single steps may clump into large step clumps as described by Mason et al. (1963). In that process, once two single steps become close enough to essentially lock together, they move more slowly, allowing steps further back to catch up. Mason et al. did not include supersaturation gradients, but such gradients may promote the clumping. In this way, a step-clump of two ~~steps~~ quickly becomes a clump of three, and the clumping continues. (Velikov et al. (1997) describes a more complex interaction for step-bunching.) Once a sufficiently tall clump forms, any single step **s** between an inside corner **c** and an edge **i** would speed up as it approached **c**, flattening the terrace as described above.

The banding in a narrow column in Fig. B2b similarly starts with a smooth curve, and may form a macrostep by the same step-clumping process. But in this case, a single step **s** flows from the center out towards the higher supersaturations at the rim. Thus, a step clump at **i** does not need to be high before the flattening effect becomes large because in this case the step is speeding up due to the higher supersaturation even without an edge at **i**. As with the terracing case, as **i** grows, it sticks out into regions of higher supersaturation, meaning that the next single step may travel even faster. Thus, a later step overcomes a previous step, quickly building up a larger macrostep, which would appear as a band in the hollow. The hollowing may start with

a single band, with ~~N~~new bands ~~would~~ forming via the same process as the crystal grows, leading to a series of nearly equally spaced bands.

This treatment suggests that step sources and dynamics, protrusive growth, the moving interface, and the shape of the supersaturation contours all likely influence hollow structure, leading to their highly variable behavior even under constant growth conditions. A similar process of banding may also apply to the 'cross-rib' features (Nelson, 2005) on the backsides of branches on broad-branch and sector-plate crystals. The suggested mechanism in that study was instead changes in temperature or supersaturation around a crystal. These changes would cause the width of the branch to vary, and the same process may also produce some terracing and banding in hollows by temporarily changing the rim width **e–i** in ~~Fig. 13~~Fig. B1d. ~~That is~~In a changing environment, more than one mechanism may alter the hollow structure.

~~3.11~~B.2 Cause of pocket-size variability

~~Consider the variability of the h~~Hollow sizes and shapes are highly variable under low normal growth rates (e.g., on different faces of the crystals in Figs. 11 and 12). Such variability is uncommon at high growth rates, so we outline here a few factors that may play larger roles at the low growth rates at low supersaturations.

One factor is the greater variability in the normal growth rates. In contrast to high-supersaturation growth, the step-sources at low supersaturations are thought to be crystal defects such as dislocation outcrops and stacking faults. The dislocation activities will in general be different on different faces of the same crystal, and between different crystals, and also may change during growth. But other factors may lead to greater variability at low supersaturation. For example, the greater relative role of lateral growth processes at low normal growth rates leads to the phenomena described in the previous section; that is, the interplay between the surface influence and the bulk vapor-diffusion influence may allow more complex nonlinear feedbacks on growth, leading to a greater chance of unstable behavior. This variability may be increased by the variation in dislocation activity, which would have a larger influence at low supersaturation because the surface has a larger direct influence on growth rates under these conditions. Finally, after a given duration, the smaller crystal sizes at low growth rates mean that variability in the initial droxtal size and properties would have a relatively larger influence on the crystal form.

In contrast to the other low-supersaturation crystals shown here, the six planar pockets in Fig. 3 are remarkably similar. The reason for the pocket symmetry is likely due partly to the equal normal-growth rates of all six prism faces. This symmetry in the growth rate must arise from having the same step source on all faces. Given that the crystal has an apparent stacking fault or stacking-disordered region that intersects all prism faces, the obvious step-promoting defect would be the fault. Fault-generating steps had been proposed by Ming et al. (1988) via a mechanism in which the fault yields a lower barrier to layer nucleation. Thus, we suggest that the six pockets open-up at the same time because the step-generation mechanism is the same stacking-fault mechanism on all six faces, producing the same normal growth rates on all faces. (That the fault could both be a source of growth and a location of hollowing is harder to explain, but possible given that the steps would start from the prism–prism edge, not the hollow location.) Concerning the hollow closing-off to form pockets, two factors occur during growth that will likely change the step-separation near the pocket, thus determining whether they close-off. One, the edge supersaturation decreases due to the larger crystal areas, and two, the relative position of the pocket-opening changes on the prism face due to one basal face growing faster than the other (i.e., the side-view in Fig. 3d shows greater advance of the right basal face than the left). As both of these factors will be equal for all six prism faces, the closing-off should occur at the same time, leading to the identical nature of the six pockets. Finally, note that the groove region, which is sublimation-rounded like the edges, did not produce a pocket during re-growth like the corners. The reason for this may be the much smaller radius of curvature in the former case.

~~3.12~~B.3 The droxtal center on t~~Two-level planar formation on droxtals,~~crystals ~~the droxtal center~~

The two-level structure occurs in planar crystals P2–P4 (Kikuchi et al., 2013) grown near water saturation around −15 °C. Some such crystals show a circle at the center, suggesting that the original droxtal largely remained unchanged. But it has been unclear how the original droxtal could remain intact as vapor deposition "filled-out" the crystal. The answer appears in Fig. B3, which shows how this circle shape can remain when the top and bottom basal planes extend by protruding growth. (Takahashi and Mori (2006) also show several cases of such sprouting.) The process of formation via protruding growth has been described by Yamashita (2014), but we include it here due to its close relation to other phenomena we describe.~~Protruding growth occurs on some frozen cloud droplets, or droxtal, causing them to directly sprout thin basal planes, leading to the two-level tabular crystal also known as crystal types P2-P4 (hereafter, we refer to the crystal-type classification in Kikuchi et al. 2013), that retain the boundaries of the original droxtal in the center. Takahashi and Mori (2006) show several cases of such sprouting. Their process of formation has already been described by Yamashita (2014) as a case of protruding growth, but we include it here due to its close relation to other phenomena we describe. See Fig. 15 for several examples of the two-level protrusions on large droxtals as well as single protrusions on rime droxtals.~~

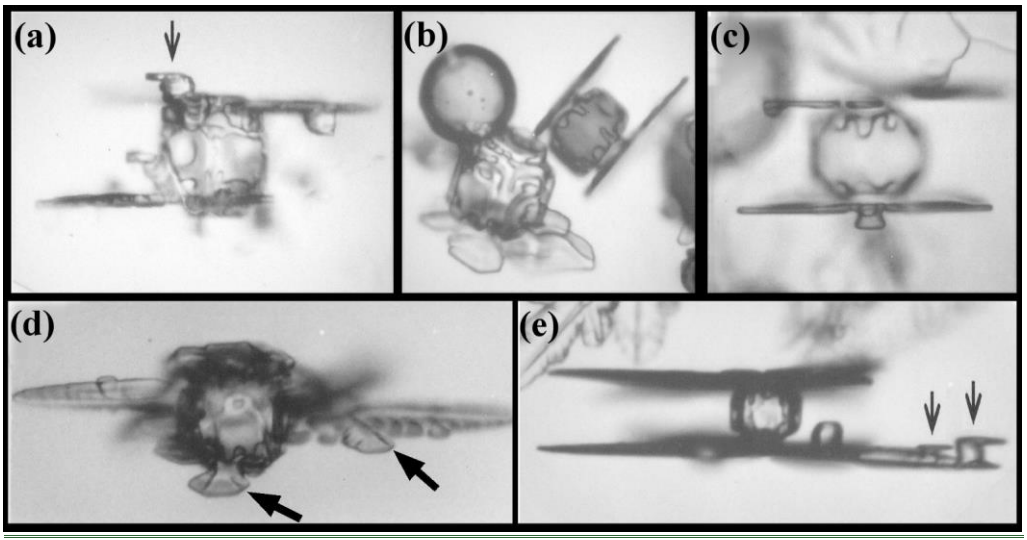

Figure ~~15~~B3: Protruding growth on large droxtals (~40–70 μm) to form the two-level structure near −15 °C. Black arrows in (a) and (e) show protruding growth on smaller rime droxtals. Black arrows in (d) shows complex structure of branch and sidebranch backside. (From the cloud chamber.)

The overall process is sketched in Fig. B4. In (a), the droxtal has just frozen. The latent heat release raises the droxtal's temperature to about 0 °C, but if the droxtal is relatively isolated, its temperature returns to the ambient value within a fraction of a second. Then, the surface quickly depletes the nearby air of vapor, driving down the surface supersaturation to a value that greatly suppresses layer nucleation on the basal faces (Nelson and Knight, 1998). Thus, after the basal facets form on the top and bottom of the droxtal (a–b), they mainly spread. The growth continues as protruding growth in (c), as was the case for corner pockets. But, unlike the corner-pocket case, protruding growth does not occur on the prism faces, and thus the basal protrusions extend out from the boundaries of the initial droxtal, creating two levels. A possible reason for the lateral-type growth being

larger on the basal than the prism may be the proposed larger x_s value on the basal in this temperature regime (Mason et al., 1963). Sketch (d) shows one level grows more than the other, which is due to asymmetry in the vapor-diffusion field around the falling crystal (Fukuta and Takahashi, 1999). As shown in Fig. B3a, and found much earlier by Nakaya (1954), branches can also occur on both levels.

~~The sprouting transition, shown in Fig. 16, can occur in the tabular-growth regime (within a few degrees of −15 °C), where, soon after freezing, the surface supersaturation quickly drops to a value that greatly suppresses layer nucleation on the basal faces (Nelson and Knight, 1998). Thus, after the basal facets form on the top and bottom of the droxtal (a–b), they mainly grow laterally. (Some prism facets also should form, but are not important here.) The growth continues as protruding growth in (c), as was the case for corner pockets. But, unlike the corner-pocket case, protruding growth does not occur on the prism faces (or, at least is much slower), and thus the basal protrusions extend out from the boundaries of the initial droxtal, creating two levels. Sketch (d) shows one level grows more than the other, which is due to asymmetry in the vapor-diffusion field around the falling crystal (Fukuta and Takahashi, 1999). As shown in Fig. 15a, and found much earlier by Nakaya (1954), branches can also occur on both levels.~~

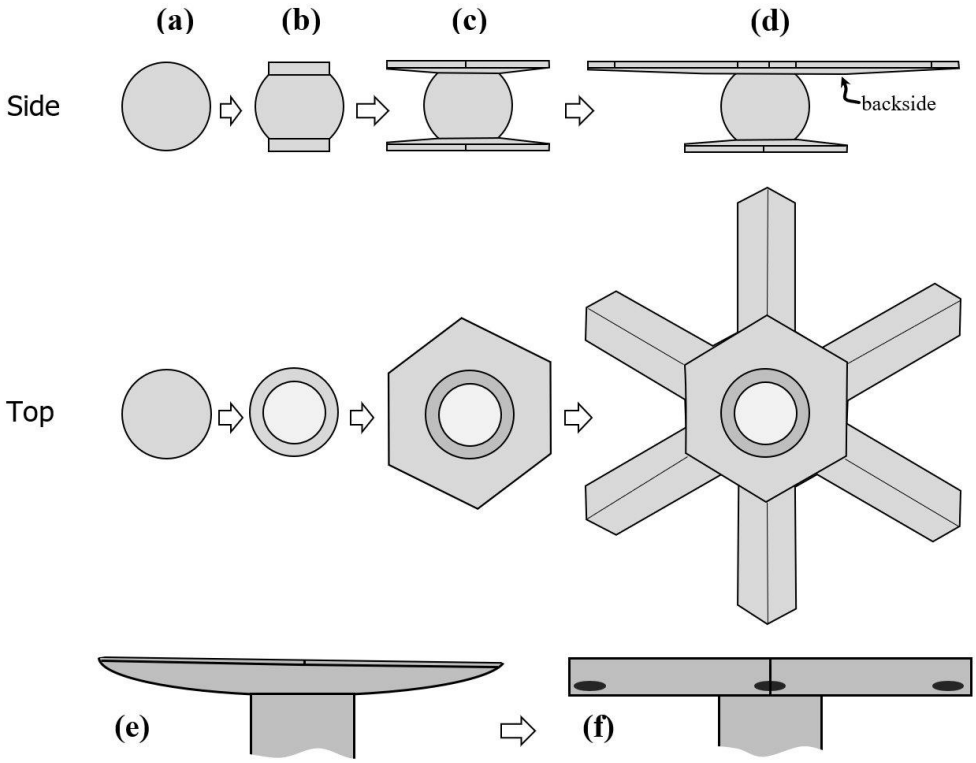

Figure ~~16~~B4: Lateral and protruding growth on a droplet or column under constant or varying conditions. (a)–(d) follow the description first given by Yamashita (2014). Here, the growth on a frozen droplet leads to protruding growth and a two-level snow-crystal. Compare side image in (d) to images in ~~Fig. 15~~Fig. B3, the top image to the snow-crystal shown in ~~Fig. 7~~Fig. 8c.

(e) Cap on one end of frozen droplet or column, showing rounded backside. (f) Same cap after a decrease in growth rate, allowing corner pockets to form. Details of the process between (e) and (f) are not shown, but would be the same as that shown in Fig. 4 except that only one side of the crystal is rounded. This latter process may explain the observed line of pockets on the crystal in Fig. 8c.

Such abrupt sprouting can explain the small center circle observed in some branched snow crystals (e.g., Fig. 8c). Not all branched, two-level crystals show such a "droxtal center". The two levels in such cases likely arise instead via the hollowing-type ("lacunary") process observed by Yamashita (1979) (see also Frank (1982), Nelson (2005)). Bentley (1924) wrote that "at least half" of the 4200 crystals he had photographed in 40 years had such a center circle, and argued that it was the frozen droplet (droxtal) upon which the crystal formed. What factors may cause the droxtal sprouting in some cases but not others? Yamashita (2014) observed sprouting on larger-than-average droxtals. Large initial droxtals may favor sprouting because their larger areas would depress the surface vapor density more than that of a much smaller droxtal, essentially shutting off the normal growth on the basal face. This effect of size may also lead to a greater vapor-density gradient where the protrusion starts, particularly at higher ambient supersaturations that would tend to produce higher supersaturation at the face edge. In addition, the AST flux should be higher when the basal face has larger x_s values. Mason et al. (1963) found x_s to peak in −9 to −15 °C, a temperature near which such two-level crystals sprout. In the recent vertical wind-tunnel experiments of Takahashi (2014), nearly all the images of planar snow crystals clearly show the center droxtal as described here. In those experiments, the crystal nucleated and grew in a droplet cloud of various liquid-water contents. The mean droplet diameter (before freezing) was 8 μm, but inspection of the images indicates that the droxtals that sprouted the two-level crystals had a slightly larger diameter (~9–13 μm). Thus, both relatively high initial supersaturations and relatively large droxtals may favor two-level initiation via protrusive growth.

~~3.13~~B.4 Corner pockets on rounded tabular backsides

The snow-crystal image in ~~Fig. 7~~Fig. 8c appears to show corner pockets on both levels of a two-level crystal. In addition, the smaller inset shows a sequence of small circles along the centerline of a branch, a pattern reproduced on the other branches as well, ruling out the possibility that these are rime. Similar series of circles appear in crystals #11, 12, and 22 in Bentley (1924). In most cases, the circles appear before the crystal branches sprout. These circles may be corner pockets by the following mechanism. During growth, the backside of the plates and branches of two-level crystals show rounded features even without sublimation (c.f., ~~Fig. 15~~Fig. B3d, Shimada and Ohtake, 2016). ~~Instead, a~~A short slowdown in growth may allow lateral and protruding growth from the rounded backside region via steps similar to those shown in ~~Fig. 8~~Fig. 4b–e, but on one side only. ~~Also, t~~The protruding growth from the side is more difficult to picture in this case due to the positioning on a ridge. Nevertheless, the basic process may be like that sketched in ~~Fig. 16~~Fig. B4e–f. If correct, the existence of each pocket marks the time when growth temporarily slowed down.

~~3.14~~B.5 Capped columns, multiple-capped columns, and florid crystals

Capped columns (CP1a, CP1b)– and multiple capped columns (CP1c) form when a columnar crystal ~~grown at near water saturation in a column regime~~ quickly moves into a high-supersaturation region ~~of~~with temperature in a tabular regime. For example, a column growing near −8 °C can be quickly lifted in a vigorous updraft to the thin planar regime starting below about −10 °C. The resulting form is similar to the droxtals with two levels~~, as in~~ (e.g., ~~Fig. 15~~Fig. B3), but with a column between ~~the~~ two basal extensions ~~(e.g., s~~such as a ~~simple~~thin plate or dendrite~~.ic plate.)~~ The left crystal in Fig. B5 shows two thin end caps and another thin, but shorter, central plane in between. At the right is a case where the central plane is longer and all three plates are

thicker than those in the other crystal. The planes in this case may have passed back into the columnar temperature regime. These two are cases of the multiple capped column.

~~One~~A previous model of ~~their~~capped-column formation involves an extreme form of hollowing in which the step-clumping region (SCR) on the prism faces forms near the step origin at the ~~corners~~basal–prism edge (Nelson, 2001). However, that model cannot readily explain the ~~capped columns with~~ central thin basal extensions that occur in the~~, also known as~~ multiple-capped column (type CP1c). Instead, the similarity to the two-level case in ~~Fig. 16~~Fig. B4 suggests an AST contribution to cap formation. If so, what is the source of the originating basal plane on the interior of the column for the CP1c case?

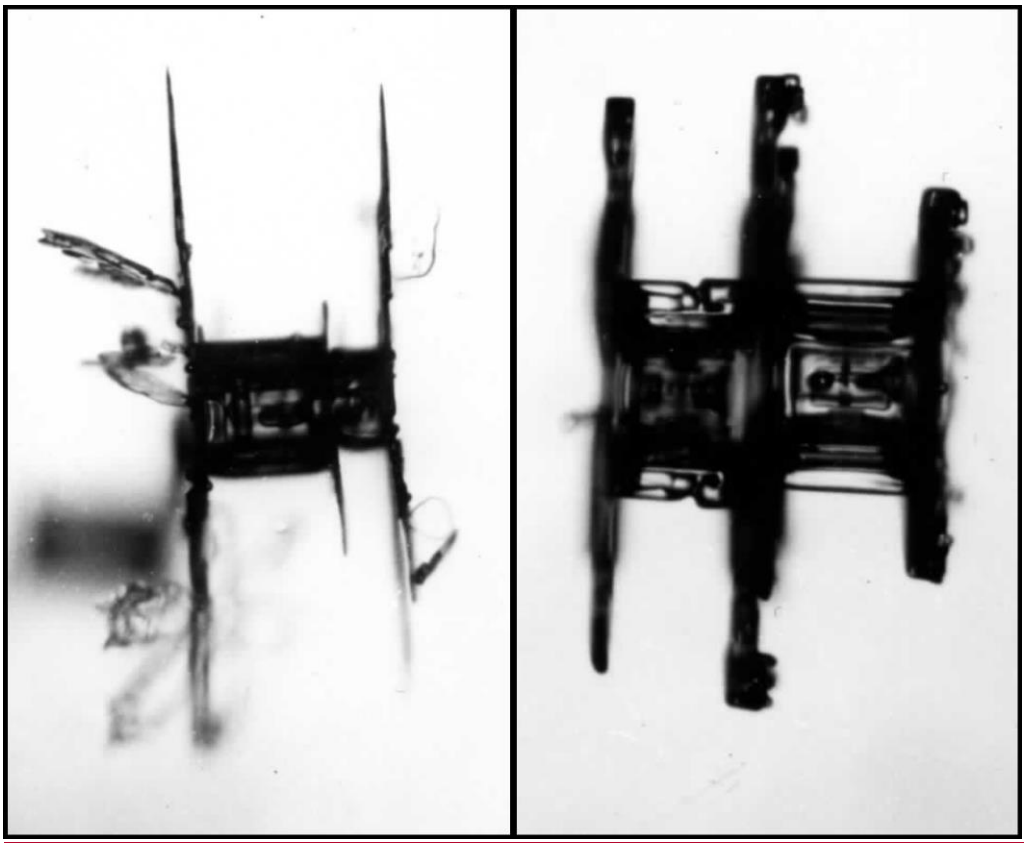

Figure B5: Multiple-capped columns from the Magono–Lee collection (Magono and Lee, 1966).

Formatted: Caption

The basal protrusions on rime in ~~Fig. 15~~Fig. B3a,e (~~narrow~~thin arrows) suggest one possible source of an interior basal extension. As sketched in ~~Fig. 17~~Fig. B6a (top), a rime droxtal could develop a basal face aligned along that of the column (assuming the droplet freezes with the same orientation). The face would grow laterally and then protrude via AST as shown in (b). Once the basal extension starts, it can grow both outward and around ~~much of~~ the column. If the two end caps have a head-start on growth, the rime droxtal nearest the center, being further from the competing vapor sinks, would have a greater vapor flux and thus be more likely to grow out into a larger basal extension. (Otherwise, two basal extensions may form relatively close together, competing for vapor until one grows significantly larger, stunting the other.) The image labeled CP1c in Fig. 1 of

Kikuchi et al. (2013) shows other rime droplets along the column, suggesting this mechanism. Without the rime, it may be unlikely that a high density of new layers could nucleate in the middle of the column, produce an SCR, and sprout a new plate.

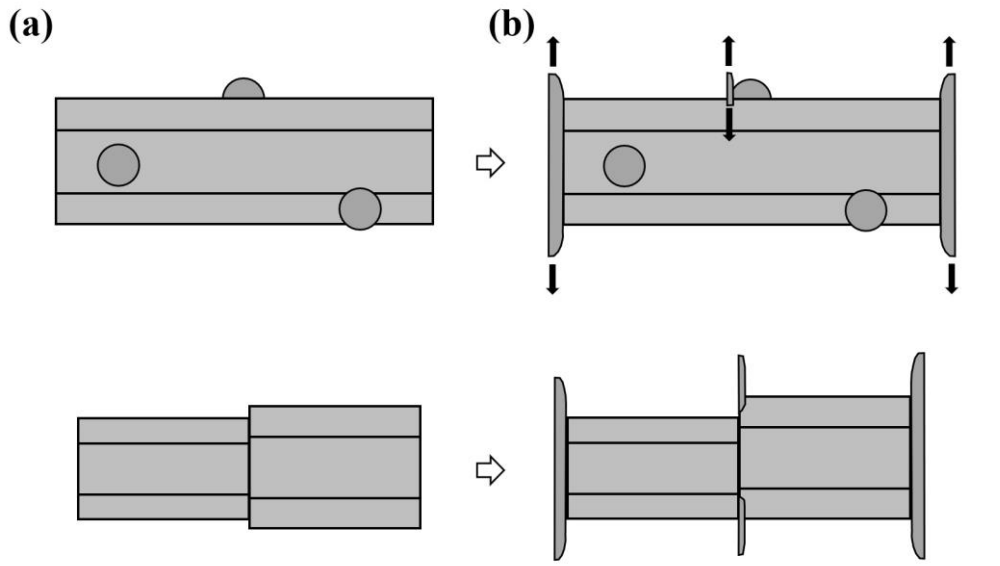

Figure ~~17~~B6: Protruding growth leading to multiple capped-column crystals. (a) A columnar crystal either with rime droplets (top) or some sort of break feature (bottom). (b) Moving into a tabular-growth temperature leads to protruding tabular growth. Black arrows in rime case show that the protruding growth extends outwards in all directions within the plane.

In addition, the examples of CP1c in ~~Magono and Lee (1966), plate 16, show examples in which the columns differ on either side of the center basal extension and do not show evidence of rime. In these cases, the column likely already had~~Fig. 5 show no rime on the column, but a shift in the column that provides an interior basal plane upon which to sprout the extension. ~~before the conditions changed to a tabular regime (e.g., Fig. 17~~Figure B6, bottom, shows how this case may proceed~~)~~. Although we know neither how common such crystals are nor how the interior planes arise, ~~but~~ we ~~know they do occur as the crystals~~show here one such case in Fig. 9 ~~demonstrates~~. Such an interior basal plane could also arise from a small bundle-type column such as a bundle of needles (C1b) or bundle of sheaths (C2b), which are discussed in ~~§3.19~~Appendix B.9. Other cases include a column with a small double-twin (e.g., §4.10 of Kobayashi et al. 1976~~, section 4.10~~), crystals such as those in Fig. 12 (possibly twins), columns with prism hollows, or a column that underwent previous transitions in the tabular regime.

Similar to the capped columns, the protruding growth process may also influence the initiation of tabular extensions on 'florid' crystals or side planes (Bacon et al., 2003). The base crystals (before sprouting) are squatter than the columns for the capped columns, and sometimes polycrystalline. See type P8b 'complex multiple plates' (Kikuchi et al. 2013). Also similar to the capped columns are the bullets with plates (CP2c), which probably form by the same processes. The left crystal in Fig. B5 shows smaller

planes on the end caps in different directions. Such new crystal orientations likely formed on rime droplets that froze in these other orientations, then extending like those in Fig. B6b (top).

B.6 AST contribution to normal growth rates of thin plates, dendrites, needles, and sheaths

To estimate the contribution of the AST flux to lateral-type growth, consider a simple treatment based on the BCF (Burton et al., 1951) model of crystal surfaces. Assume here that the region over the face edge (i.e., the lateral-growth front) is rough, and thus this region can be treated as BCF do for a step edge, that is, as having an equilibrium concentration of mobile surface molecules. Assume further that, as suggested by step-motion experiments (Hallett, 1961), molecular migration over the edge encounters no barrier. In this case, straightforward use of BCF gives a flux of molecules f_L (per edge length) that equals

$$f_L = x_s \frac{v}{4} N_{eq} \sigma_e \,, \quad \text{(B3)}$$

where x_s is the surface migration distance, v is the mean molecular speed in the vapor, N_{eq} is the equilibrium vapor density, and σ_e is the vapor supersaturation near the edge. This result suggests that we can view the adjoining face region within x_s of the edge as a collection region of molecules impinging from the vapor. Assuming that this face edge has n adjacent facets from which to draw the flux, and the edge has thickness t over which the AST flux is distributed, the effective flux (per area) F_{AST} is

$$F_{AST} = n \frac{x_s}{t} \frac{v}{4} N_{eq} \sigma_e \,, \quad \text{(B4)}$$

an amount we compare to the direct vapor flux F_v (e.g., Nelson and Baker, 1996),

$$F_V = \frac{v}{4} N_{eq} \sigma_e \,, \quad \text{(B5)}$$

where the deposition coefficient is assumed to be unity (effectively rough surface), consistent with the assumption of a step edge in the derivation of Eq. (B3). Thus, as a crude estimate, the ratio of AST flux to standard vapor flux is just $n \cdot x_s/t$, with n = 1 or 2 depending on whether the thin edge is bound by one facet, as in a dendrite branch, or two facets, as in a thin disc. In general, n can vary between 1 and 2 when two faces meet on one edge, such as the two prism faces along the edge of a sheath, and may exceed 2 in the case of a thin whisker. In the next two subsections, it will be convenient to view the total flux as equivalent to having an effective supersaturation of $\sigma_{eff} \equiv \sigma_e \cdot (1 + n \cdot x_s/t)$.

Concerning x_s/t, early estimates of x_s from step-motion experiments on the basal face gave a range of values, depending on temperature, of about 1–6 µm (Mason et al., 1963; Kobayashi, 1967). A more recent measurement gives a value of about 5–10 µm at −8.6 °C (Arakawa et al., 2014). For the thickness t, a recent study shows that the tip region of a dendritic snow crystal has a tapered tip (Shimada and Ohtake, 2016; 2018). The measurement does not give a precise value of t exactly at the edge, but an average value within ~10 µm of the edge gives about 0.3 µm. Thus, the estimates of x_s/t here suggest that the AST flux could be up to ~3–60x the direct vapor flux in certain cases. The resulting increase in growth rate from this flux would be less than this factor due to the vapor-diffusion process. ~~Also, the~~Further analysis ~~in Appendix B~~(to be included in part II) suggests that a partial barrier to migration over the edge may exist, and the resulting reflection of some admolecules at the edge would reduce this AST flux. Nevertheless, such a flux could significantly increase the rate of growth (maximum dimension) of thin planar growth forms such as the dendrite (P3b) and fern (P3c) crystals, as well as sheath (C2) and needle (C1) forms.

B.7 Rounding of plates and tips of fast-growth forms

Fast-growing crystals have leading growth fronts that can appear rounded, and some thin tabular crystals can be disc-shaped or scalloped. For example, the sheath extensions in Fig. B7 include some with tips that appear rounded and some that appear flat-faced. Similarly, Knight (2012) observed sheath-needles with rounded tips. Sei et al. (2000) shows rounded sheath-needles sprouting from prism corners that later flatten upon becoming larger. An increase in supersaturation would then cause smaller, round tips to sprout on the larger, flat tips. Round tips also seem to appear on the faster-growing dendrites near −15.0 °C (P3b,c). Gonda and Nakahara (1996) even found such rounding on dendritic crystals grown with their basal face against glass. (However, for the fast-growing dendrite cases, the small scale of the tips makes it hard to discern small facets with limited image resolution, and a slight amount of rounding may quickly occur in brief undersaturated conditions, so the phenomenon is not well-established yet.) Away from the tip, rounding of the side vertices has been attributed to SCR forming due to decaying gradient in surface supersaturation (Nelson, 2001; Frank, 1974). In slower-growing tabular crystals, Keller et al. (1980) observed disc crystals faceting as they became larger and thicker, as did Knight (2012). In our previous experiments (Nelson and Knight, 1996), we also saw small disc crystals develop facets as they grew (Nelson, 2014). Also, Yamashita and Asano (1984) grew rounded tips of "serrated" dendrites at about −2.0 °C, and noted that they were thinner and grew faster than the thicker, facetted tips around −3.0 °C. Thus, rounding can occur in several situations. But, as argued in Nelson (2001), the supersaturations are too low for the phenomenon to arise from kinetic roughening, so we ask if AST may drive such rounding.

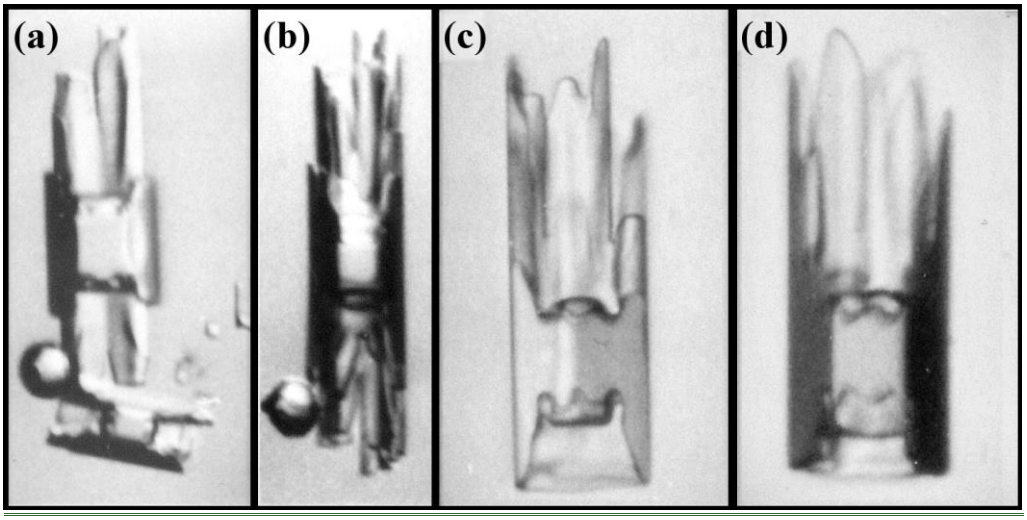

Figure ~~18~~B7: Initial sheath protrusions sprouted from droxtals of ~40–70 μm diameters at −4.8 °C (a,b) and −5.9 °C (c,d). (From the cloud chamber.)

Consider first a thin tabular crystal with two basal faces, focusing on the region near a prism–prism edge as sketched in ~~Fig. 19~~Fig. B8a. As shown in the top sketch, the collection area for AST flux at the tip **c** has an angle of just 120° compared to the 180° further down (at least a distance of ~x_s) at **e**, making the AST flux ~2/3rds the value at the tip. If the total molecular flux is dominated by the AST flux, then this effect would move the point of highest total flux away from the tip. Equivalently, we can

view position **e** as having higher effective supersaturation than **c**. Thus, as shown in the bottom sketch, the point **e** of new-layer nucleation has moved down from the tip. Moreover, if the edge region is effectively rough, then the regions of higher effective supersaturation will advance faster than regions with lower values, changing the vertex or tip shape until a steady-state shape emerges. Such a shape would be rounded, as shown in the sketch. Thus, if the crystal edge is nearly rough, then AST flux can cause the corner or tip to round as steps travelling from their source at **e** to further down the tip toward **c** can readily clump. In this case, $n = 2$ due to AST flux from the top and bottom basal faces. Thus, the edge plan view may be similar to that shown at the top in Fig. B8b.

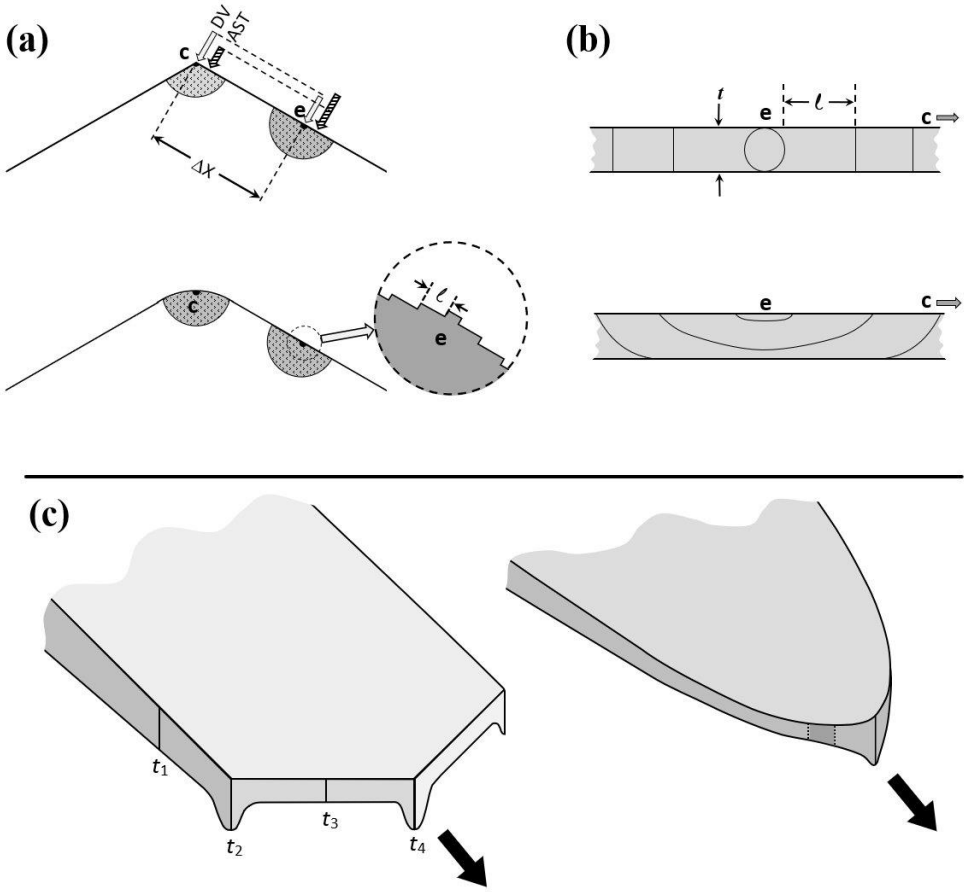

Figure ~~19~~B8: AST-induced rounding. (a) Direct vapor flux DV and AST at the corner **c** and edge **e** of a thin tabular crystal. Shaded regions are effective collection regions for AST flux, arrows show relative magnitudes. Inset at bottom is shown in top case of (b). (b) Nucleation and step flow on edge region of thin crystal in (a), plan view of edge. Top sketch is symmetric case. Layer-nucleation point **e** of (a), has steps moving away with initial separation l. ~~Middle~~Bottom sketch shows asymmetric case leading to step separation $l \sim t$. ~~Bottom sketch is step configuration used in calculation in Appendix B. The small circle is a closed step loop, used to approximate collection by a straight step of length t, the crystal thickness.~~ (c) Thin-branch case with

non-crystallographic backside. Thickness t is greater at the vertices t_2 and t_4 and thus has less growth from AST flux. Rounded case at right with small prism face bound by dotted lines.

A dendrite branch has a different tip shape, with the edge prism faces bound by just one basal face, the other being non-crystallographic. Thus, the edge plan view may be more like that at bottom in Fig. B8b. In this case, a second factor may cause the vertices to round. As sketched in (c), the leading prism faces are expected to be thicker at the vertices, that is, $t_2 > t_{1,3}$ and $t_4 > t_3$. (Although the thickness variation right at the perimeter was not detected by recent interferometry studies (Shimada and Ohtake, 2016; 2018), the formation of a main ridge and side ridge, which are clearly visible in nearly all tips, appear to require such an increase in thickness.) Their formation mechanism, as described in Nelson (2005), relies upon the influence of the direct vapor flux. But if their growth is also significantly influenced by AST flux, and they are thicker at the vertices, then Eq. B4 shows that their growth rates will be slower. In this case, they may advance more slowly at the vertices, leading to the rounding shown in (c).

These rounding mechanisms depend upon the prism faces being nearly rough. ~~Section 3.22 discusses various mechanisms for such roughening, but o~~One possible factor is illustrated by the ~~middle~~bottom sketch in ~~Fig. 19~~Fig. B8b. Here, layers nucleate at one basal–prism edge and can reorient parallel to the edge with a separation l of roughly the crystal thickness t, which may make the edge effectively rough. For a face to essentially collect all surface ad-molecules, the step spacing l need only be smaller than x_s. But if the spacing becomes significantly smaller than x_s, the normal growth rate becomes proportional to the local effective supersaturation (as all the flux is incorporated into the crystal), meaning that a decrease in this supersaturation would cause the surface to respond, producing rounding. Such a case is akin to the kinetic roughening that is driven by high supersaturations (Elwenspoek and van der Eerden, 1987), but in this case the supersaturations are ~~too~~relatively low.

Although AST ~~is~~ may be a ~~likely~~key factor in some of these cases of crystal rounding, rounding in general on vapor-grown ice is more complex than ~~the~~our simple ~~arguments above~~treatment here. In different situations, c~~C~~rystal rounding on vapor-grown ice may involve a combination of the above AST mechanism, ~~supersaturation gradients, defects,~~thermal roughening, a thin solute layer, and perhaps yet undiscovered factors.

~~3.17~~B.8 Tip shapes of sheath and sharp needles

Other aspects of tip shape may also influence the normal growth rates of needle crystals. Needle crystals (C1a) are long, thin, columnar crystals with "tops shaped like a knife edge" (Kikuchi et al., 2013) that form near −5 °C. In their initial growth, they appear as narrow prism planes that sprout from the edges of the basal plane, similar to the sprouting of basal planes during the formation of two-level crystals ~~(§3.12)~~examined above (§B.3). Examples shown in ~~Fig. 18~~Fig. B7, as well as in Sei et al. (2000), suggest that they initiate via ~~protrusive~~P-growth. Knight (2012) observed both sheath-needles and, less often, a newly reported type he called sharp needles. The sheath needles would grow at a rate of about 0.3–1.0 μm/s, whereas the sharp needles grew about twice as fast, about 1.5–2.5 μm/s. The sharp needles also had a smaller diameter and appeared more nearly round in cross-section. Why did they have different tips and why the distinct growth rates?

The different tip shapes may be the reason for the bimodal growth rate. ~~Given that both~~If each side (prism plane) of the needle tips are ~~likely to be~~ of order 10 μm or less, the AST flux ~~is likely to~~can be significant, perhaps even dominant. The net effect of this flux should depend on the ratio of the collection area (on the adjoining prism faces) to the growth-front area. Consider the two tip shapes at the bottom of ~~Fig. 20~~Fig. B9. The left case, with the 120° interior angle, ~~appears to be the same as~~is like the sheaths in ~~Fig. 18~~Fig. B7, whereas the right has the 60° angle like that of "iii" in the right scroll of ~~Fig. 21~~Fig. B10b in which one prism face is missing. If the arrows represent the AST flux, then the right case of ~~Fig. 20~~Fig. B9 has almost twice the AST flux

to the growth-front area at the tip (dashed circle) than the left case; that is, n is near 1 on the left, but almost 2 on the right. Another factor is the influence of the backside of the tip on the surrounding vapor density. The backside, being non-crystallographic, is effectively rough and thus efficiently draws in vapor. Neither the front-side prism faces ($\boldsymbol{p}_1$,$\boldsymbol{p}_2$ or $\boldsymbol{p}_1$,$\boldsymbol{p}_5$) nor the tip are collecting much mass from the vapor. But for a given length of needle, the open sheath on the left has a greater backside area than the proposed sharp needle on the right. This backside may dominate the mass-uptake, just as it appears to do on dendritic crystals (Nelson, 2005). With the smaller area for the sharp-needle case comes a smaller mass uptake, and with a smaller mass uptake, a higher surface supersaturation and higher normal growth rate. In this way, the sharp needle should grow significantly faster than the sheath needle, as was observed. An approximate calculation (to appear in part II) finds these effects cause an increase in rate by about 50%. A possibly larger effect, though harder to accurately model, may come from the direction of the supersaturation gradients between the two needle cases. This gradient is likely larger in the sharp-needle case due to the smaller interior angle, which would have the effect of sharpening the needle, which in turn could greatly increase its growth rate.

Consistent with ~~this argument~~our hypothesis that the two case have different interior angles, Knight (2012) found that when the temperature of the sharp needle was raised to slow down growth, it thickened enough to discern that it had a triangular shape (Fig. 4 of Knight, 2012). This 60° interior angle of the proposed sharp needle is a feature of trigonal crystals. In Appendix ~~§3.21~~B.11 below, we argue that this angle is stable in the columnar regime, which includes the needle case.

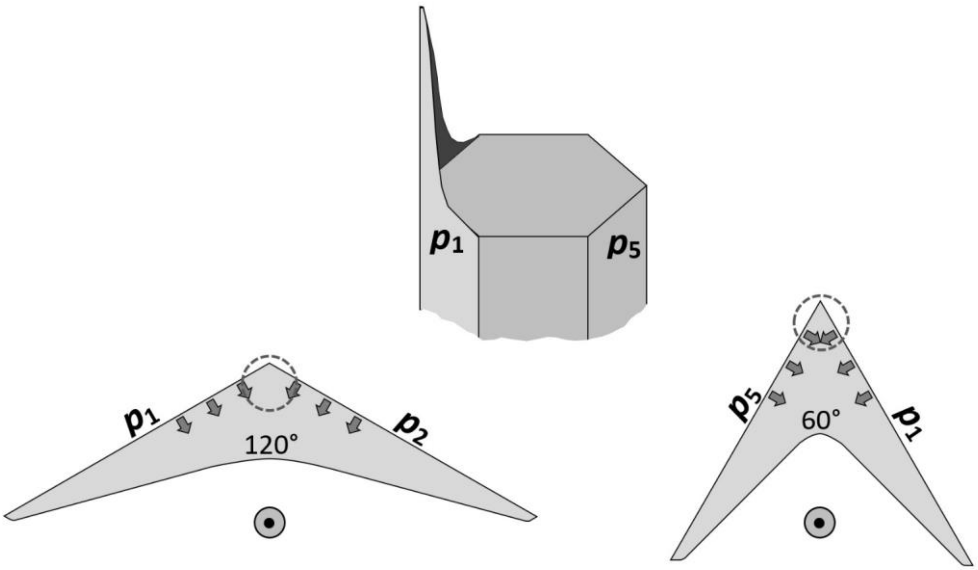

Figure ~~20~~B9: Needle-tip cross-sections. Prism face $\boldsymbol{p}_1$ through $\boldsymbol{p}_6$ run clockwise around crystal sketch in middle-top. Bottom shows views looking straight down. Left: case from sheath with prisms $\boldsymbol{p}_1$ and $\boldsymbol{p}_2$. Right: case from sheath initially with prisms $\boldsymbol{p}_1$, $\boldsymbol{p}_6$, and $\boldsymbol{p}_5$, but middle prism $\boldsymbol{p}_6$ vanished. Arrows show AST flux from adjoining prism faces.

B.8 Scroll crystal features

A perplexing growth feature is the scroll (C3c). With a scroll feature, thin prism-face "sheets" or side-planes tend to curl inward while maintaining a prism orientation, somewhat resembling a paper scroll as shown in Fig. B10. (For formation sequences, see Figs. 3 and 5 in Sei et al., 2000.) In the atmosphere, the original Nakaya diagram (e.g., Nakaya et al. 1958) shows scrolls forming at and above water saturation near −7 °C, which is consistent with later diagrams by other authors. Later, Nakata et al. (1992) found scrolls to be very common features of certain polycrystals (Gohei twins, CP7a). But perhaps one of the earliest descriptions of a scroll is in Seligman (1936), where he finds large examples in crevasse hoar. However, with the aid of a standard macro lens on a common digital camera, one can observe them frequently in hoar frost. A description of their formation is briefly mentioned in Higuchi et al. (2011), but their proposed mechanism differs from that presented next.

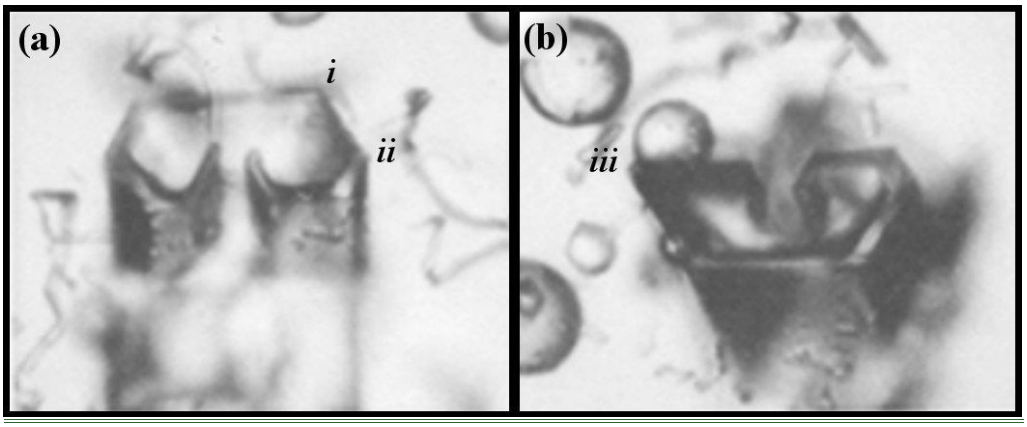

Figure ~~21~~B10: Scrolls formed on crystals of approximate diameter of 60 µm. (From the cloud chamber.)

The scroll may start as a protrusion, like a sheath, except on a larger-area basal face as shown in ~~Fig. 22~~Fig. B11a. When this protrusion is thin, it can grow rapidly because the AST flux is depositing onto a small-area region at the growth front. (Growth may be more rapid normal to the page, but we focus on the side growth.) This rate is marked by the large arrow pointing across prism p_2 in (a). But normal growth is also occurring on the backside (or inside), causing it to gradually thicken. (In this description, we assume that the backside, or inside, of the scroll is mostly non-crystallographic.) This normal growth rate is marked by the smaller arrow pointing down, towards the basal interior. On the leading front of the protrusion, direct vapor flux is also contributing to growth, but when the feature is thin, this flux is overcome by the larger AST flux from prism p_2 (Eq. B4). Eventually ~~though~~, this protrusion thickens enough to reduce the protruding growth rate, at which point ~~lateral growth on the front can form~~ prism facet p_3 can form and spread there, essentially ceasing the lateral growth of p_2 as shown in the sketch. Now the process starts on the edge of these new prism faces, causing new protruding growth at 60° to the old protrusive growth ~~as shown at~~(-right side), and the process repeats, later curling around another 60° into a scroll-like shape. Each new "wing" of the scroll may have a smaller area due to it moving ~~interior of the structure where the~~towards lower vapor density, ~~is less, and thus the protruding growth rate is less~~allowing the edge-front faceting to start sooner. ~~This~~Such a process would ~~lead to the observed~~produce a curling feature ~~of scrolls. Compare vertices *i* and *ii* in Fig. 21a and Fig 22a~~.

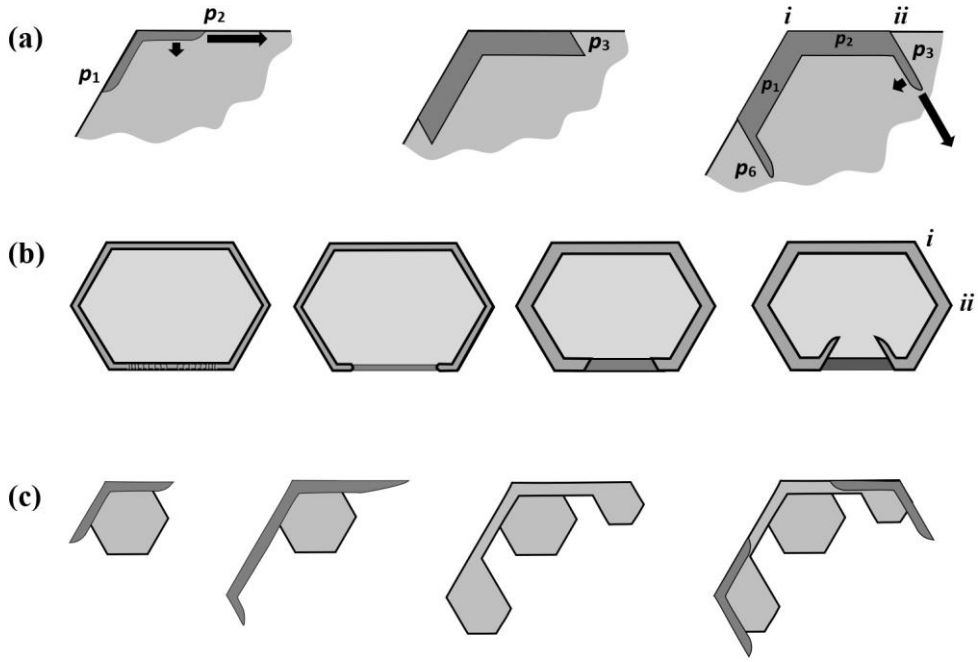

Figure ~~22~~B11: Scroll and sheath bundles via protruding and normal growth. (a) The basic process, viewed along c-axis (normal to basal). The darker region is a sheath protrusion from prisms p_1 and p_2 going up out of the page. Arrows indicate relative rates of growth in width (via AST) and thickness (via normal growth). In middle sketch, protruding region has thickened, slowing the rate of protruding growth, allowing significant lateral growth on the ends that leads to new prism facets p_3 and p_6. In the right sketch, protrusion growth occurs on these new prism faces. The process can continue (not shown), generating facets p_4 and p_5. Compare ***i*** and ***ii*** vertices to ones in ~~Fig. 21~~Fig. B10. (b) A complete sheath has its rim broken at the bottom (left), due to a vapor-density gradient or asymmetry. The process in the next three sketches follows the same process as explained in (a). Vertices ***i*** and ***ii*** correspond to those in ~~Fig. 21~~Fig. B10. (c) Possible source of sheath and needle bundles from protruding-growth overshoot. Leftmost sketch follows from start of case (a) except protruding growth overshoots the base. (Overshooting is exaggerated to clarify the concept.) In middle sketches, the edge of the protrusion thickens and facets as in case (a). Far right, process repeats.

A scroll may also initiate from a cup-type crystal form or sheath (C2a) after part of its rim forms a break, which may in turn be due to an axial asymmetry in the nearby vapor-density field. As sketched in ~~Fig. 22~~Fig. B11b, the sides of the break (at bottom) could then curl around via the same process as that sketched for (a). Supersaturations high enough to produce cup crystals are rare in the atmosphere, but are very common near hoar frost. As hoar cup crystals tend to be closely clustered, and thus having large local variations in vapor density, this initiation process may be likely for hoar scrolls. Large examples of this type are in Knight and Devries (1985). This ~~case also more closely resembles that~~mechanism may have produced the crystal in ~~Fig. 21~~Fig. B10a (compare vertices *i* and *ii*).

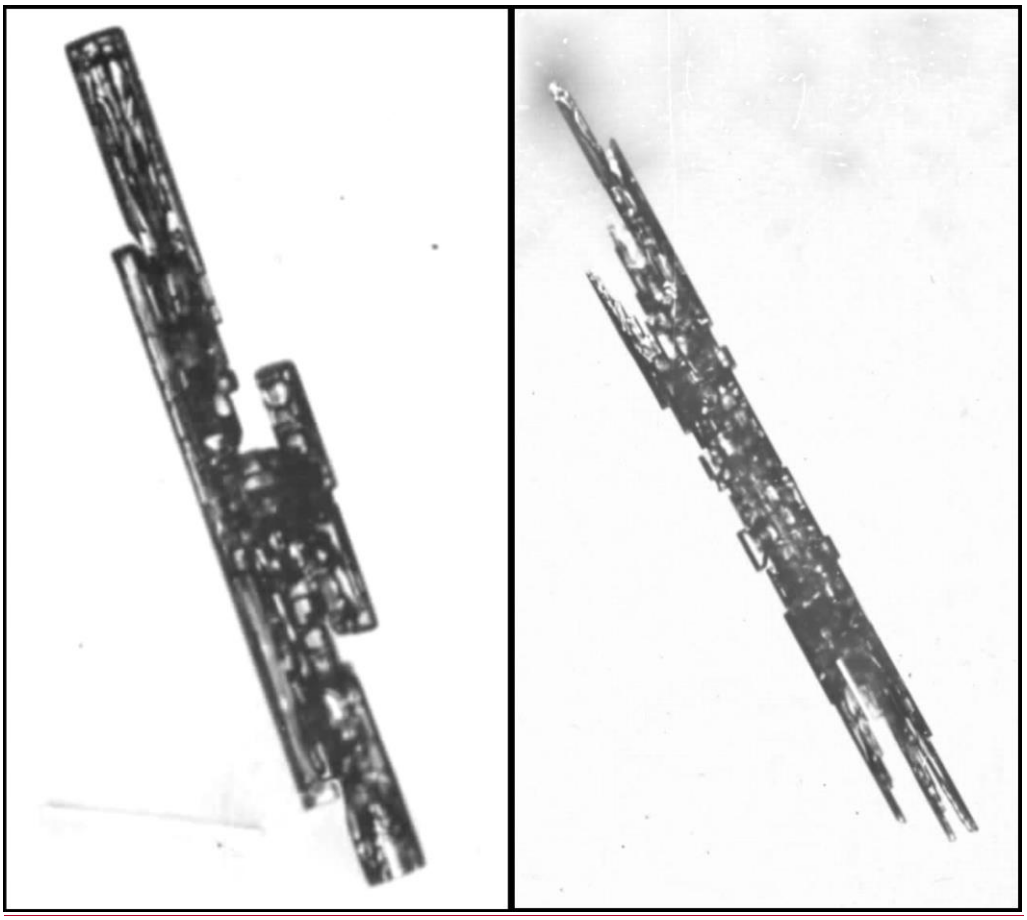

Figure B12: Bundle of sheaths (left) and bundle of needles (right) from the Magono–Lee collection (Magono and Lee, 1966).

Another perplexing growth form is the bundle of sheaths (C2b), and similarly, the bundle of needles (C1b). These habits form in a narrow temperature regime near −5 °C where growth is almost exclusively in the c-axis direction (e.g., Takahashi et al., 1991). However, unlike the needles, these crystal forms have widened significantly perpendicular to the c-axis. Such widening is hard to reconcile with our knowledge of growth driven by layer nucleation, which may effectively shut off all normal growth of the prism faces. Two mechanisms may overcome this nucleation barrier. One is riming. A rimed drop on a prism plane may then sprout a new sheath protrusion along the c-axis. The second mechanism is sketched in Fig. B11c. In this mechanism, the protruding sheath widens as in the scroll form in (a), but overshoots the base crystal, thus advancing the crystal width perpendicular to the c-axis. The protrusion will thicken, and may then develop a new prism face by the mechanism suggested in (a) for the scroll. In this way, a new sheath or needle can develop to the side of the original, producing a "bundle". Such overshooting of the prism planes in this case is analogous to the overshooting of the basal planes in the two-level crystal (§B.3).

B.10 Protruding growth on branch backsides and ridge pockets

The backsides of branches on tabular crystals appear to be largely non-crystallographic during growth under constant conditions. But they are not gently curved; rather, various ridges and ribs are common, which show up as dark interior lines in images. However, when part of a relatively fast-growing crystal branch slows down, due to either a change of conditions or to the gradual drift toward the crystal interior as the outer parts grow out, the ridges and cross-ribs may form planar protrusions. For example, such protrusions appear relatively common on the slower-growing planar crystals in Takahashi (2014) at temperatures of −12.5 and −16.3 °C. Libbrecht (2006) refers to them as "aftergrowth plates", though they form while the crystal is growing. ~~An e~~Examples ~~is shown~~are marked with arrows in ~~Fig. 23~~Fig. B13a. Also, fairly common are long pockets that we call ridge pockets. Ridge pockets include the main-ridge pockets aligned towards the vertex and coming in a pair, as well as the side-ridge pockets aligned toward each side and generally having numerous pairs. Several examples appear in ~~Fig. 23~~Fig. B13b. This image shows main-ridge pockets at A (enlarged inset upper left) and side-ridge pockets at B.

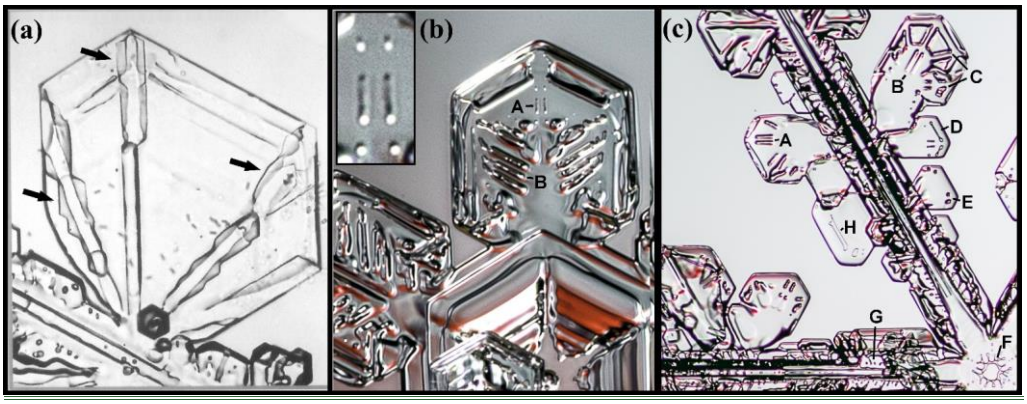

Figure ~~2~~B13: Protruding growth on branch backsides and branch pockets. (a) Sidebranch of dendrite. Arrows show protrusion features on ridges. (b) Branch of broad-branch crystal. Inset is close-up of main ridge pockets A on one branch, B marks side-ridge pockets. (c) Branch of dendrite. Sublimation has apparently exposed several pocket features A–H described in text. Image in (a) from large hoar crystal grown in an unforced air-flow cloud chamber of Yamashita and Ohno (1984). Crystals in (b) and (c) from snow crystals collected at ground level (courtesy of Mark Cassino).

The dendrite branch in Fig. B13c shows numerous pocket features. (This crystal has undergone significant sublimation just before imaging, and thus most of the pockets appear to have re-opened. But it provides clear examples of pockets seen on other crystals.) Here, A and B mark main ridge pockets. C marks an example in which pockets can form where a main ridge meets a thickened cross-rib. At bottom is a pocket and at top is a position that may produce a pocket by such an intersection. D appears to be an elongated edge pocket (§4.6). E and G appear to be side-ridge pockets, and F is a center ring pocket (Yamashita, 2018). H may be a center pocket or an edge pocket like D. The main ridge pockets at B fade towards the main branch, indicating that the base of the pocket has a downward slope towards the tip. In images such as these, which show only one view, it is difficult to be sure that the features are pockets as opposed to channels or small hollows. Nevertheless, they appear to be common and whether or not they are pockets or channels, their effect on scattering may be similar.

The ridge pockets may form as sketched in ~~Fig. 24~~Fig. B14. The branch backside often has a main ridge from the tip, shown in cross-section at (a). As pointed out by Frank (1982), the ridge produces a vapor-shadowing effect leading to the two parallel

channels to both sides in the next sketch. These channels are clearly seen in images of most branched snow crystals and was noticed much earlier by Nakaya (1954). With a local growth slow-down, which may arise simply due to the branch tips growing further out, thus depleting the crystal inner regions of vapor, lateral growth may start to dominate, creating the protruding growth in the next two sketches. This may continue and eventually close-off the channels making the two main ridge pockets at the bottom in (a). The mechanism for side-ridge pockets is sketched in (b). The process is like that of the main ridge, except side ridges can form close together, creating a central channel gap. Protrusion growth at the crest starts bridging the gap, and completes the pocket at the bottom. These sketches do not show the 3-D structure of the branch, in which the top surface slopes downward towards the thinner outermost prism faces at the tip. Thus, the protrusions likely also grow from the interior region towards the tip (as in the corner-pocket case), eventually covering the entire backside.

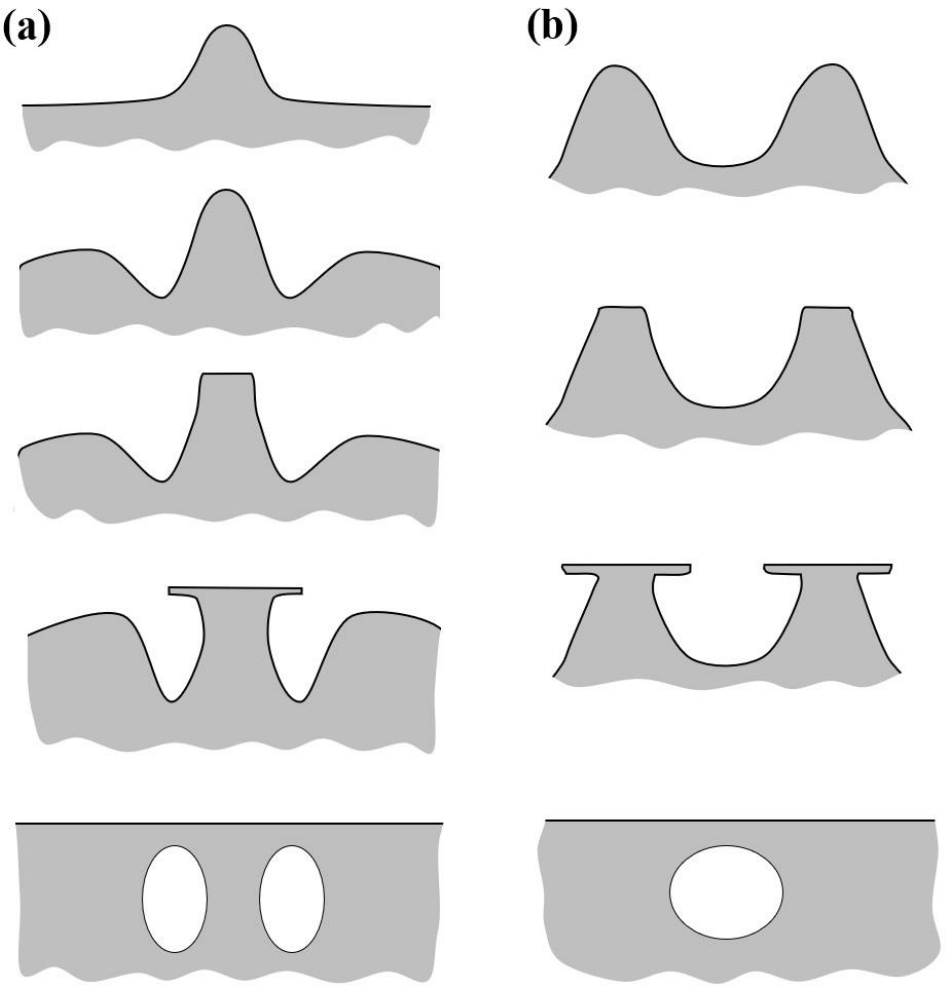

Figure 2B14: Development of ridge channel pockets. (a) Adjacent to main ridge. (b) Between side ridges. Compare to A and B in Fig. B13b.

3.21B.11 AST contributions to trigonal formation and primary habit

Trigonal crystals have only three clearly observable prism faces, a striking feature that begs for an explanation. Another crystal type with three-fold symmetry is the scalene hexagonal, which is shown together with the trigonal type in Fig. B15. Bentley (1901) finds both types rare in precipitation, but Heymsfield (1986) reports on a very cold cloud in which roughly 50% of the crystals had three-fold symmetry. In the laboratory, Yamashita (1973) found that numerous trigonal and scalene forms

would result from seeding with an adiabatic-expansion method to create sub-micron ice nuclei, but only hexagonal crystals would result from nucleating cloud droplets of much larger size. This finding may explain the difference in Bentley's and Heymsfield's findings because the latter observations were of crystals that likely formed on sub-micron droxtals. In Yamashita's sub-micron seeding experiments, the crystals grew at temperatures down to about −26 °C. The trigonal forms appeared stable when columnar; for example, about 10–20% of all crystals were trigonal in the columnar regime above −10 °C. But the trigonal tabular forms appeared to transition to the scalene hexagonal at small sizes, with the latter types occurring in over 40% of the crystals at all temperatures except around −12 to −18 °C. In all cases the trigonal were more common than rhombohedral and pentagonal forms.

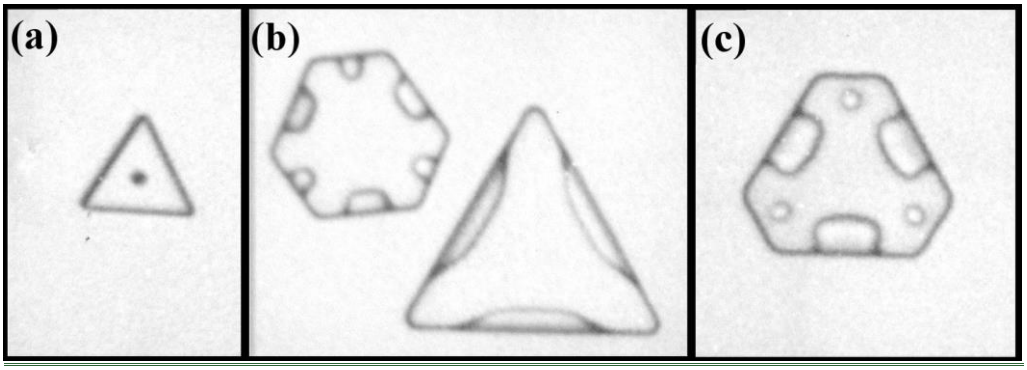

Figure ~~2~~B15: Trigonal and scalene hexagonal. (a) Trigonal. (b) Both types. (c) Scalene hexagonal. Crystals grown for about 310 s at −10.2 °C in the cloud chamber. Diameters are about 15–35 µm.

A recent review proposes three possible explanations for trigonal formation (Murray et al., 2015). In one, they suggest that stacking disorder can lead to growth of trigonal forms, but do not give a specific formation mechanism. ~~Concerning a possible mechanism, s~~Stacking faults in cubic crystals can produce trigonal forms (e.g., Millstone et al., 2009), but the mechanism involves growth on alternating re-entrant corners that have not yet been shown to occur in stacking-disordered ice. Also, it is not clear how such a mechanism would explain Yamashita's observations above. ~~Moreover, o~~Our observations here (discussed in §B.2) suggest that regions of stacking disorder may instead lead to near-symmetric hexagonal forms (e.g., Fig. 3)~~). Thus, the stacking disorder mechanism is both implausible and contrary to observations.~~ Another explanation involves having equivalent dislocation step sources on just three alternating prism faces (e.g., Sei and Gonda, 1989; Wood et al., 2001). Such a mechanism cannot explain the preponderance of trigonal over rhombohedral and pentagonal forms. The third explanation involves aerodynamic factors (Libbrecht and Arnold, 2009) that would influence habit more for tabular and larger crystals. Such an explanation also appears inconsistent with Yamashita's findings above, specifically the greater stability of the trigonal form on columnar ~~forms~~habits and the transition from trigonal to scalene hexagonal as the tabular forms grew larger. Instead of these proposed explanations, we suggest a closer look at the growth mechanism, focusing on two factors: a mechanism for their initial formation in sub-micron droxtals, and a mechanism for their stability as they grow larger.

A possible explanation for the formation of an initial trigonal habit from a sub-micron droxtal is sketched in Fig. B16a–d. When the sub-micron droplet freezes, one prismatic plane forms first. Assume, as in sketch (b) that it is $\boldsymbol{p_1}$ on the left side. If the crystal is smaller than x_s, facet spreading of $\boldsymbol{p_1}$ may be dominated by AST yet increase in rate as the

face expands. This rate would increase in proportion to the increase in area because all the vapor impinging on the area can migrate to the edge. Thus, lateral growth would greatly favor the first face that develops. Moreover, this growth may overshoot, and effectively bury, the neighboring faces p_2 and p_6. If the next face that develops is either p_3 or p_5, then face p_4 would be similarly buried as shown in (c). As p_3 and p_5 expand, the crystal fills out as a trigonal form with only p_1, p_3, and p_5 faces as shown in (d). In this way, if after step (b), the three remaining faces were equally likely to form next, then the likelihood of a trigonal would be twice that of a crystal with four prism faces. Experimentally, the trigonals formed much more frequently than those of the rhombohedral and pentagonal (except at −4.2 °C), and thus the formation of the second prism face may depend on the formation of the first. For example, the region marked **u** in sketch (b) may immediately develop into p_3 (ditto for p_5 on the other side), leading to trigonal in all cases. Or, a small crystal with four prisms may be unstable compared to one with three. Regardless, the basic mechanism would lead to trigonal crystals in most cases.

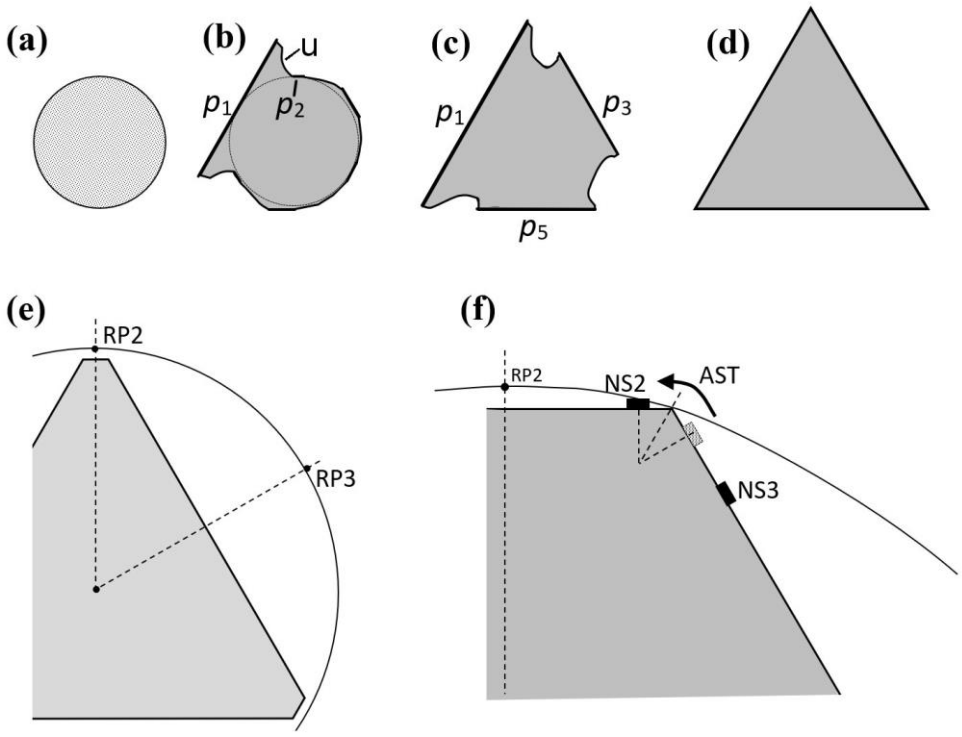

Figure 2B16: Formation and growth of a trigonal crystal. (a) Droplet before freezing. (b) Upon freezing, Pprism face p_1 forms before the others, growing laterally via AST, stunting neighbors p_2 and p_6. The region "u" may have a range of slopes, sometimes lining up along p_3. (c) Prism face p_3 or p_5 develop next, also stunting p_4. (d) Trigonal forms. (e) Vapor density contour around nearly trigonal form (scalene hexagonal) with small prism faces. RP2 and RP3 are points on p_2 and p_3 where a reflection-symmetry plane crosses the contour. (f) Close up of corner between prisms p_2 and p_3. Solid boxes are the layer nucleation sites NS2,3. Shaded box on p_3 is the nucleation site in the absence of AST.

The trigonal form may then be maintained via an effect of the vapor-supersaturation contours on layer nucleation. The supersaturation contours around the crystal, viewed in the plane of Fig. B16e, should have the same symmetry as the crystal. In the sketch, the contour is a circle, but in general needs to only have reflection symmetry about the dashed lines from the center to points RP2 (reflection-symmetry point, face 2) and RP3 as shown. (Far from the crystal, the contour will be a circle, but closer to the surface, the lines will bend closer to the surface as suggested in (f). The consequence is the asymmetry in the contour about the vertex between $\boldsymbol{p}_2$ and $\boldsymbol{p}_3$, as shown. Assuming that the growth is via layer nucleation, with layer nucleation points near to, but not exactly at, the vertex, then such points on either side of the vertex will experience different vapor supersaturations. In particular, point NS2 on face $\boldsymbol{p}_2$ will have greater supersaturation and thus nucleate new layers at a faster rate than at the corresponding point on face $\boldsymbol{p}_3$. This factor will increase the normal rate of growth of $\boldsymbol{p}_2$ over that of $\boldsymbol{p}_3$.

This factor, though small, can be amplified by AST. Consider that the rate of layer nucleation depends on the density of surface-mobile molecules, not the adjacent vapor density directly. Thus, as indicated in (f), the faster production of new layers at NS2 will draw a net AST flux from face $\boldsymbol{p}_3$, thus reducing the surface ad-molecule concentration there. As a result, the layer nucleation point NS3 must move further away from the vertex, as shown in the sketch, further reducing the layer-nucleation rate on face $\boldsymbol{p}_3$. In this way, the normal growth rate of $\boldsymbol{p}_2$ can significantly exceed that of $\boldsymbol{p}_3$ even with a relatively small vapor-density asymmetry, driving its area lower. The difference in growth rates between the faces may lead to the smaller face becoming relatively smaller or larger, depending on the ratio of the rates. (With a little trigonometry, you can readily work out the condition for a relative decrease.) But if the face area shrinks, the effect here may increase, causing further shrinkage; conversely, if the face area grows, the effect may weaken, leading first to the scalene hexagonal and then to fully hexagonal. This AST effect on the relative layer nucleation rates between adjoining faces was previously proposed by Frank (1982) to explain the abruptness of primary-habit change with temperature. As he suggested, it should apply in general to the basal–prism edge as well, influencing the primary habits (aspect ratios) of snow crystals in general.

About the higher stability of columnar trigonal forms, consider the magnitude of the effect. The magnitude should depend on the size of the mean migration distance x_s on the prism faces compared to the crystal size. When the value of x_s is a significant fraction of the large-face diameter (e.g., 0.1 or more), the effect is likely to be stronger as NS3 is pushed further from the vertex. In contrast, when x_s is much smaller, then the shift of NS3 will be insignificant. The values of x_s for the prism face are unknown, but Mason et al. (1963) argued that ~~in the tabular regime, x_s~~they should be relatively ~~small (compared to the basal's value), but relatively~~ large in the columnar regime (compared to the tabular regime). Such a trend in x_s, if verified by experiment, could the explain the higher stability of trigonal columns as well as the transition to scalene hexagonal for the tabular case. The instability of the tabular case here is also consistent with the argument that an imposed gradient in supersaturation has little effect on the direction of tabular branches (Nelson and Knight, 1998), that is, prism faces adjacent to a supersaturation maximum should grow at the same normal growth rate (unlike the case in ~~Fig. 26~~Fig. B16f) because in the tabular regime, x_s for the prism face would instead be relatively small.

In addition, the AST flux from the basal to the prism should be smaller towards the narrow prism in a scalene hexagonal crystal than to the wider prism (following §~~3.16~~B.7 above). This effect would further de-stabilize the tabular trigonal and scalene hexagonal forms, particularly for the thinner tabular crystals, ~~and~~but have less effect on the columnar crystals. Concerning the role of the vapor mean-free path, this mechanism for the stability would have a vanishing role ~~as~~when the vapor mean-free path ~~approached or~~ exceeded the crystal size. But in an atmosphere of air, this condition would require crystal diameters below a few tenths of a micron. Finally, if the layer nucleation rate increased more rapidly at higher supersaturation, as is expected, then the influence of the AST flux would increase as well, strengthening the mechanism. In general, the supersaturation in a cloud is

higher when the first crystals nucleate, and is also higher at the crystal surface when the crystal is small, but as each crystal grows and more crystals nucleate, the supersaturation drops. This effect also predicts a transition from trigonal to scalene hexagonal, and eventually, to hexagonal. However, if the crystal develops branches while still scalene hexagonal, the nearly three-fold symmetry should remain as the branches grow independently of one another. This may explain the large, nearly three-fold symmetric branched crystals in Bentley's collection (Bentley, 1924; Bentley and Humphreys, 1962).

Finally, consider what would result if, instead of $\boldsymbol{p_3}$ or $\boldsymbol{p_5}$ developing after $\boldsymbol{p_1}$, that $\boldsymbol{p_4}$ developed in Fig. B16c. In this case, one can argue that the resulting crystal would have two large-area prisms $\boldsymbol{p_1}$ and $\boldsymbol{p_4}$, with the latter smaller than the former, and just two other equal-sized faces $\boldsymbol{p_3}$ and $\boldsymbol{p_5}$. That is, the shape in cross-section would be an isosceles trapezoid. Such a shape falling with $\boldsymbol{p_4}$ side down could generate the suncave Parry arc in a thin cloud. Upon growing larger, the $\boldsymbol{p_2}$ and $\boldsymbol{p_6}$ faces would likely develop, and then regardless of whether the falling orientation had $\boldsymbol{p_4}$ side down or up, a suncave Parry arc would result (e.g., Westbrook, 2011). A sampling of crystals from a Parry-arc display found no evidence of the trapezoid form (Sassen and Takano, 2000), so such a form may transition to the six-sided form while still small.

Author contributions. The experiments with the capillary apparatus were done by JN and BS, Text, figures, and calculations were prepared by JN, with input from BS.

Competing interests. The authors declare that they have no conflict of interest.

Acknowledgements. The National Science Foundation provided support for this research through grant #1348238 from the Division of Atmospheric and Geospace Sciences (AGS). We also thank the Laucks Foundation for research funds, equipment, and laboratory space. JN thanks Charles Knight for discussions about the distinction between lateral and normal growth. We thank Prof. Akira Yamashita (AY) for kindly supplying the images for Figs. 1, B3, B7, B10, B13a, and B15. We also thank Art Rangno for supplying the original digital copies of the Magono–Lee collection shown in Figs. B5 and B12. Mark Cassino and Martin Schnaiter also kindly supplied useful photographs. The concept of protruding growth is from AY, as is the basic mechanism of trigonal initiation on sub-micron droxtals, and two-level formation. JN also thanks AY for numerous discussions of protruding growth and pocket formation. Some crystal images were processed in ImageJ using auto-contrast and background subtraction.

References

Arima, Y. and Irisawa, T.: The back-force effect in the multinucleation growth process. J. Cryst. Gr., 104, 297–309, 1990.

Avramov, I.: Kinetics of growth of nanowhiskers (nanowires and nanotubes). Nanoscale Res Lett., 2, 235–239, doi 10.1007/s11671-007-9054-8, 2007.

Bacon, N. J., Baker, M. B., and Swanson, B. D.: Initial stages in the morphological evolution of vapour-grown ice crystals: A laboratory investigation. Q. J. R. Meteorol. Soc., 129, 1903–1927, 2003.

Bailey, M. and Hallett, J.: Growth Rates and Habits of Ice Crystals between -20 and -70 C, J. Atmos. Sci., 61 514–544, 2004.

Bentley, W. A.: Twenty years' study of snow crystals. Monthly Weather Rev. May, 212–214, 1901.

Bentley, W. A.: Forty years' study of snow crystals. Monthly Weather Rev. Nov., 530–532, 1924.

Bentley, W. A. and Humphreys, W. J.: Snow Crystals. Dover Publications, 226 pp., 1962.

Burton, W. K., Cabrera, N., and Frank, F. C.: The Growth of Crystals and the Equilibrium Structure of their Surfaces. Phil. Trans. R. Soc. A , 243, 299–358, 1951.

Demange, G., Zapolsky, H., Patte, R., Brunel, M.: Growth kinetics and morphology of snowflakes in supersaturated atmosphere using a three-dimensional phase-field model. Phys. Rev. E, 96, 022803 (1–13), 2017.

Elbaum, M.: Roughening transition observed on the prism facet of ice. Phys. Rev. Lett. 67, 2982-2985, 1991. https://doi.org/10.1103/PhysRevLett.67.2982

Elwenspoek, M. and van der Eerden, J. P.: Kinetic roughening and step free energy in the solid-on-solid model and on naphthalene crystals. J. Phys. A: Math. Gen. 20, 669-678, 1987.

Frank, F. C.: Snow Crystals. Contemp. Phys., 3–22, 1982.

Frank, F.C.: personal communication, 1993.

Frenkel J.: On the surface motion of particles in crystals and the natural roughness of crystalline faces. J. Phys. USSR 9, 392–398, 1945.

Elwenspoek, M. and van der Eerden, J. P.: Kinetic roughening and step free energy in the solid-on-solid model and on naphthalene crystals. J. Phys. A: Math. Gen. 20, 669-678, 1987.

Gilmer, G. H., Ghez, R., and Cabrera, N.: An analysis of combined surface and volume diffusion processes in crystal growth. J. Cryst. Gr., 8, 79–93, 1971. https://doi.org/10.1016/0022-0248(71)90027-3

Gonda, T. and Gomi, H.: Morphological instability of polyhedral ice crystals growing in air at low temperature. Annals of Glaciology, 6, 222−224, 1985.

Gonda, T. and Koike, T.: Growth mechanisms of single ice crystals growing at a low temperature and their morphological stability. J. Cryst. Gr., 65, 36−42, 1983.

Gonda, T. and Nakahara, H.: Formation mechanism of side branches of dendritic ice crystals grown from vapor. J. Cryst. Gr., 160, 162−166, 1996.

Gonda, T., Kakiuchi, H., and Moriya, K.: In situ observation of internal structure in growing ice crystals by laser scattering tomography. J. Cryst. Gr., 102, 167–174, 1990.

Gonda, T., Matsuura, Y., and Sei, T.: In situ observations of vapor-grown ice crystals by laser two-beam interferometry. J. Cryst. Gr., 142, 171–176, 1994.

Field Code Changed

Formatted: Pattern: Clear

Gonda, T., Sei, T., and Gomi, H.: Surface micromorphology of columnar ice crystals growing in air at high and low supersaturations. Mem. Natl. Inst. Polar Res., Special issue, 39, 108–116, 1985.

Gonda, T., and Yamazaki, T.: Morphology of ice droxtals grown from supercooled water droplets. J. Cryst. Gr., 45, 66−69, 1978.

Gonda, T., and Yamazaki, T.: Initial Growth forms of Snow Crystals Growing from Frozen Cloud Droplets. J. Meteor. Soc. Jpn., 62, 190–192, 1984.

Hallett, J. and Mason, B. J.: The influence of temperature and supersaturation on the habit of ice crystals grown from the vapour. Proc. Roy. Soc. London, A247, 440–453, 1958.

Hallett, J.: The growth of ice crystals on freshly cleaved covellite surfaces. Philos. Mag. 6 (69), 1073−1087, 1961.

Harrington, J. Y., Moyle, A., and Hanson, L. E.: On Calculating Deposition Coefficients and Aspect-Ratio Evolution in Approximate Models of Ice Crystal Vapor Growth. J. Atmos. Sci., 76, 1609–1625, 2019. https://doi.org/10.1175/JAS-D-18-0319.1

Heymsfield, A. J.: Ice Particles Observed in a Cirriform Cloud at −83 °C and Implications for Polar Stratospheric Clouds. J. Atmos. Sci. 43, 851–855, 1986.

Hobbs, P. V. and Rangno, A. L.: Ice Particle Concentrations in Clouds. J. Atmos. Sci., 42, 2523-2549, 1985. https://doi.org/10.1175/1520-0469(1985)042<2523:IPCIC>2.0.CO;2.

Hudait, A., and Molinero, V.: What Determines the Ice Polymorph in Clouds? J. Amer. Chem. Soc., 138, 8958–8967, 2016. DOI: 10.1021/jacs.6b05227.

Itoo, K.: Forms of Ice Crystals in the Air: On Small Ice Crystals (II). Papers in Meteorology and Geophysics, 3, 207–216, 1953.

Järvinen, E., Jourdan, O., Neubauer, D., Yao, B., Liu, C., Andreae, M. O., Lohmann, U., Wendisch, M., McFarquhar, G. M., Leisner, T., Schnaiter, M.: Additional Global Climate Cooling by Clouds due to Ice Crystal Complexity. Atmos. Chem. Phys. Discuss., https://doi.org/10.5194/acp-2018–491, 2018.

Keller, V. W., McKnight, C. V., and Hallett, J.: Growth of ice discs from the vapor and the mechanism of habit change of ice crystals. J. Cryst. Gr. 49, 458–464, 1980.

Kelly, J. G., Boyer, E. C.: Physical Improvements to a Mesoscopic Cellular Automaton Model for Three-Dimensional Snow Crystal Growth. Cryst. Growth Des., 14, 1392–1405, 2014.

Kikuchi, K., Kameda, T., Higuchi, K., and Yamashita, A.: A global classification of snow crystals, ice crystals, and solid precipitation based on observations from middle latitudes to polar regions. Atmos. Res., 132-133, 460–472, 2013.

Knight, C. A.: Another look at ice crystal growth habits. Trans. Amer. Geophys. Union, 53, 382, 1972.

Knight, C. A.: Ice Growth from the Vapor at −5 °C, J. Atmos. Sci., 69, 2031–2040, 2012.

Knight, C. A. and Devries, A. L.: Growth forms of large frost crystals in the Antarctic. Journal of Glaciology, 31, 127-135, 1985.

Kobayashi, T.: On the Variation of Ice Crystal Habit with Temperature. Physics of Snow and Ice. Proceedings, Institute of Low Temperature Science, Hokkaido University: Sapporo, 95−104, 1967.

Kobayashi, T., Furukawa, Y., Kikuchi, K., and Uyeda, H.: On twinned structures in snow crystals. J. Cryst. Gr., 32, 233–249, 1976.

Kobayashi, T., and Ohtake, T.: Hexagonal Twin Prisms of Ice. J. Atmos. Sci. 31, 1377–1383, 1974.

Kuroda, T., Irisawa, T., and Ookawa, A.: Growth of a polyhedral crystal from solution and its morphological stability. J. Cryst. Gr., 42, 41–46, doi: 10.1016/0022-0248(77)90176-2, 1977.

Lamb, D. and Scott, W. D.: Linear growth rates of ice crystals grown from the vapor phase. J. Cryst. Gr., 12, 21–31, 1972. https://doi.org/10.1016/0022-0248(72)90333-8.

Field Code Changed

Libbrecht, K. G.: Explaining the formation of thin ice crystal plates with structure-dependent attachment kinetics. J. Cryst. Gr., 258, 168–175, 2003.

Libbrecht, K. G.: The physics of snow crystals. Rep. Prog. Phys. 68, 855–895, 2005.

Libbrecht, K. G.: Field Guide to Snowflakes. Voyageur Press, Minneapolis, MN, 112 pps, 2006.

Libbrecht, K. and Arnold, H. M.: Aerodynamic stability and the growth of triangular snow crystals. arXiv:0911.4267 (http://arxiv.org/abs/0911.4267), 2009.

Magee, N. B., Miller, A., Amaral, M., Cumiskey, A.: Mesoscopic surface roughness of ice crystals pervasive across a wide range of ice crystal conditions. Atmos. Chem. Phys. 14, 12357–12371, doi:10.5194/acp-14-12357-2014, 2014.

Maeno, N. and Kuroiwa, D.: Gas Enclosures in Snow Crystals. Low Temperature Science, Ser. A, 24, 81–89, 1966. (in Japanese)

Magono, C. and Lee, C. W.: Meteorological Classification of Natural Snow Crystals. J. Faculty of Science, Hokkaido Univ. Ser. 7, Geophysics, 2(4), 321–335, 1966.

Malkin, T. L., Murray, B. J., Brukhno, A. V., Anwar, J., and Salzmann, C. G.: Structure of ice crystallized from supercooled water. Proc. Nat. Acad. Sci., 109, 1041–1045, 2012.

Mason, B. J., Bryant, G. W., and van den Heuvel, A. P.: The growth habits and surface structure of ice crystals, Philos. Mag., 8, 505–526, 1963.

Millstone, J. E., Hurst, S. J., Métraux, G. S., Cutler, J. I. and Mirkin, C. A.: Colloidal gold and silver triangular nanoprisms. ~~small~~Small, 5, 646–664, 2009.

Ming, N-b., Tsukamoto, K., Sunagawa, I., and Chernov, A. A.: Stacking faults as self-perpetuating step sources, J. Cryst. Gr., 91, 11–19, 1988.

Moon, P. and Spencer, D. E.: Field Theory for Engineers. D. Van Nostrand, New York, 1961.

Murray, B. J., Salzmann, C. G., Heymsfield, A. J., Dobbie, S., Neely, R. R. III, Cox, C. J.: Trigonal ice crystals in Earth's atmosphere. Bulletin American Meteor. Soc. Sept. issue 1515–1531, 2015.

Myers-Beaghton, A. K. and Vvedensky, D. D.: Nonlinear equation for diffusion and adatom interactions during epitaxial growth on vicinal surfaces. Phys. Rev. B 42, 5544-5554, 1990. https://doi.org/10.1103/PhysRevB.42.5544

Nakata, M., Asano, A., Yamashita, A.: Morphology of Giant Ice Polycrystals Grown from the Vapour, Physics and Chemistry of Ice. Ed. N. Maeno and T. Hondoh, Hokkaido University Press, Sapporo, 311–317, 1992.

Nakaya, U.: Snow Crystals: Natural and Artificial. Harvard Univ. Press, 510 pp, 1954.

Nakaya, U., Hanajima, M., Muguruma, J.: Physical Investigations on the Growth of Snow Crystals. J. Faculty of Science, Hokkaido University. Ser. 2, 5(3), 87–118, 1958.

Nelson, J.: A Theoretical Study of Ice Crystal Growth in the Atmosphere. Ph.D. Dissertation, University of Washington, 1994.

Nelson, J.: Sublimation of Ice Crystals. J. Atmos. Sci., 55, 910–919, 1998.

Nelson, J.: Growth mechanisms to explain the primary and secondary habits of snow crystals. Philosophical Magazine A, 81, 2337-2373, 2001.

Nelson, J.: Branch Growth and Sidebranching in Snow Crystals. Crystal Growth & Design, 5, 1509–1525, 2005.

Nelson, J.: http://www.storyofsnow.com/blog1.php/ April 10th, 2014 post (Accessed June, 2018), 2014.

Nelson, J., and Baker, M. B.: New Theoretical Framework for Studies of Vapor Growth and Sublimation of Small Ice Crystals in the Atmosphere. J. Geophys. Res. D **101**, 7033–7047, 1996.

Nelson, J., and Knight, C.: A new technique for growing crystals from the vapor. J. Cryst. Gr. 169, 795–797, 1996.

Nelson, J., and Knight, C.: Snow Crystal Habit Changes Explained by Layer Nucleation. J. Atmos. Sci., 55, 1452–1465, 1998.

Formatted: Font: Times New Roman, 10 pt, Font color: Auto, Pattern: Clear

Field Code Changed

Neshyba, S., Adams, J., Reed, K., Rowe, P. M., Gladich, I.: A quasi-liquid mediated continuum model of faceted ice dynamics. J. Geophys. Res., 121, 14,035–14,055, doi.org/10.1002/2016JD025458, 2016.

Pfalzgraff, W. C., Hulscher, R. M., and Neshyba, S. P.: Scanning electron microscopy and molecular dynamics of surfaces of growing and ablating hexagonal ice crystals. Atmos. Chem. Phys., 10, 2927–2935, 2010.

Rosenberg, R.: Why is Ice Slippery? Physics Today 58, 12, 50-55, 2005. doi: 10.1063/1.2169444

Sassen, K. and Takano, Y.: Parry arc: a polarization lidar, ray-tracing, and aircraft case study. Appl. Opt., 39, 6738–6745, 2000.

Sears, G. W.: A growth mechanism for mercury whiskers. Acta Metal., 3, 361–366, 1955.

Seligman, G.: Snow structure and ski fields: being an account of snow and ice forms met with in nature and a study on avalanches & snowcraft. Macmillan & Co., Ltd. 555 pp, 1936.

Schnaiter, M., Järvinen, E., Abdelmonem, A., and Leisner, T.: PHIPS-HALO: the airborne particle habit imaging and polar scattering probe – Part 2: Characterization and first results. Atmos. Meas. Tech., 11, 341–357, 2018.

Sei, T. and Gonda, T.: Growth Rate of Polyhedral Ice Crystals Growing from the Vapor Phase and Their Habit Change. J. Meteorol. Soc. Jpn. 67, 495–502, 1989.

Sei, T., Gonda, T., and Goto, Y.: Formation process of branches of needle ice crystals grown from vapor. Polar Meteorol. Glaciol. 14, 27–33, 2000.

Shimada, W. and Ohtake, K.: Three-Dimensional Morphology of Natural Snow Crystals. Crystal Growth & Design, 16, 5603−5605, doi: 10.1021/acs.cgd.6b01263, 2016.

Shimada, W. and Ohtake, K.: Asymmetrical Three-Dimensional Morphology of Growing Snow Crystals Observed by a Michelson Interferometer. Crystal Growth & Design, 18, 6426−6430, doi: 10.1021/acs.cgd.8b01377, 2018.

Smith, H. R., Connolly, P. J., Baran, A. J., Hesse, E., Andrew R.D. Smedley, A. R. D., Webb, A. R.: Cloud chamber laboratory investigations into scattering properties of hollow ice particles. J. Quant. Spectrosc. & Radiat. Transf., 157, 106–118, 2015.

Swanson, B., and Nelson, J.: ~~(in preparation)~~ Low-Temperature Triple-Capillary Cryostat for Ice Crystal Growth Studies. Atmos. Measurement Techniques, https://doi.org/10.5194/amt-2019-137, 2019.

Takahashi, C. and Mori, M.: Growth of snow crystals from frozen water droplets, Atmos. Res., 82, 385–390, doi:10.1016/j.atmosres.2005. 12.013, 2006.

Takahashi, T.: Influence of Liquid Water Content and Temperature on the Form and Growth of Branched Planar Snow Crystals in a Cloud. J. Atmos. Sci., 71, 4127–4142, 2014.

Takahashi, T., Endoh, T., Wakahama, G., and Fukuta, N.: Vapor Diffusional Growth of Free-Falling Snow Crystals between -3 and -23 °C. J. Meteorol. Soc. Japan, 69, 15–30, 1991.

ten Wolde, P. R. and Frenkel, D.: Homogeneous nucleation and the Ostwald step rule. Phys. Chem. Chem. Phys., 1, 2191-2196, 1999. DOI: 10.1039/A809346F

Vekilov, P. G., Lin, H., and Rosenberger, F.: Unsteady crystal growth due to step-bunch cascading. Phys. Rev. E. 55, 3202–3214 doi.org/10.1103/PhysRevE.55.3202, 1997.

Voigtländer, J., Chou, C., Bieligk, H., Clauss, T., Hartmann, S., Herenz, P., Niedermeier, D., Ritter, G., Stratmann, F., and Ulanowski, Z.: Surface roughness during depositional growth and sublimation of ice crystals, Atmos. Chem. Phys., 18, 13687–13702, https://doi.org/10.5194/acp-18-13687-2018, 2018.

Westbrook, C. D.: Origin of the Parry arc. Q. J. R. Meteorol. Soc., 137, 538–543, 2011.

Wood, S. E., Baker, M. B., and Calhoun, D.: New model for the vapor growth of hexagonal ice crystals in the atmosphere, J. Geophys. Res., 106, 4845–4870, 2001.

Formatted: No underline

Formatted: No underline

Formatted: No underline

Field Code Changed

Field Code Changed

Formatted: Default Paragraph Font

Formatted: Font color: Auto

Woodruff, D. P.: How does your crystal grow? A commentary on Burton, Cabrera and Frank (1951) 'The growth of crystals and the equilibrium structure of their surfaces'. Phil. Trans. Roy. Soc. A 373, 20140230, 2015. https://doi.org/10.1098/rsta.2014.0230

Yamashita, A.: Skeleton Ice Crystals of Non-Hexagonal Shape Grown in Free Fall, J. Meteorol. Soc. Jpn., 49, 215–231, 1971.

Yamashita, A.: On the Trigonal Growth of Ice Crystals. J. Meteorol. Soc. Jpn., 51, 307–317, 1973.

Yamashita, A.: Small artificial snow crystals grown in free fall. J. Japanese Association of Crystal Growth, 6, 75–85, 1979. (In Japanese)

Yamashita, A.: Morphology of Plate-type Snow Crystals Grown in a Supercooled Cloud. Tenki, 60. ~~23~~165–~~33~~176, 2013. (In Japanese).

Yamashita, A., unpublished manuscript "Protruding Growth of Snow Crystals -Potential Role of an Adjoining-face Process", 2014.

Yamashita, A.: Adjoining Face Process and growth of Snow Crystals. JSSI&JSSE Joint Conference, Matsumoto, Japan 2015.9.13-9.16. p 24 (C1-1), 2015. (In Japanese)

Yamashita, A.: Study on Air Pockets Enclosed in Snow Crystal Part I—-Air Pockets of Plate—-. Tenki 63, ~~15~~393–~~22~~400, 2016. (In Japanese)

Yamashita, A.: Study on Air Pockets Enclosed in Snow Crystal Part II—Analysis of Air Pockets Taking Growth Process of Prism Faces into Consideration—. Tenki 66, 239–251, 2019. (In Japanese)

Yamashita, A.: unpublished manuscript "Study on comparatively large air pockets" AP Note No. 4, Nov. 2018.

Yamashita, A., Asano, A.: Morphology of Ice Crystals Grown from the Vapour at Temperatures between −4 and −1.5 °C. *J. Meteorol. Soc. Japan*, 62, 40–45, 1984.

Yamashita, A., Ohno, T.: Ice Crystals Grown in an Unforced Air Flow Cloud Chamber, J. Meteor. Soc. Jpn., 62, 135–139, 1984.